NRPB-R302

Atmospheric Dispersion Modelling Liaison Committee

Annual Report 1996/97

NRPB-R302

National Radiological Protection Board

The National Radiological Protection Board was established by the Radiological Protection Act 1970 and is responsible for conducting research and providing advice and services for protection against ionising and non-ionising radiations.

Any questions relating to this report should be addressed to the Publications Office, National Radiological Protection Board, Chilton, Didcot, Oxfordshire, OX11 0RQ, UK.

Further copies are available from the Stationery Office and through booksellers.

NRPB-R302

Atmospheric Dispersion Modelling Liaison Committee

Annual Report 1996/97

National Radiological Protection Board
Chilton
Didcot
Oxon OX11 0RQ

Approval date: March 1998
Publication date: May 1999

The Stationery Office, £22.50
ISBN 0 85951 422 6

Preface

In 1977 a meeting of representatives of government departments, utilities and research organisations was held to discuss methods of calculation of atmospheric dispersion for radioactive releases. Those present agreed on the need for a review of recent developments in atmospheric dispersion modelling, and a Working Group was formed. Those present at the meeting formed an informal Steering Committee, that subsequently became the UK Atmospheric Dispersion Modelling Liaison Committee. That Committee operated for a number of years. Members of the Working Group worked voluntarily and produced a series of reports. A workshop on dispersion at low wind speeds was also held, but its proceedings were never published.

The Committee has recently been reorganised and has adopted terms of reference. The organisations represented on the Committee, and the terms of reference adopted, are given in this report. The organisations represented on the Committee pay a small annual subscription. The money thus raised is used to fund reviews on topics agreed by the Committee, and to support in part its secretariat, provided by NRPB. The new arrangements came into place for the start of the 1995/96 financial year. During its first year, the Committee placed contracts for three reviews, which were described in its Annual Report for that year. This report describes the second year in which the Committee has operated under the new arrangements, and during which it placed contracts for two studies. The technical specifications for these contracts are given in this report. The reports from its contractors are attached as annexes to this report. In addition, the Committee organised a presentation on the work undertaken to validate the ADMS model and the more general work on validation of the Gaussian plume dispersion model.

The Committee intends to place further contracts in future years and would like to hear from those interested in tendering for such contracts. They should contact the Secretary:

Mr J G Smith
National Radiological Protection Board
Chilton
Didcot
Oxon OX11 0RQ

Contents

Atmospheric Dispersion Modelling Liaison Committee

1 Organisations represented on the Committee

Amersham International plc
Atomic Weapons Establishment, Aldermaston
British Nuclear Fuels plc
Department of the Environment Northern Ireland
Environment Agency
Health and Safety Executive
  Major Hazards Assessment Unit
  Nuclear Installations Inspectorate
Magnox Electric
Ministry of Agriculture, Fisheries and Food
Meteorological Office
National Nuclear Corporation
National Radiological Protection Board
Nuclear Electric
Royal Naval College, Greenwich
Rolls Royce and Associates plc
Scottish Nuclear
Scottish Office (HMIPI)
Urenco (Capenhurst)
Westlakes Research Institute

The Chairman and Secretary are provided by NRPB.

2 Terms of reference

1 To review current understanding of atmospheric dispersion and related phenomena and to identify suitable models for application primarily in authorisation or licensing, in the context of discharges to atmosphere resulting from nuclear industry activities.

2 The Committee shall consist of representatives of government departments, government agencies and primarily the nuclear industry. Each organisation represented on the Committee shall pay an annual membership fee of £1000.

3 The Committee will consider selected topics. These should be selected following discussion and provisional agreement at meetings of the Committee, followed by confirmation after the meeting. Where possible, it will produce reports describing suitable models for that topic. These will reflect either the views of an Expert Working Group appointed by the Committee or the outcome of a workshop organised on behalf of the Committee. The Working Group will determine who should be invited to speak at workshops, and to subsequently review their outcome and identify suitable models.

4 The money raised from membership fees and registration fees for the workshops will be used to support the Working Group, the drafting of reports, and any other matters which the Committee may decide.

3 Reports published

Clarke, R H (1979). The first report of a Working Group on Atmospheric Dispersion: a model for short and medium range dispersion of radionuclides released to the atmosphere. Harwell, NRPB-R91.

Jones, J A (1981). The second report of a Working Group on Atmospheric Dispersion: a procedure to include deposition in the model for short and medium range dispersion of radionuclides. Chilton, NRPB-R122.

Jones, J A (1981). The third report of a Working Group on Atmospheric Dispersion: the estimation of long range dispersion and deposition of continuous releases of radionuclides to atmosphere. Chilton, NRPB-R123.

Jones, J A (1981). The fourth report of a Working Group on Atmospheric Dispersion: a model for long range atmospheric dispersion of radionuclides released over a short period. Chilton, NRPB-R124.

Jones, J A (1983). The fifth report of a Working Group on Atmospheric Dispersion: models to allow for the effects of coastal sites, plume rise and buildings on dispersion of radionuclides and guidance on the value of deposition velocity and washout coefficients. Chilton, NRPB-R157.

Jones, J A (1986). The sixth report of a Working Group on Atmospheric Dispersion: modelling wet deposition from a short release. Chilton, NRPB-R198.

Jones, J A (1986). The seventh report of a Working Group on Atmospheric Dispersion: the uncertainty in dispersion estimates obtained from the Working Group models. Chilton, NRPB-R199.

Atmospheric Dispersion Modelling Liaison Committee. Annual Report 1995/96. Chilton NRPB-R292. Includes annexes:

Atmospheric Dispersion at Low Wind Speed
Application of Computational Fluid Dynamics Codes to Near-field Atmospheric Dispersion
Rise of a Buoyant Plume from a Building Wake

4 Specifications for technical annexes

A Atmospheric dispersion at low wind speed

1 Background

W S Atkins has produced a report on low wind speed conditions for HSE with particular reference to quantitative risk assessment (QRA). A subsequent phase of this study will extend the work to consider the development of a simple methodology for estimating dispersion in low wind speeds. It will also consider the effects that the inclusion of these low wind speeds has on the results of QRAs. The proposal for additional work for ADMLC is given in Sections 2 and 3 below.

2 Objectives

To determine the importance of low wind speed, stable conditions when calculating the annual average concentration from a constant source at distances of a few hundred metres.

3 Tasks

(a) Agree on typical release (size, buoyancy, momentum, height, release duration), and ranges of values for release parameters.

(b) Synthesise wind data, using sonic anemometer or lightweight cup data (as analysed in WSA Phase 1 report) as far as possible.

(c) Develop simple dispersion methodology for low wind speeds. This will include justified criteria for the lower limit on the use of standard models, which may depend on release rate and distance from source.

(d) Calculate annual averages and concentrations from a short release, varying the following parameters:

- release height (fully entrained, from a building roof, from a stack),
- distance of target from source (in the range 100 m to 10 km),
- averaging time for wind data,
- release characteristics (neutral and a buoyant release).

(e) Present and discuss results. This will take the form of a stand-alone report to ADMLC which will form an appendix to the HSE phase 2 report.

B Review of models for calculating air concentrations when plumes impinge on buildings or the ground

Releases of material to atmosphere can occur in situations where the plume can impinge on other buildings or on elevated ground close to the release point. In some instances, the plume can pass over air intakes or windows in the building from which the material is released. Methods for calculating the concentration on the surface of, or inside, buildings or at ground level on elevated terrain should be reviewed. The review should identify the situations when plumes might impinge, and describe existing methods for calculating the concentration on the ground or the building surface. Methods that are suitable for incorporation in personal computer programs should be identified if possible. The extent to which the Gaussian plume model could be modified for application in such situations should also be addressed.

The review should concentrate on existing models. The possibility of developing improved models should be identified, but the development of such models is outside the scope of this contract.

ANNEX A

Atmospheric Dispersion at Low Wind Speed

I G LINES AND D M DEAVES
WS ATKINS SAFETY & RELIABILITY

Contents

Summary

Background

WS Atkins, as part of its support to the Major Hazards Assessment Unit of the Health and Safety Executive (HSE), has undertaken studies of dispersion in low mean wind speeds. The primary application of the work is to short timescale accidental releases of toxic or flammable gases, and the results of the first phase of the study were presented by Lines and Deaves (1996). The second phase is considering the possible improvements in current applications of low wind speed effects in qualified risk assessment (QRA) studies in more detail, and this has been extended to cover the interests of the Atmospheric Dispersion Modelling Liaison Committee (ADMLC). These interests relate primarily to the dispersion of passive or buoyant releases from stacks or buildings, as described in the brief, which is outlined in Section 1.

Structure

Sections 2 and 3 describe the main findings of this study, and will be included as appendices to the final HSE report. Section 2 presents a brief review of possible alternative modelling approaches for low wind speed conditions. Section 3 then uses examples to demonstrate the effects of different implementations, both of weather data and of modelling approaches, on annual averages and short-term ground-level concentrations. Conclusions are presented in Section 4, and references are then included as Section 5.

Conclusions

This project has shown that there are several ways in which simple methodologies can be applied to ensure that the effect of low wind speeds is incorporated. These include:

(a) simply using a greater number of representative weather conditions,
(b) defining additional low wind speed weather categories (eg on the basis of Weibull distributions),
(c) applying simple low wind speed dispersion models for low wind speed or calm conditions,
(d) applying additional conditions/provisos to standard dispersion models.

However, having reviewed all of these approaches, it is felt that the best advice is to consider the type of application for which the dispersion modelling is required, and then use an appropriate methodology with suitable assumptions.

In summary, for annual average concentrations or risk assessment type applications, the cross-wind spread of a plume is generally unimportant, as the results depend on the cross-wind integrated concentrations. Many simple low wind speed models essentially just modify the horizontal spread parameter, and so their use would not result in any significant changes to the results. However, this study has shown that the frequency of low wind speed categories may be significant, and so it is preferable to use a larger number of representative weather categories in order to ensure that low wind speeds can be included. It should be noted, however, that low wind speed categories should not be used to predict concentrations at distances beyond those which could be reached by the plume (ie considering the persistence of these low wind speed conditions).

For safety case applications, where the requirement is often to consider the dispersion of a release in typical and worst case weather conditions, the assessment of dispersion in low wind speeds is more important. First, it is necessary to define what constitutes the worst case conditions.

In the past, F2 has often been chosen, but this report shows that, at short to medium distances, it may be more appropriate to consider F0.5 or F1 conditions, depending on whether such conditions could persist to the distance of interest. A variety of models may be applied, most of which involve modifying the cross-wind spread according to the wind speed, resulting in wider but less concentrated plumes than would be obtained by simply applying a standard Gaussian plume approach. Having considered a number of such models, it is felt that, for most practical purposes, the inclusion of a 'meander' or time averaging correction to the standard NRPB-R91 model provides a reasonable approach for use at low wind speeds of 0.5 to 2 m s^{-1}. This approach results in a $u^{-1/2}$ dependence of the concentration on wind speed, rather than the u^{-1} dependence usually quoted for Gaussian plume models. This $u^{-1/2}$ dependence implies a 'softer' singularity as $u \rightarrow 0$, implying that it may be appropriate to use such models down to fairly low wind speeds (eg 0.5 m s^{-1}).

In certain special cases, such as when a prediction of upwind spread is required, then it may be necessary to use either a puff type model or some form of three-dimensional diffusion equation, rather than any form of standard plume model.

1 Introduction

Under contract to the Health and Safety Executive (HSE), WS Atkins has produced a report on low wind speed conditions with particular reference to qualified risk assessment (QRA) (Lines and Deaves, 1996). A subsequent phase of this study will extend the work to consider the development of a simple methodology for estimating dispersion in low wind speeds. It will also consider the effect that the inclusion of these low wind speeds has on the results of QRAs. The technical proposals for this phase were supplied separately to HSE, and the proposals for additional work for the Atmospheric Dispersion Modelling Liaison Committee (ADMLC), as presented in this report, are described below.

The objective of this study is to determine the importance of low wind speed, stable conditions when calculating the annual average concentration from a steady source at distances of a few hundred metres. It was agreed that this objective would be met by undertaking the following tasks, the results of which are presented in this report.

(a) Agree on typical release (size, buoyancy, momentum, height, release duration), and ranges of release parameters.

(b) Synthesise wind data, using sonic anemometer or lightweight cup data (as analysed in WSA Phase 1 report) as far as possible.

(c) Develop simple dispersion methodology for low wind speeds. This will include justified criteria for the lower limit on the use of standard models, which may depend on release rate and distance from source.

(d) Calculate annual averages and concentrations from a short release, varying the following parameters:

- release height (fully entrained, from a building roof or stack),
- distance of target from source,
- averaging time for wind data,
- release characteristics (neutral and a buoyant release),
- presence or not of building wake effects.

(e) Present and discuss results.

2 Review of models for passive dispersion in low mean wind speeds

2.1 Relevant atmospheric structure

For dense gas releases, the early stages of dispersion are often dominated by the motions set up by the release itself. For passive releases, since there is generally little effect on the flow, the structure of the atmosphere and its turbulence is dominant in determining the details of the dispersion. This section therefore discusses the relevant effects of atmospheric structure in order to provide a background to the more detailed discussions of specific models which are presented in Sections 2.2 and 2.3.

It is well known that the state of the atmosphere may be unstable (much convective mixing), neutral (mostly mechanical mixing) or stable (little mixing of any kind). In Phase 1 of the study for HSE, Lines and Deaves (1996) analysed some good quality meteorological data (obtained from sonic anemometers), and determined the distribution of low wind speeds within the various stability classes. It was found that, for mean wind speeds $\leq$ 2kt, only 35% were neutral, with 45% stable and 20% unstable. This compares with around 75% neutral, 15% stable and 10% unstable for

all conditions, irrespective of wind speed. It is therefore apparent that non-neutral stability classes assume a much greater significance when considering low wind speed conditions.

As indicated above, the main difference between dispersion in stable and unstable conditions is in the rather greater mixing in the latter case. This implies that stable conditions represent a 'worst case' for ground-level releases, which remain close to the ground and dilute slowly. For elevated (eg stack) releases, unstable (convective) conditions are worst, since the more rapid dilution will cause a large plume spread, and bring pollutants down to ground level more rapidly than in stable conditions.

As far as dispersion modelling is concerned, there are rather different problems associated with stable and unstable conditions. For stable conditions, plumes remain thin but meander significantly. Mean concentrations may therefore bear little relationship to the rather intermittent concentration traces which may be recorded in dispersion experiments. This problem is considerably exacerbated in the low wind speed case, since wind direction can change rapidly and frequently, and the mean direction cannot always be defined. For unstable conditions, pollutants may be spread rapidly to fill the complete depth of the mixing layer, making concentrations dependent on this depth, with wind speed appearing only as a secondary parameter which may influence that depth.

The structure of atmospheric mean wind and turbulence profiles also depends on small-scale topography. For high winds, any such effects are secondary, whereas they become more significant at low mean wind speeds, and may then be the dominant factor in determining the local dispersion conditions. This is particularly likely to be the case for stable conditions, as indicated by Jones (1997).

2.2 Models for low wind speed stable conditions

Problems relating to dispersion under stable conditions have been addressed by a number of authors over the last ten years or so. The approaches have ranged from modifying standard Gaussian plume models to reviewing the turbulence characteristics of such atmospheric conditions, and, in some cases, developing new models either for low wind speed or for completely calm conditions.

A useful starting point for the assessment of the current status of such modelling is the review of Cirillo and Poli (1992). They considered the performance of four different models as compared with observations presented by Sagendorf and Dickson (1974). These were:

(a) Puff model,

(b) Split σ model,

(c) Puff model for σ_y, standard model for σ_z,

(d) Cagnetti and Ferrara (1982) zero wind model:

$$c = \frac{Q}{2\pi r^{3/2}\sqrt{u_d K_z}} \tag{2.1}$$

where $u_d = 0.5$ m s^{-1} and $K_z = 1$ m^2 s^{-1}.

The application of models (a) and (c) required the input of actual meteorological data, but gave the best fits. Model (b) gave concentration profiles which were far too peaky, with peak centreline concentrations overpredicted by factors of around two to five. Model (d) performed poorly, except for one very low wind speed case (0.5 m s^{-1}), where the horizontal stability was

quoted as *A*, giving a value of σ_θ of around 50° at the 2 m level, while the vertical stability was quoted as *E*. Since this particular trial gave a plume spread of 360°, it was hardly surprising that the zero wind model fitted it well.

The main conclusion from Cirillo and Poli (1992) therefore seems to be that best fits are obtained where site-specific and incident-specific meteorological data are available. This conclusion is not surprising, but does not help in determining improvements to standard models for general application.

Several authors have developed improved models to allow for non-Gaussian concentration profiles in the lower part of the atmospheric boundary layer. Brown *et al* (1993) derived one such model using *k* theory, although it has not been specifically produced for low wind speeds. The final form of the concentration equation is rather complex, and depends on power law indices for the wind speed and eddy diffusivity profiles with height. Its implementation, however, still retains dependence on a negative power of *U*, giving a singularity at the origin. An alternative interpretation may perhaps suggest dependence on u_*^{-n}, which may remain finite as $U \rightarrow 0$.

A similar dependence was suggested by Venkatram (1982) who presented much simplified semi-empirical models for cross-wind integrated concentration against normalised distance. Specifically,

$$\overline{C_y} = \frac{Q}{u_* x} \qquad x < 1.4L$$

$$= \frac{0.89Q}{u_* L^{1/3} x^{2/3}} \qquad x > 1.4L \tag{2.2}$$

where *L* is the Monin-Obukhov length and u_* is the friction velocity. Again, this may suggest the use of a limiting value of u_* which remains constant as the wind speed drops to zero.

The stable boundary layer can be defined by

$$u = \frac{u_*}{k}\left(\ln\frac{z}{z_o} + \beta\frac{z}{L}\right) \tag{2.3}$$

where β is a constant and *L* is the Monin-Obukhov length. Venkatram suggests that $L = Au_*^2$ for low wind speed stable conditions, where $A = 1100\ s^2\ m^{-1}$. Substituting this into equation A2.3 gives

$$u = \frac{u_*}{k}\ln\frac{z}{z_o} + \frac{\beta z}{Aku_*} \tag{2.4}$$

If this is differentiated with respect to u_*, it can be seen that *u* has a minimum when:

$$u_* = \left(\frac{\beta z}{A\ln z/z_o}\right)^{1/2} \tag{2.5}$$

Taking $\beta = 7$, this minimum will occur at a value of around 0.05–0.06 m s^{-1} for $z = 2$ m and $z_o = 0.01$–0.1 m. The resulting variation of *u* with u_* is then as indicated in Table 2.1 for $z = 2$ m and $z_o = 0.1$ m.

TABLE 2.1 Variation of 2 m wind speed with friction velocity for stable boundary layers

u_* (m s^{-1})	0.01	0.02	0.05	0.1	0.2
u (m s^{-1})	3.28	1.75	1.02	1.07	1.66
u/u_*	328	88	20	11	8.3

It is clear that this model breaks down for wind speeds at 2 m height of less than 1 m s^{-1} (3.2 m s^{-1} at 10 m). For low wind speeds, however, it is expected that u_* may remain finite as $u \rightarrow 0$, because of residual turbulence. A similar analysis has been given by Hanna and Paine (1989), who used a minimum value of u_* as a cut-off in their hybrid plume dispersion model.

Now, as noted in the Phase 1 report, Smith (1992) identified wind speeds at which $\sigma_u = u$ as being around 0.35–0.50 for stable (E/F/G) conditions. As noted in Table 2.2 below, σ_u/u_* is around 5–6 for such conditions, suggesting a value of u_* of around 0.06–0.1. This implies that the u/u_* variation indicated in Table 2.1 breaks down for wind speeds below about 1.5 m s^{-1}. It is probable, therefore, that the variation of u_* with u asymptotes in some way as indicated in Figure 2.1, with a minimum value of u_* at around 0.05–0.06 m s^{-1}. A further constraint on the asymptotic value for u_* as $u \rightarrow 0$ can be obtained by considering the minimum value of L, which is quoted by Hanna and Paine (1989) as 5 m. Using $L = Au_*^2$, with the value of A given by Venkatram, gives a minimum value of $u_* = 0.067$ m s^{-1}. The asymptotic line on Figure 2.1 has been set to this value at $u = 0$. If it is assumed that $\sigma_u = 6u_*$ (see Table 2.2), this gives a minimum σ_u of 0.4 m s^{-1}.

Jones (1997) suggests that, where the mean wind speed is zero, the dispersing material would form an expanding disc of radius $\sigma_u t$. The upwind spread would then depend on the maximum time for which such conditions may exist, which has been observed, from sonic anemometer data at Cambourne and Cardington, to be around 20–30 minutes. This suggests a maximum upwind spread of around 500–700 m; further discussion and quantification of this phenomenon is given in Section 3.3.

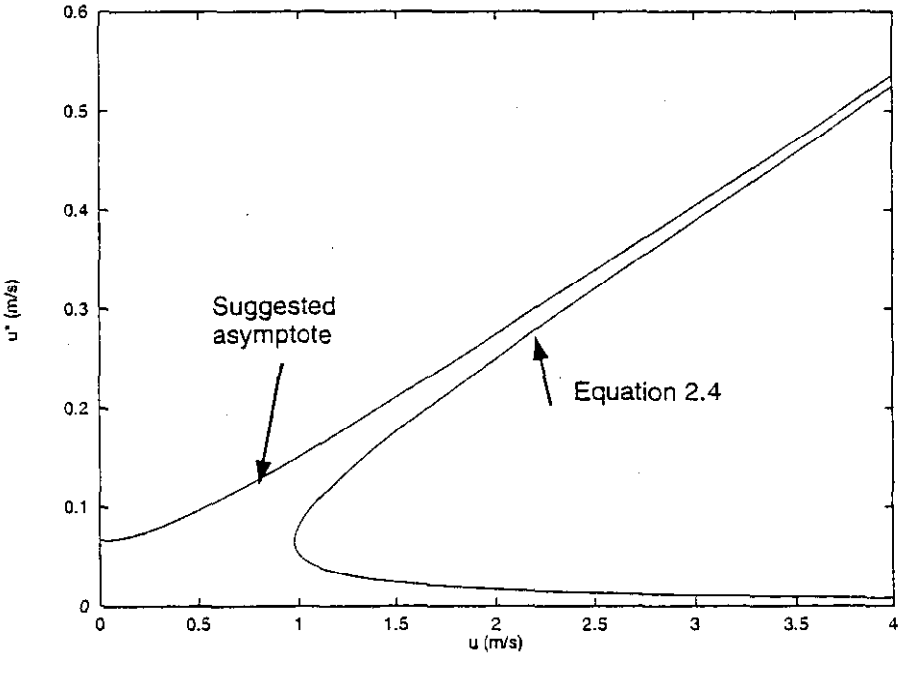

FIGURE 2.1 Asymptotic behaviour of u_* for low mean wind speed u

Lines and Deaves (1996) have identified a number of authors who adopt an equivalent assumption regarding the lateral dispersion parameter, such that the product $\sigma_\theta u$ remains constant as the velocity tends to zero. Specifically, a value of 0.5 (taking σ_θ in radians) has been suggested by Jones (1997), and a value of 45 (σ_θ in degrees) has been given by Etling (1990), corresponding to 0.8 with σ_θ in radians.

Sharan *et al* (1995) undertook a review similar to that presented by Cirillo and Poli (1992). Tests were undertaken against the same set of dispersion data, and similar conclusions were drawn. They did, however, introduce two further types of model:

(a) short-term averaging, in which standard parameters were applied over each subinterval,

(b) U_{min} approach, where the σs are adjusted for the 'calm condition' periods, to remove the singularity at $u = 0$.

The application of U_{min} is not entirely clear, but appears to involve breaking down the meteorological record into discrete periods for which a mean $\overline{U}$ is calculated by adding the individual components from these periods. The value of U_{min} is stated to be related to the performance of the anemometer, which is evidently reasonable when applying wind data for the actual period during which the measurements were made. This latter approach seems to have considerable merit, although it would have to be applied carefully with due regard to the nature of the meteorological information which is used.

Further background information on turbulence velocities etc. are discussed by Agarwal *et al* (1995). The data presented were obtained in the tropics, so may have to be adjusted if used in temperate latitudes. Specifically, they showed that the turbulence velocities varied significantly with both windspeed and stability, as shown in Table 2.2.

TABLE 2.2 Variation of turbulence velocities

Wind speed	Stability	σ_u/u_*	σ_v/u_*	σ_w/u_*
$U > 1$ m s^{-1}	Neutral	2	1.6	1.2
$U < 1$ m s^{-1}	Unstable	2	2	1.6
	Stable	6	5	1.6

Although σ_u, σ_v and σ_w are not generally used directly in most dispersion models, this information may be usable either in defining a minimum value of u_* (see above), or in application to certain specific zero wind models (see below).

A model which can be used in calm conditions has been developed by Arya (1995). For zero wind speed, this reduces to

$$c = \frac{Q\sigma_u}{(2\pi)^{3/2}\sigma_v\sigma_w r_m^2} \tag{2.6}$$

where $$r_m^2 = x^2 + \left(\frac{\sigma_u}{\sigma_v}\right)^2 y^2 + \left(\frac{\sigma_u}{\sigma_w}\right)^2 z^2$$

If it is assumed that $\sigma_u = \sigma_v$ and $\sigma_w = 1.6u_*$ (as suggested by Table 2.2) this reduces to

$$c = \frac{Q}{25u_* r^2} \tag{2.7}$$

or, for a minimum u_* of 0.067,

$$c = \frac{0.6Q}{r^2} \tag{2.8}$$

This gives concentrations which are everywhere lower than those given by the Cagnetti and Ferrara model (shown on Figure A10), ranging from a factor of 3 at x = 100 m to 100 at x = 100 km.

There are several potential drawbacks with the use of this model. One is that it depends on using σ_u, σ_v and σ_w, which may each tend to zero with u, re-introducing the singularity at $u = 0$, although the minimum u_* approach described above may circumvent this problem. The paper also points out that the dispersion parameters used are valid for small timescales, whereas the steady-state solution is valid for large timescales, implying an inconsistency in the derivation. Some results are given for low wind speeds which show the symmetrical dispersion for calm conditions, and significant upwind dispersion for values of wind speed up to w_*, the convective velocity scale. The model derivation appears to be general, although the primary applications given are to convective conditions.

2.3 Models for low wind speed convective conditions

For elevated releases, the worst ground-level concentration will normally be experienced in unstable (convective) atmospheric conditions. There is rather more emphasis, therefore, when dealing with convective conditions, on the behaviour of elevated plumes, and two models have been derived for this specific scenario.

Deardorff (1984) derived a model for tall stack releases in low wind convective conditions, on the assumption of complete mixing throughout the depth of the mixing layer. The solution depends on a numerical integration, which makes it less attractive for general use. However, the results presented do show the clear effects of along-wind and upwind diffusion. The author concludes that his model provides a basis on which more refined models could be built.

The model of Hanna and Paine (1989) does not purport to be a low wind speed model, but does deal with dispersion from a tall stack. It aims to provide the peak ground-level concentration, and then assumes a Gaussian cross-wind profile and a vertical profile which is only Gaussian for neutral and stable conditions; for vertical dispersion, either a pdf model or a convective scaling model is used. The paper is useful in that it provides an equation for the maximum concentration in extreme light wind conditions as a function of buoyancy flux, mixing depth and release height.

The models of Arya (1995) and Sharan *et al* (1996) both have been developed for any stability classes, although their primary applications appear to be for convective conditions. The Arya model has been described in Section 2.2; his main conclusion is that longitudinal diffusion becomes important in weak winds with high turbulence intensity. Arya also indicated the intention to undertake a physical simulation of near-source diffusion in a convective mixed layer with no mean wind, using the convection tank of the USEPA Fluid Modelling Facility.

The model of Sharan *et al* (1996) is based on K theory, and gives a solution in term of the diffusivities K_x, K_y and K_z. It is shown how this reduces to the classical Gaussian plume model using the slender plume approximation, which is shown to be equivalent to neglecting downwind diffusion. The results showed that the centreline concentration is unchanged, compared with the Gaussian model, whereas the off-centreline concentrations are reduced. Validation was provided against tracer experiments conducted in Delhi in 1991. Agreement was good for convective conditions, although the lowest wind speed recorded for such conditions was 0.74 m s^{-1}.

2.4 Use of low wind speed models

The main application for which such models are to be used in this study is the stable low mean wind speed case. The requirement is for a straightforward modification to standard Gaussian plume models, or to their application, which will allow existing techniques to be used as far as possible. The following options are therefore suggested.

(a) U_{min} approach (Sharan *et al,* 1995) – requires an estimate of the proportion of time for which $u < u_{min}$.

(b) Use of u_* (Venkatram, 1982) – see Table 2.4.1 of Lines and Deaves (1996) and the discussion in Section 2.2; set lower limit of (say) 0.05–0.06 for u_*.

(c) Zero wind model (Cagnetti and Ferrera, 1982) – needs similar information to approach (a).

(d) Set $\sigma_\theta u$ = constant (0.5–0.8) (Jones, 1997) – use this for u below value at which σ_θ matches to standard plume parameters.

(e) Set lower limit on velocity (eg $u = 0.5$ m s^{-1}) – similar to (a), but adjust frequency distribution rather than undertaking separate calculation for very low wind speeds; can perhaps use minimum u_* arguments.

3 Importance of low wind speeds for passive dispersion

3.1 Introduction

The main objective of this report is to consider the importance of low wind speeds in the modelling of the dispersion of radioactive releases and other passive pollutants. These types of release tend to be either passive or buoyant, and may be from a stack or from within a building wake. Releases may be of relatively short duration, such as in an accident, or may involve routine emissions continuing throughout the year.

The significance of low wind speeds for each of these types of release will be considered, and various alternative methodologies will be evaluated.

In order to ensure that the discussion remains focused on the types of release of most interest, the following set of typical conditions has been agreed.

(a) release height:
- 20 m (eg a short stack),
- 60 m (eg top of a reactor building),
- fully entrained in the wake of a 60 m cubical building,

(b) momentum: negligible,

(c) buoyancy:
- zero buoyancy,
- positively buoyant (buoyancy flux $F = 1.81$),

(d) duration:
- continuous (long-term or annual average calculations),
- short duration (eg 30 minute),

(e) size: any possible release rate (Bq s^{-1}).

It is emphasised that it is not within the scope of this project to consider all possible combinations of the above parameters with every possible type of model, but rather to try to draw some general conclusions that would be applicable to the range of conditions summarised above.

3.2 Use of wind data

When undertaking a safety report or risk assessment, the approach that has traditionally been adopted is to consider a number of representative weather categories, and to assess the dispersion of the release in each case. In safety reports, the principal requirement is generally to predict the consequences of potential accidents in typical or worst case weather conditions, and so the frequency of such conditions is of secondary relevance. However, when undertaking a full quantified risk assessment, or when predicting long-term average concentrations from routine or long duration releases, it is obviously important that the likelihood of the various atmospheric conditions is taken fully into account. In these sorts of assessment, the frequency of each representative weather category may be obtained from long-term average meteorological data. Varying degrees of sophistication can be used for the categorisation, and it is important that the choice of representative categories is suitable for the application being considered.

To illustrate the importance of the choice of representative weather categories, data has been used from a site where it is known that the frequency of low wind speeds is above average (ie Herstmonceux).

3.2.1 Simple NRPB-R91 approach

Figure 11 in NRPB-R91 suggests that low wind speed areas of the UK, such as Herstmonceux, can be modelled using the representative weather categories (the 50% D case) given in Table 3.1.

TABLE 3.1 Example of representative weather categories from NRPB-R91

Pasquill stability	Wind speed ($m\ s^{-1}$)	Percentage frequency
A	1	1
B	2	9
C	5	21
D	5	50
E	3	8
F	2	10
G	1	2

This approach was used in NRPB-R91 to obtain annual average concentrations for a unit release (see Figure 34 in that report). However, although this approach does include some low wind speed conditions (in A, B, F, G), it assumes a single wind speed for each Pasquill stability. This may lead to misleading results if any of the categories 'conceals' a significant frequency of low wind speeds. For example, F1 and D1 are probably both fairly common at a low wind speed site. (Note that, hereafter, notation such as D1 will be used to refer to $1\ m\ s^{-1}$ wind speed in D stability conditions, for example.)

It should also be noted that the precise location of Herstmonceux (close to the south coast of England), on Figure 11 in NRPB-R91, would suggest that it should correspond to the 65% D weather conditions. However, this appears to contradict the actual meteorological data for Herstmonceux (see below), emphasising the fact that Figure 11 in NRPB-R91 needs to be applied with caution as it may not lead to a satisfactory choice of representative weather categories.

3.2.2 Standard meteorological data

Table 3.2 summarises the percentage frequency of the various combinations of stability and frequency based on standard hourly meteorological data for Herstmonceux over the 10-year period 1981–1990.

TABLE 3.2 Representative weather categories based on Meteorological Office data

	Wind speed						
Pasquill stability	*Calm* <0.5 m s^{-1}	*1–3 kts* 1.0 m s^{-1}	*4–6 kts* 2.6 m s^{-1}	*7–10 kts* 4.4 m s^{-1}	*11–16 kts* 6.9 m s^{-1}	*17–98 kts* >8.8 m s^{-1}	Total
A	–	0.041	–	–	–	–	0.041
A/B	0.088	0.978	0.103	–	–	–	1.169
B	0.717	3.588	1.273	0.240	–	–	5.818
B/C	–	–	0.833	2.781	–	–	3.614
C	0.261	1.464	5.515	6.544	0.225	0.051	14.059
C/D	–	–	–	0.743	1.21	–	1.953
D	1.237	4.833	4.874	10.702	18.498	11.240	51.385
E	–	–	2.920	1.863	–	–	4.783
F/G	3.272	11.996	1.911	–	–	–	17.179
Total	5.575	22.901	17.428	22.873	19.932	11.291	100.00

The table implies 29 representative weather categories, many of which involve wind speeds which are significantly less than the typical values used in NRPB-R91. It is noted that, for the purposes of simple dispersion modelling, the frequencies associated with categories A/B, B/C, C/D and F/G are modelled as A, B, C and F, respectively, resulting in 24 distinct weather conditions that need to be assessed.

However, this approach still leads to problems in that it is not clear how the frequency associated with calms (5.575%) should be treated. Some authors have suggested that it should be modelled as a low wind speed (eg 0.5 m s^{-1}), distributed around all wind directions.

3.2.3 Synthesis of data using Weibull distribution

The basic meteorological data for Herstmonceux shows some significant frequencies associated with low wind speeds and calms, and it may therefore not be appropriate to assume a single representative wind speed for the low wind speed categories (ie the calm and 1–3 knot categories). An alternative approach would be to assume that the frequency distribution of wind speeds in a particular stability category follows a Weibull distribution, and hence it would be possible to derive a more refined set of categories at low wind speeds.

For the Herstmonceux site, this sort of refinement is probably most important for the stable F/G category, which could, for example, be divided into 0.25, 0.5, 0.75, 1.0, 1.5, 2.0 and 2.6 m s^{-1} representative wind speed categories. These conditions could either all be analysed with a standard dispersion model (eg NRPB-R91) or alternatively, the low wind speed categories could be analysed using a more suitable low wind speed dispersion model (see Section 2 for a review of such models).

In some cases, the Weibull distribution may be considered a too sophisticated approach, and its use may not be justifiable owing to the lack of suitable data. In such cases, it may be

preferable to assume that a linear relation exists at low wind speeds, so that the cumulative frequency of wind speeds < U is proportional to U (at low wind speeds).

It is emphasised that, before attempting to fit any kind of distribution to any low wind speed data, it is necessary to consider the instrumentation that was used to collect the data. For example, if a standard Munro anemometer was used to collect the data, then it is likely that some very rough approximations will need to be made when fitting a Weibull distribution, as the low wind speed data are bound to be very uncertain because of the inertia and finite start-up speed of the anemometers. Data from light weight cup or, ideally, sonic anemometers should be used to derive the best possible frequency distribution of wind speeds, and this distribution should be used as the basis for selecting appropriate representative wind speeds, as discussed by Deaves and Lines (1997).

3.2.4 Other forms of meteorological data

The preceding discussion has concentrated on the use of statistical meteorological data, which involves average frequencies for particular types of condition. However, the use of sequential meteorological data is becoming more common in recent dispersion models (such as ADMS). Sequential data have some advantages, but great care must be taken if they are to be used in risk assessment applications, as it is important that worst case conditions are incorporated, even if their frequency is very low. For the purposes of most safety cases, where a simple assessment of typical and worst case conditions is required, it is often preferable to use statistical data.

3.3 Effects of weather categorisation on dispersion calculations

The preceding sections have discussed various alternative schemes that may be used to include low wind speeds within the representative weather categories required for long-term average or risk assessment type applications. In order to demonstrate the relative importance of some of the issues considered, it is necessary to consider some simple examples.

Figure 3.1 shows the annual average ground-level concentration for a unit release (1 Bq s^{-1}) from a 20 m high stack, based on the weather categories and frequencies quoted in NRPB-R91 for a 50% D location (see Table 3.1). The uppermost line on the figure is the total concentration, and corresponds closely with Figure 34 in NRPB-R91. The other lines on the graph show the contributions from each of the seven representative weather categories. All concentrations have been calculated using the standard methods and data described in NRPB-R91 (although it is noted that the G stability category has been modelled using the same plume spread parameters as for F stability). At distances of up to 150 m, the B2 conditions give the largest contribution, as the unstable mixing causes the plume to spread rapidly down to ground level. From 150 to 1500 m, the D5 category dominates, largely due to the high frequency of such conditions (50%). It is only at distances beyond 1500 m that the low wind speed stable conditions (F2) become most important.

The importance of the D5 results is that they imply that, in order to improve the assessment of long-term average concentrations in the near to medium field, it is probable that it would be necessary to represent the D stability conditions with a range of wind speeds, and not simply use a typical value of 5 m s^{-1}. Similarly, in the medium to far field, it may be necessary to give more detailed consideration to the low wind speed stable conditions. It may also be concluded that there is probably little point in giving a great deal of consideration to low wind speed unstable conditions (eg A1) as these do not appear to be significant.

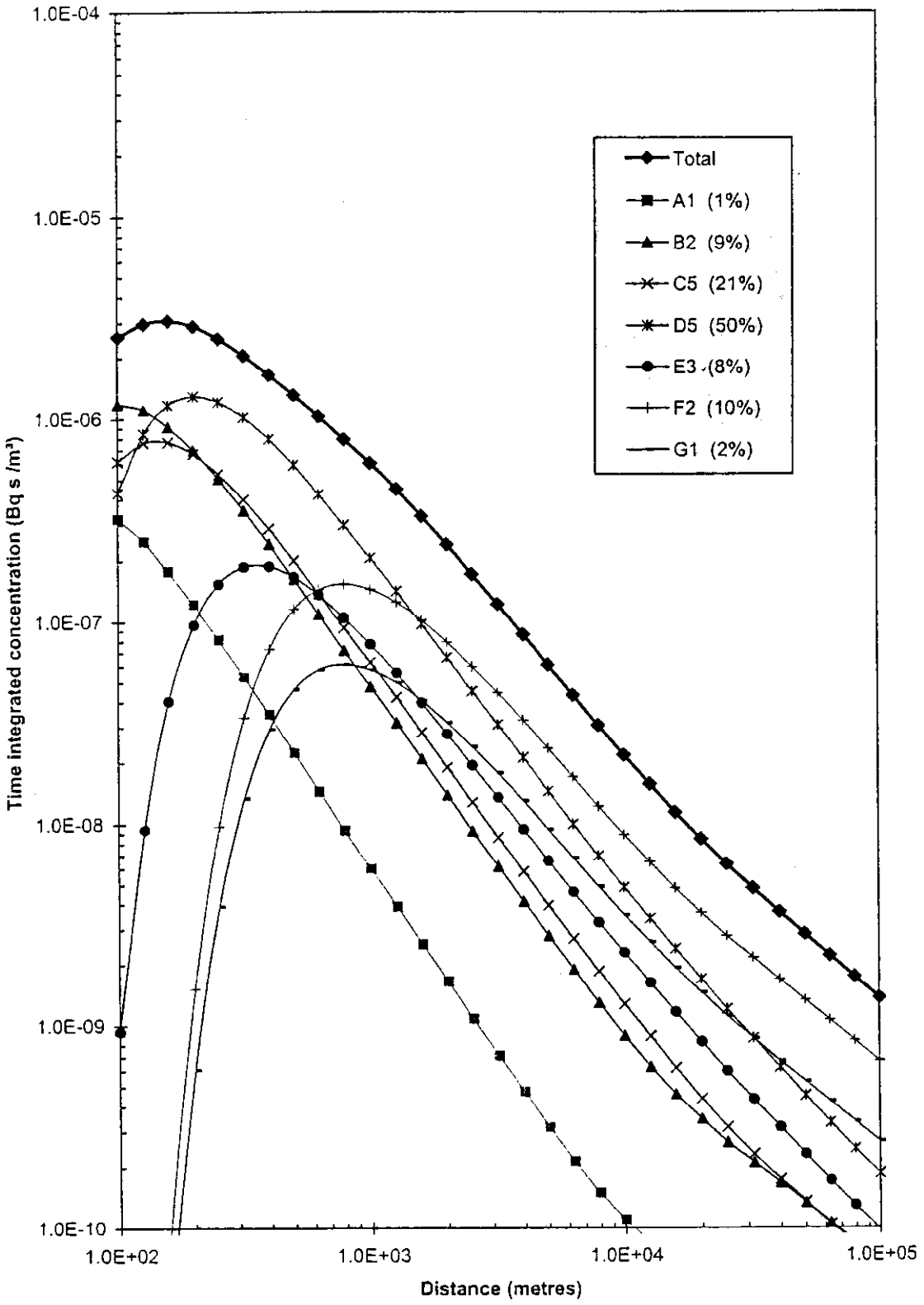

FIGURE 3.1 Annual average ground-level concentrations for a unit release from a 20 m stack, showing the contribution from various weather categories; weather categories and frequencies from NRPB-R91

Figure 3.2 is very similar to Figure 3.1, except that the frequencies used for each of the six representative weather categories have been calculated on the basis of actual standard hourly meteorological data for Herstmonceux over the 10-year period from 1981 to 1990. The overall total concentration in Figure 3.2 is within 13% of that predicted in Figure 3.1 at all distances from 100 m to 100 km. This indicates that, if one accepts the limitations and restrictions imposed by a small number of weather categories (see below), then the simple NRPB-R91 approach is quite adequate and is not improved significantly by using site-specific data.

Although Figures 3.1 and 3.2 agree very closely, they tend to imply that refining the choice of representative weather categories could lead to significantly different results. Therefore, the same situation has also been modelled using all 24 representative weather categories shown in Table 3.2. Calm conditions were arbitrarily modelled as having a wind speed of 0.5 m s^{-1}, but it is noted that this first approximation may not be ideal and is therefore discussed further in Section 3.4. Figure 3.3 shows the results of this analysis, together with the overall total results from Figures 3.1 and 3.2. It is also interesting to calculate the results based on assuming weather categories and frequencies based on the 65% D distribution from Figure 11 of NRPB-R91, which is the assumption that one might make if no meteorological data were available, ie Figure 3.3 shows the results of four types of analysis:

(a) using the seven categories and frequencies from Figure 11 of NRPB-R91 (50%D),
(b) using the seven categories and frequencies from Figure 11 of NRPB-R91 (65%D),
(c) standard six categories but frequencies from real Herstmonceux data,
(d) using 24 representative categories with real Herstmonceux data.

The clear conclusion from Figure 3.3 is that, by including the full set of representative weather categories, the annual average concentrations are predicted to be about a factor of two higher than those predicted using the standard NRPB-R91 approach. The increase is largely due to the inclusion of low wind speed neutral conditions (D0.5, D1.0, D2.6) for distances up to 1500 m, and at greater distances the increase is due to the inclusion of low wind speed stable conditions (F0.5 and F1). It should be noted that Herstmonceux is a low wind speed area, and so the importance of these conditions is much greater at this location than at many other sites within the UK.

It is also noted that there is relatively little difference in the results corresponding to the 50% and 65% D contours, implying that, if one is using the standard NRPB-R91 approach, with its implicitly coarse weather categorisation scheme, then the effect of site location in the UK is relatively unimportant. A more refined set of weather categories is required in order to demonstrate that there may be significant differences between low and high wind speed areas of the UK.

3.3.1 Effect of stack height

The example calculations described above are for an isolated 20 m high stack. However, all the general conclusions described above would still be appropriate for any stack height in the range 0 to 60 m, except for the fact that the distances at which the various weather categories would dominate the results would alter. For stacks higher than 20 m, unstable conditions would remain important out to larger distances, and stable conditions would only become significant at distances of several kilometres. Conversely, with shorter stacks (or ground-level releases), the unstable conditions will probably never be important, and the stable conditions may dominate the results even close to the source.

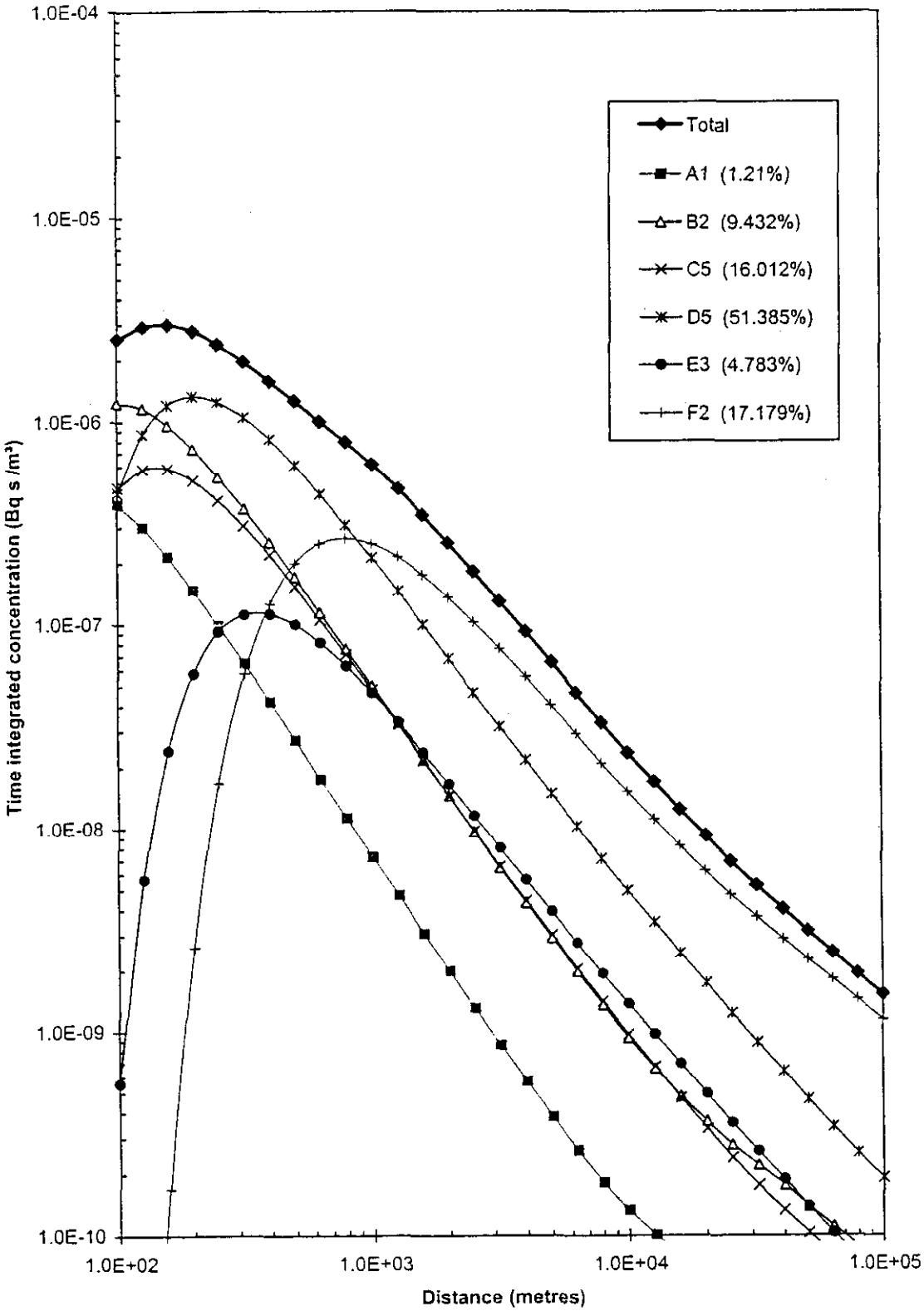

FIGURE 3.2 Annual average ground-level concentrations for a unit release from a 20 m stack, showing the contribution from various weather categories; weather categories from NRPB-R91 but frequencies from actual Herstmonceux data

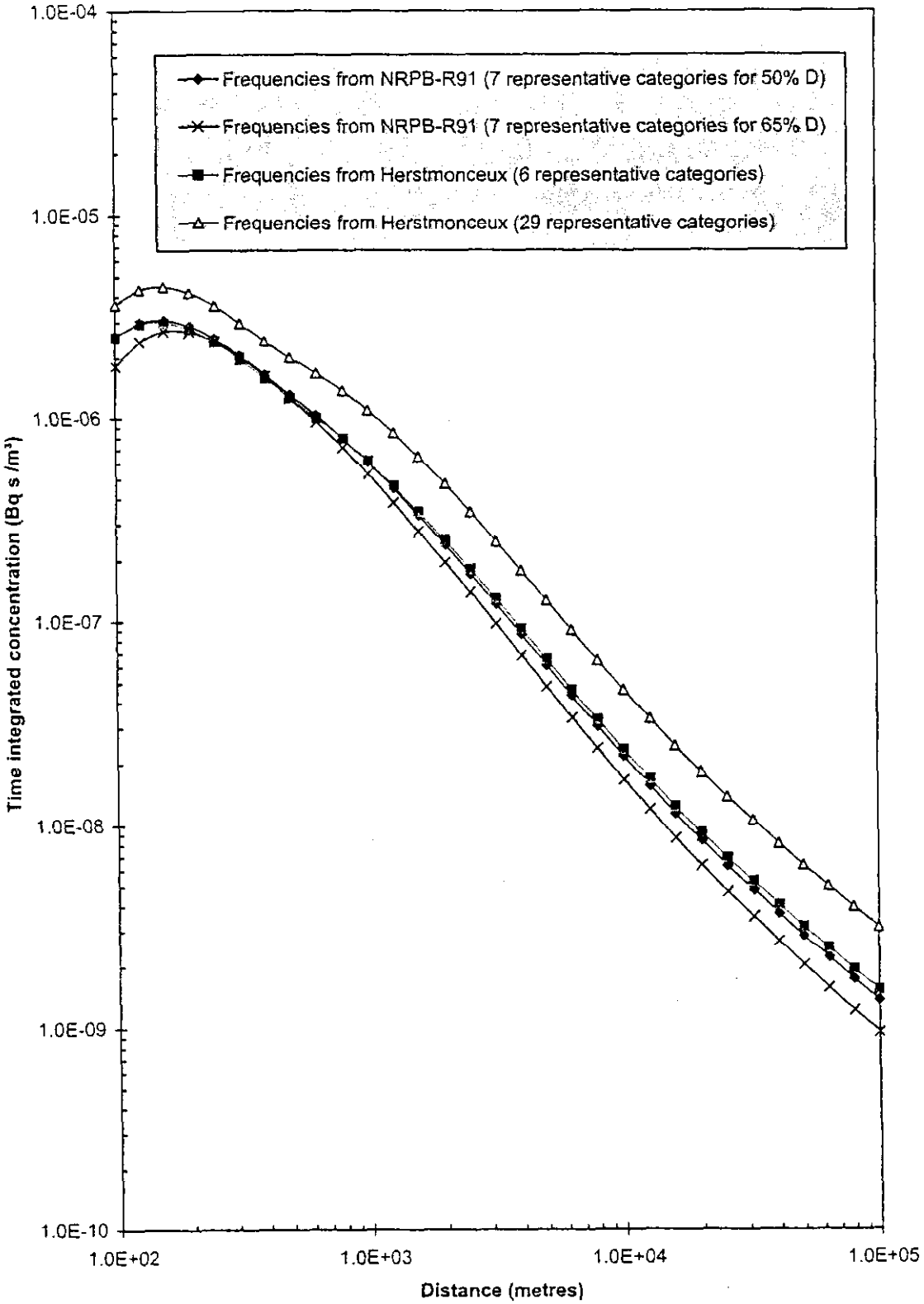

FIGURE 3.3 Annual average ground-level concentrations for a unit release from a 20 m stack, showing the effect of the choice of representative weather categories

The effect of stack height is illustrated quite clearly in Figures 13–19 and Figures 27–40 of NRPB-R91. The general conclusion that may be reached is that, in terms of annual average concentrations or risk assessment type applications, low wind speeds will be more significant for short stacks than for tall stacks. This will be illustrated further in Section 3.5.

3.3.2 Effect of buoyancy

The example calculations described above all relate to passive releases. The effect of source buoyancy (for example, releases at greater than ambient temperature) is principally to increase the effective stack height, the effect of which has been discussed above. It should be noted, however, that the degree of plume rise is generally dependent on the wind speed. For example, simple plume rise formulae for stable conditions tend to predict a plume rise which is inversely proportional to the cube root of the wind speed. Therefore, at lower wind speeds, the degree of plume rise increases, leading to a greater effective stack height and, consequently, to lower ground-level concentrations. This implies that any predicted increase in ground-level concentration due to the inclusion of low wind speed categories may be compensated for by a reduction in concentration due to increased plume rise. In practice, the relative importance of these two effects will be dependent on the precise situation, and it is therefore difficult to draw any more general conclusions.

For example, halving the wind speed in stable conditions increases the plume rise by 26%. Therefore, close to the source the increased plume rise at low wind speeds will generally lead to reduced concentrations, but at greater distances the concentrations become dependent on the mixing layer depth and so the low wind speed case would tend to lead to greater concentrations.

Hanna and Paine (1989) quote Briggs' formulae for plume rise in stable conditions as

$$\Delta h = 2.6\left(\frac{F}{us}\right)^{1/3} \quad \text{for bent-over plumes in stable conditions}$$

$$\Delta h = 4F^{1/4}s^{-3/8} \quad \text{for calm stable conditions}$$

where $$F = w_s R_s^2\left(\frac{g}{T_p}\right)\left(T_p - T_a\right) \qquad s = \frac{g}{T}\frac{\mathrm{d}q}{\mathrm{d}z}$$

and w_s is the initial plume vertical speed, R_s is the initial plume radius, T_p is the initial plume temperature and T_a is the ambient temperature. For example, taking some typical values for a vent stack as w_s = 5 m s^{-1}, R_s = 0.5 m, T_p = 338 K, T_a = 288 K, and dθ/dz = 1 K m^{-1} leads to a plume buoyancy flux F = 1.81 and s = 0.034, and hence the dispersion profiles as shown in Figure 3.4. The peak ground-level concentrations are compared in Table 3.3.

TABLE 3.3 Effect of plume rise at low wind speeds

Wind speed (m s^{-1})	Plume rise Δh (m)		Maximum ground-level concentration for a 30 minute unit release from a 20 m stack in F stability
	Bent-over	Calm	
0	n/a	16.49	2.26 10^{-5}*
0.5	12.32	n/a	3.10 10^{-5}
1	9.78	n/a	2.61 10^{-5}
2	7.76	n/a	2.14 10^{-5}
3	6.78	n/a	1.84 10^{-5}

*Calculated using an effective wind speed of 0.5 m s^{-1}.

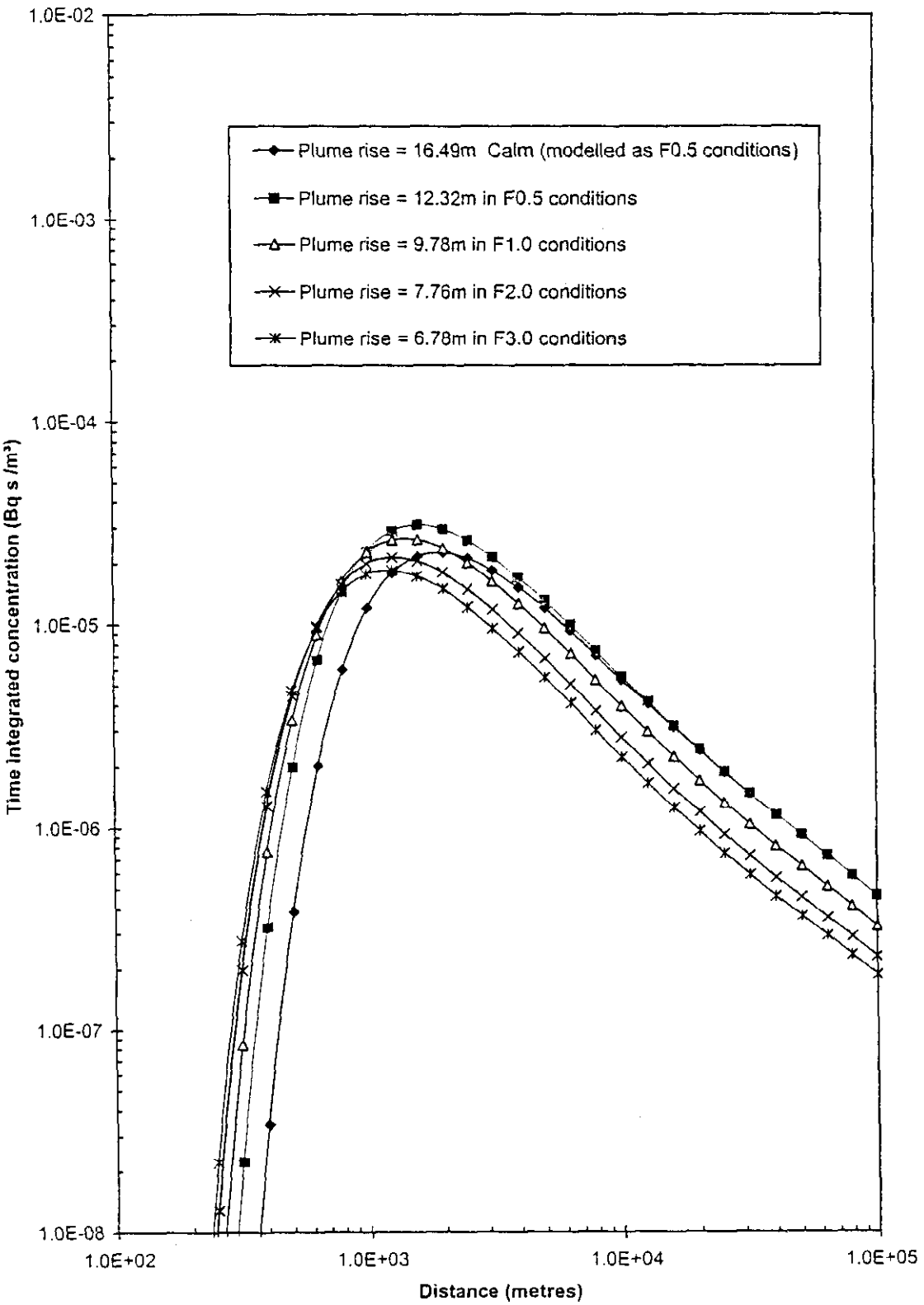

FIGURE 3.4 On-axis ground-level time-integrated concentrations as a function of wind speed for a 30 minute release from a 20 m stack in category F conditions with various degrees of plume rise depending on wind speed

The table shows that, reducing the wind speed from 3 m s^{-1} to 0.5 m s^{-1} only leads to a 68% increase in the maximum ground-level concentration, indicating that the increased plume rise at low wind speeds has a significant mitigating effect. The increase in concentration at low wind speed does, however, increase in the far field, to a factor of around 2.5. Clearly, for a very buoyant plume, or for a shorter stack, it is quite possible that there would be reduced concentrations at low wind speeds.

The plume rise predicted for the zero wind case, using the 'calm' formula, is only slightly larger than that predicted for the 0.5 m s^{-1} 'bent-over' plume, and therefore the peak ground-level concentration (assuming an effective wind speed of 0.5 m s^{-1}) is remarkably similar to that predicted for higher wind speeds. It is also interesting to note that the 'calm' and 'bent-over' plume rise equations give the same plume rise when $u = 0.275F^{1/4}s^{1/8}$, which would be $u = 0.21$ m s^{-1} in the example above.

In summary, the overall effect of buoyancy at low wind speeds can only be predicted by consideration of specific cases, but, in general, plume buoyancy will tend to reduce the significance of low wind speed conditions.

3.3.3 Effect of building wake entrainment

In the standard Fackrell model, the actual wake concentration is inversely proportional to the wind speed, and therefore, if this type of model is used, low wind speeds will clearly have a major significance. For example, a release of 1 Bq s^{-1} in F1 conditions would lead to exactly double the wake concentration predicted for F2 conditions. If a virtual source type model is used to predict the subsequent downwind dispersion, then the difference between the F1 and F2 results would gradually reduce towards that predicted for the 'no building' case.

The effect of using a conventional wake model is illustrated in Figure 3.5 for a unit release in F stability into the wake of a 60 × 60 × 60 m building. The wake is modelled using Fackrell's model, leading into a standard virtual source model at larger distances.

It should be noted that conventional wake models are likely to break down at low wind speeds because of convective motions becoming dominant. This is likely to be particularly relevant when the buildings themselves are at above ambient temperature, as may well be the case at power stations or many other industrial sites.

3.3.4 Effect of averaging time or release duration

The overall cross-wind spread of a plume depends on both the averaging time and the microscale turbulence. Long averaging times (or release durations) lead to greater plume meander and thus lower average concentrations. Moore has characterised this by

$$\sigma_y^2 = (0.065x)^2\left(\frac{7}{u}\right)T + \sigma_{yt}^2$$

where the first term represents the plume meander and the second term is due to atmospheric turbulence. Hence, if the averaging time T (hours) is significant, then reducing the wind speed by a factor of two, for example, leads to less than a factor of two increase in the predicted concentration using a Gaussian plume model, as the cross-wind spread σ_y is increased. In fact, as T/u becomes large, the concentration predicted by the standard Gaussian plume model varies as $u^{-1/2}$ rather than as u^{-1}. This means that the $u \rightarrow 0$ singularity in the standard Gaussian plume model is somewhat 'softer' than might otherwise be thought.

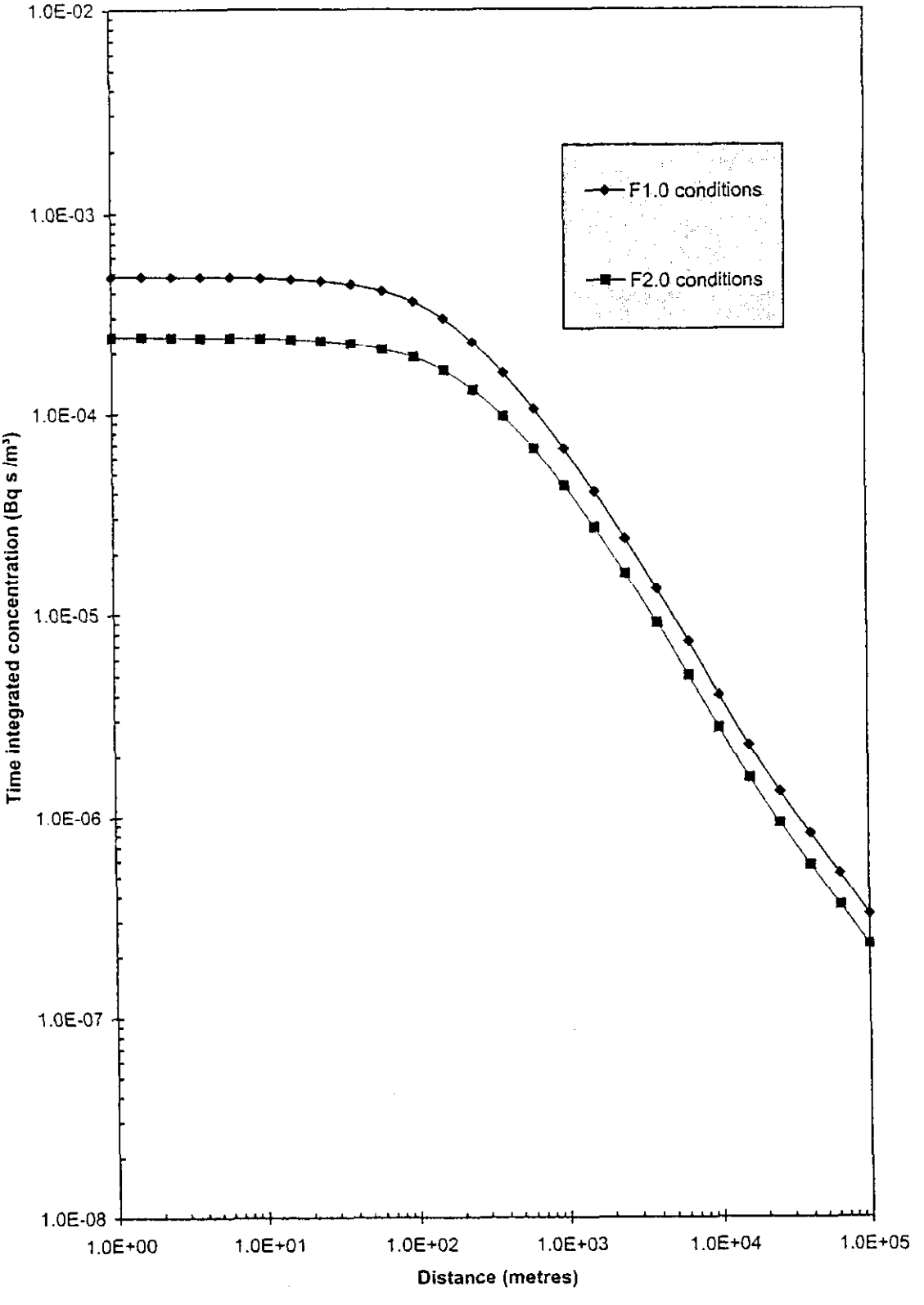

FIGURE 3.5 On-axis ground-level time-integrated concentrations as a function of wind speed for a 30 minute release from within the wake of a 60 m cubiodal building in category F conditions

Briggs' formula for elevated small releases in open country states that

$$\sigma_y = \frac{ax}{(1+0.0001x)^{0.5}}$$

where a is a constant depending on the stability category. Assuming that x is small, it is possible to determine the value of u/T at which the 'meander' term begins to dominate, ie $u/T = 7(0.065/a)^2$, as shown in Table 3.4.

TABLE 3.4 Determination of wind speed at which plume meander becomes dominant

Pasquill stability category	Value of Briggs' parameter 'a'	Value of u/T below which 'meander' term begins to dominate
A	0.22	0.6
B	0.16	1.2
C	0.11	2.4
D	0.08	4.6
E	0.06	8.2
F	0.04	18.5

For example, in stable F conditions the 'meander' term begins to dominate when $u/T < 18.5$, for u in m s^{-1} and T in hours. This means that, even for a 0.5 hour release in stable conditions, the 'meander' term will dominate for all wind speeds less than 9.25 m s^{-1}, and therefore that the concentrations predicted by a Gaussian plume model in stable conditions will almost certainly vary as $u^{-1/2}$, and not as u^{-1}. This is illustrated in Figures 3.6 and 3.7 which are discussed below.

Figure 3.6 shows the results of using the standard NRPB-R91 approach for these three cases. The F2 case is similar to Figure 18 in NRPB-R91. It is noted that the concentrations predicted for the F0.5 case are only about a factor of two above those predicted for the F2 case (and not a factor of four as one might expect). This is simply because the value of σ_y depends on the averaging time. This is illustrated in Figure 3.7 which shows the same case, but with a very short averaging time. The F0.5 results are now a factor of four above those for F2. As discussed above, this appears to indicate that, provided the effects of the averaging time are incorporated, the difficulties associated with low wind speeds (ie infinite C as $u \rightarrow 0$) may not begin to be a significant problem until $u << 0.5$ m s^{-1}.

The general conclusion is that, as most releases of interest will have release durations of 30 minutes or more, an averaging time correction should be applied when using a Gaussian plume model. At low wind speeds, particularly in stable conditions, this averaging time correction implies that concentrations will vary as $u^{-1/2}$, and not as u^{-1}, and so the difficulties as $u \rightarrow 0$ may not be so significant.

3.3.5 Persistence of wind speed

Low wind speeds are generally unlikely to persist for very long periods. It is therefore inappropriate to assume that concentrations at large distances in low wind speeds can be predicted by simply applying a Gaussian plume model, as the required plume travel time may be much greater than the persistence time for those conditions. For example, since stable conditions do not generally occur during the day, the maximum persistence time for any stable condition is approximately

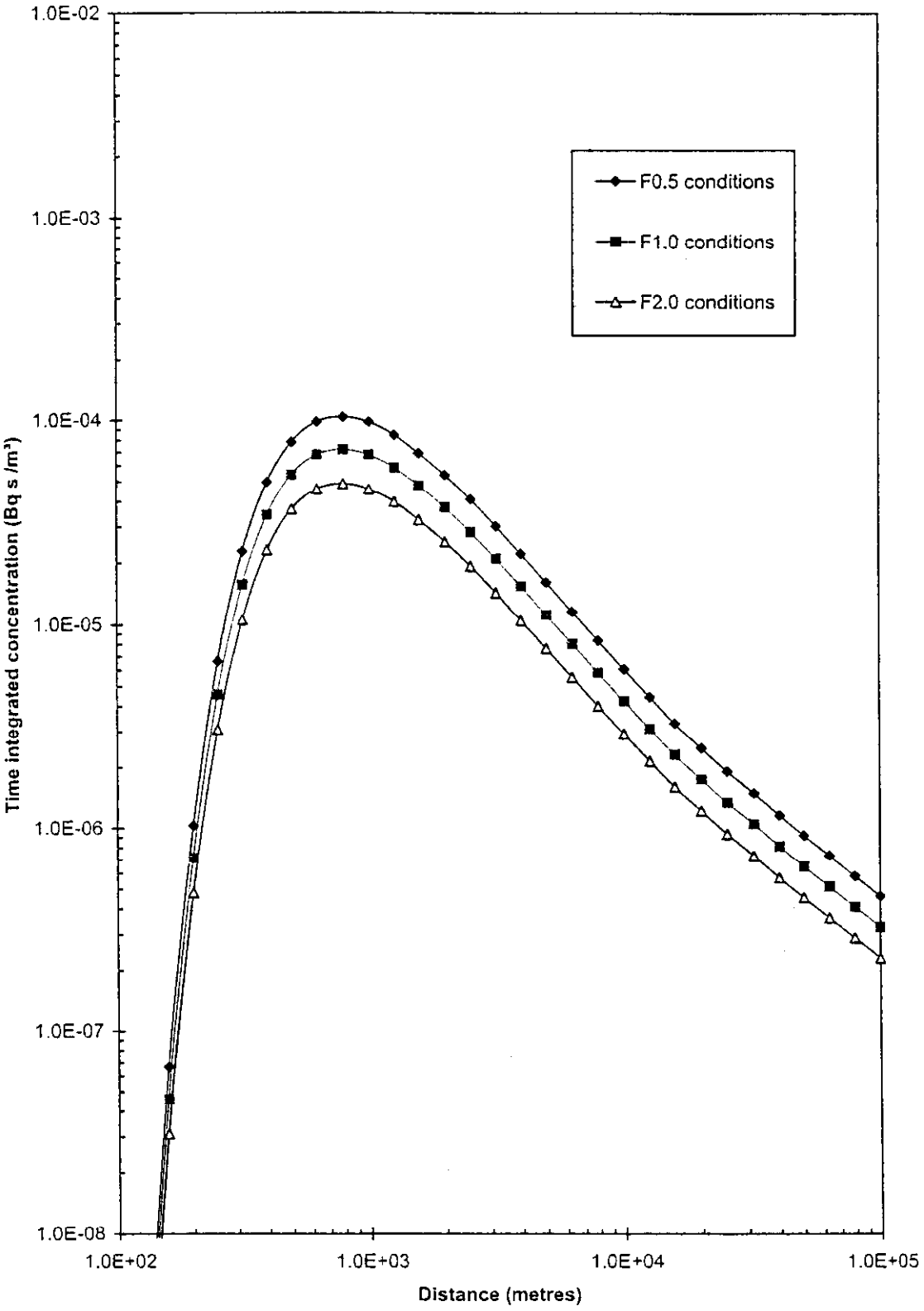

FIGURE 3.6 On-axis ground-level time-integrated concentrations as a function of wind speed for a 30 minute release from a 20 m stack in category F conditions

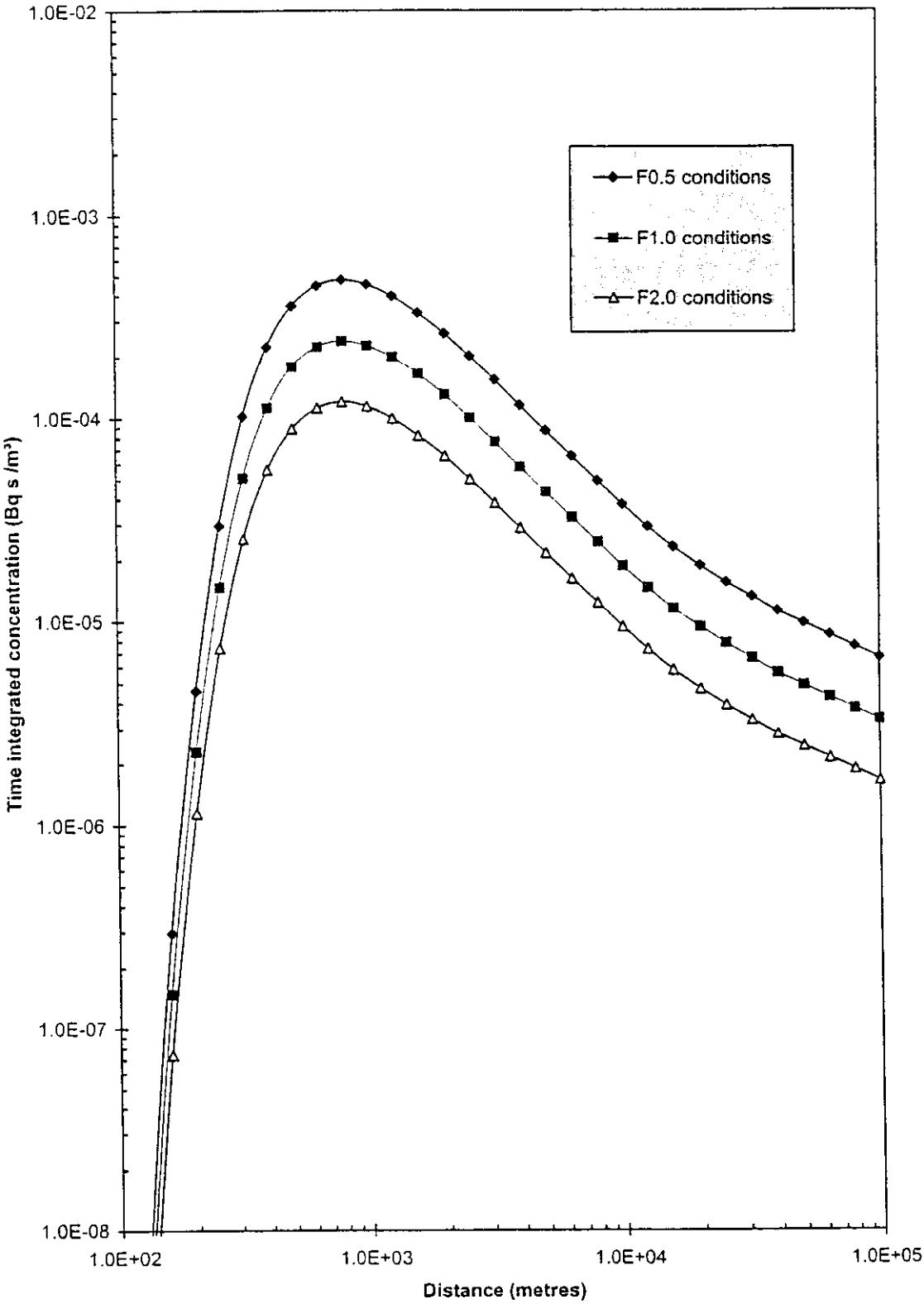

FIGURE 3.7 On-axis ground-level time-integrated concentrations as a function of wind speed for a very short duration release from a 20 m stack in category F conditions

17 hours (or about 7 hours in the summer). This 17-hour period would imply the following maximum distances at which a low wind speed stable condition should be applied (Table 3.5).

This table indicates that plumes may travel considerable distances, even at low wind speeds. However, examination of detailed meteorological data indicates that the typical persistence time of low wind speed conditions is generally much less than the 17-hour period assumed above. Although it may be appropriate to consider this type of worst case long persistence time in a safety case, it would not be appropriate when calculating long-term averages or when conducting a risk assessment.

TABLE 3.5 Maximum distances for low wind speed stable conditions

Wind speed ($m\ s^{-1}$)	Maximum applicable distance (based on 17 hour travel time) (km)
0.5	30.6
1	61.2
2	122.4
3	183.6

If the cumulative probability of a low wind speed persisting for a period t is given by $p(t)$, then the analysis presented by Lines and Deaves (1996) suggests that it is reasonable to assume a relationship of the form:

$$p(t)/p_0 = e^{-t/t_0} \qquad t < t_{max}$$
$$p(t)/p_0 = 0 \qquad t \geq t_{max}$$

where p_0 = probability of 10 minute wind speed < u, t_0 = persistence 'half-life' (minutes), and t_{max} = maximum persistence time (minutes).

It is unlikely that t_0 is an intrinsic property of any given site, but estimates for typical t_0 values have been obtained from the Camborne and Cardington datasets, as shown in Table 3.6.

TABLE 3.6 Persistence times (minutes) based on meteorological data

	Camborne		Cardington	
Wind speed u ($m\ s^{-1}$)	t_0	t_{max}	t_0	t_{max}
0.5	22	30	22	20
1.0	87	230	87	70
1.5	173	510	115	210
2.0	231	540	173	340
2.5	346	570	303	>600
3.0	361	>600	433	>600

These data suggests that, for wind speeds of less than 3 $m\ s^{-1}$ at these sites, a reasonably conservative rule of thumb for estimating t_0 is given by

$$t_0 = 2u$$

where t_0 is in hours and u is in $m\ s^{-1}$.

It should be noted that this is a reasonable fit for $u \geq 1.5$ m s^{-1}, but rather overpredicts t_0 for very low wind speeds. Applying this result would lead to the maximum plume travel distances shown in Table 3.7; distances in brackets are obtained by using t_0 = 22 min and 87 min directly from Table 3.6.

TABLE 3.7 Maximum distances for low wind speed conditions based on estimated values of t_0

Wind speed (m s^{-1})	t_0 (hours)	Maximum applicable distance (based on t_0 travel time)
0.5	1	1.8 km (660 m)
1	2	7.2 km (5.2 km)
2	4	28.8 km
3	6	64.8 km

These results show that, in contrast to Table 3.5, the low wind speed conditions such as 0.5 or 1.0 m s^{-1} are only applicable out to a few kilometres from the site. The implication is that, if one were interested in the annual average concentration (or risks) at any distance over 1.8 km, then it would be inappropriate to include the results of any dispersion modelling using wind speeds of 0.5 m s^{-1}. The frequency associated with any such low wind speed or calm conditions should be allocated to the next higher wind speed category (eg 1 m s^{-1}). A similar argument would apply at 7.2 km etc.

3.3.6 Upwind spread

At very low wind speeds, where the mean wind speed is comparable with the turbulence velocities, it is possible for significant concentrations to be observed upwind of the release. This effect cannot be predicted by standard continuous plume models, and so some alternative form of model would be required if such effects are likely to be important. The maximum upwind spread distance may be estimated as $x = \sigma_u t$, where σ_u is the turbulence velocity and t is the persistence time for such conditions (see above). Suitable values might be approximately $\sigma_u = 0.35$ m s^{-1} (at low wind speeds), and t = 1800 seconds (typically), implying a maximum upwind spread in low wind speeds of about 630 m.

These values are only very rough estimates, but they do appear to indicate that upwind spread is unlikely to be important at distances of more than a few hundred metres.

3.4 Simple methodologies for low wind speed dispersion

The question that now arises is whether it is appropriate to model the dispersion of releases in calm and low wind speed categories using the types of simple approach described above, or whether some alternative methodologies are required for low wind speeds. Section 2 provided a summary of various alternative simple models that could be applied when considering the dispersion of releases at low wind speeds. Each of these methodologies is evaluated below by attempting to apply the models to the sort of releases likely to be of interest. In general, the results are compared with those that would be obtained using the standard NRPB-R91 model.

Section 3.5 will consider a range of possible cases, based on the typical conditions identified in Section 3.1. However, in order to illustrate the predictions of the various types of model considered, the remainder of this section focuses on a 30 minute release from an isolated

20 m stack in F2, F1 and F0.5 conditions. The NRPB-R91 results for these base cases have already been presented in Figures 3.6 and 3.7, which were discussed in Section 3.3.

3.4.1 Sharan *et al* (1996)

This is based on the assumption that, for wind speeds less than some specified value U_{min}, the dispersion coefficients are modified such that:

$$\sigma = a\,x^{b} \qquad U \geq U_{min} \text{ (transport condition)}$$

$$\sigma = a'\,x^{b'} \qquad U < U_{min} \text{ (calm condition)}$$

where $a' = a(U_{min}/U)^b$ and $b' = b$.

Sharan *et al* do not make it clear whether this increased spread should apply to just σ_y and σ_x, or whether it should also apply to σ_z. Assuming that it does not apply to σ_z, then the centreline concentrations predicted by this approach are reduced by a factor of $(U_{min}/U)^b$, and the plume width is increased by a similar factor. This implies no change in the cross-wind integrated concentration as the wind speed decreases to zero. Furthermore, if b = 1 (as in Briggs' formulae for σ_y), then the centreline concentrations predicted as $U \rightarrow 0$ remain identical to those calculated for U_{min}, ie if U_{min} were chosen as 1 m s^{-1}, then the F0.5 result in Figure 3.7 would be identical to the F1 result. However, Sharan *et al* would predict a wider plume for the F0.5 case.

In summary, the Sharan *et al* approach would lead to similar annual average or risk assessment results to those from the simple Gaussian plume model. However, for the purposes of a worst case analysis in a safety case, this approach leads to a wider, but less concentrated plume than would be obtained by simply using a Gaussian plume model, although the difference would be reduced if an averaging time correction were used in the latter.

3.4.2 Venkatram (1982)

In order to apply Venkatram's methodology, it is necessary to estimate the values of the Monin-Obukhov length L and the friction velocity u_*. We shall consider a release in stable F conditions, where L = 17.497 m. For the purposes of the example, the value of u_* is assumed to depend linearly on the wind speed, ie

$$u = 2 \text{ m s}^{-1} \qquad u_* = 0.0958103 \text{ m s}^{-1}$$

$$u = 1 \text{ m s}^{-1} \qquad u_* = 0.0479052 \text{ m s}^{-1}$$

$$u = 0.5 \text{ m s}^{-1} \qquad u_* = 0.0239526 \text{ m s}^{-1}$$

The F2 condition has been modelled and the results are shown in Figure 3.8, which also shows the results that would be obtained using the standard NRPB-R91 approach, bearing in mind that, in a simple Gaussian plume model, the cross-wind integrated concentration is given by $C_0(2\pi)^{1/2}\sigma_y$, where C_0 is the centreline concentration.

Figure 3.8 shows that the results obtained using Venkatram's approach are not significantly different from those produced by the NRPB-R91 method, except in the far field where the NRPB-R91 results show the effect of plume trapping within the mixing layer. At lower wind speeds, Venkatram's approach still suffers from difficulties as $u_* \rightarrow 0$, and so it would still be necessary to specify some arbitrary lower limit on u_*, as discussed in Section 2.2. It is also noted that Venkatram's approach only applies to ground-level releases, and does not predict either plume spread or peak concentrations. It is therefore considered that Venkatram's approach is probably not worth further consideration.

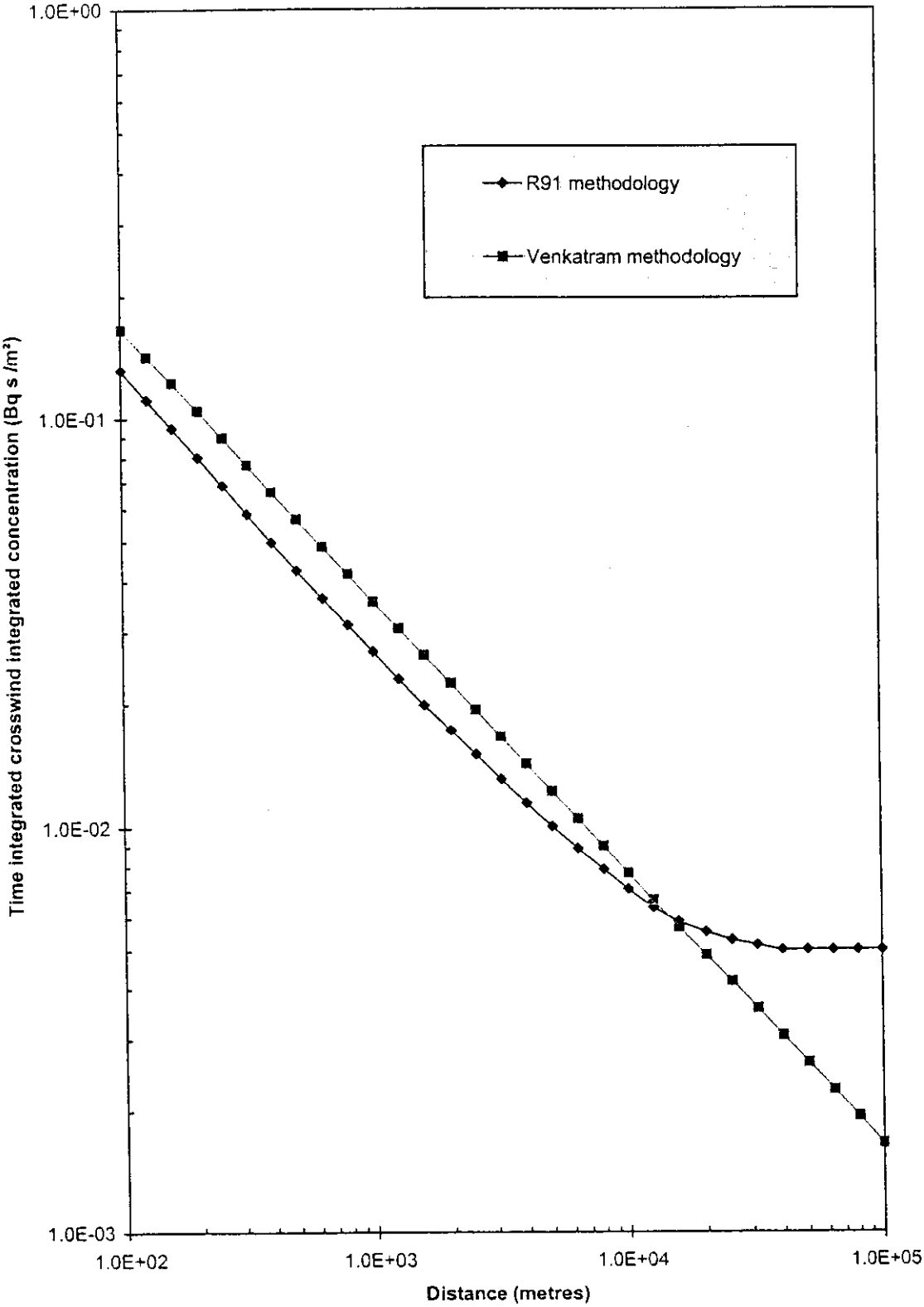

FIGURE 3.8 Cross-wind integrated concentrations for a 30 minute release at ground level in category F2 conditions

3.4.3 Cagnetti and Ferrara (1982)

The model proposed by Cagnetti and Ferrara for describing diffusion under zero wind stable conditions is

$$\chi = \frac{Q}{2\pi r^{3/2}\sqrt{u_d K_z}}$$

where, as in Cirillo and Poli (1992) $u_d = 0.5$ m s^{-1} and $K_z = 1$ m s^{-1}. The results of using this model, as compared to the NRPB-R91 approach for a 1-hour release in F0.5 conditions, are shown in Figure 3.9. As one would expect, the zero wind model predicts much lower concentrations than the *on-axis* concentrations from the standard Gaussian plume model. However, one would expect the cross-wind integrated concentrations to be more similar, as shown in Figure 3.10.

The small difference (a factor of 2.5 to 3) between the results in Figure 3.10 indicates that, for the purposes of risk assessment or long-term average concentration estimates, it does not matter very much which model is chosen. However, when assessing a release of short duration, the zero wind speed model may significantly underestimate the peak on-axis concentration. Therefore, in general, it would appear that there is little to be gained by using this type of zero wind speed model for the sorts of applications relevant to this project.

3.4.4 Hanna/Jones

Jones (1997) quotes Hanna's approach for low wind speeds as $\sigma_\theta = 0.5u^{-1}$, with σ_θ in radians. This implies that $\sigma_y = 0.5xu^{-1}$, which is quite different to the standard Gaussian plume model where $\sigma_y = ax$. However, it is essentially similar to the Sharan *et al* approach with $U_{min} = 0.5/a$.

The effect of using this approach for a release from a 20 m isolated stack in stable F conditions is shown in Figure 3.11. It is emphasised that Hanna's approach implies centreline concentrations which are independent of wind speed. Figure 3.11 also shows some results using the standard NRPB-R91 model. The results for F1 conditions (with no averaging time correction) are an order of magnitude higher than those predicted by Hanna. Conversely, the results for F2 conditions (with a 2-hour averaging time) correspond quite closely with those of Hanna.

One of the difficulties associated with Hanna's approach is that it is not clear at what threshold wind speed it should begin to apply. For example, if one chose 1 m s^{-1}, then Hanna's approach would result in a significant step change (a factor of about ten in F stability) in predicted concentrations in going from a standard model at 1.1 m s^{-1} to Hanna's model at 1.0 m s^{-1}. In order to avoid such a step change, the threshold wind speed would have to be about 10 m s^{-1} (in F stability).

In essence, Hanna's approach can be viewed as just an approximation of the averaging time approach, without having to specify the averaging time (T) or wind speed (u). However, although it may be suitable for some combinations of u and T, it is unlikely to be generally applicable for all possible combinations of u and T, and therefore it should only be used with caution.

3.4.5 Three-dimensional diffusion models

A number of authors have described analytic solutions to the three-dimensional diffusion equation, which could, in principle, be used to predict dispersion in very low wind speeds. One of the main advantages of such models is that they can evaluate upwind spread, which may be important in some special cases. However, it should be noted that the results of such three-dimensional models depend largely on the choice of eddy diffusivity parameters, and that the simple analytic solutions generally require that these diffusivities are constant. Lines and Deaves (1996) have illustrated how this type of model may be used.

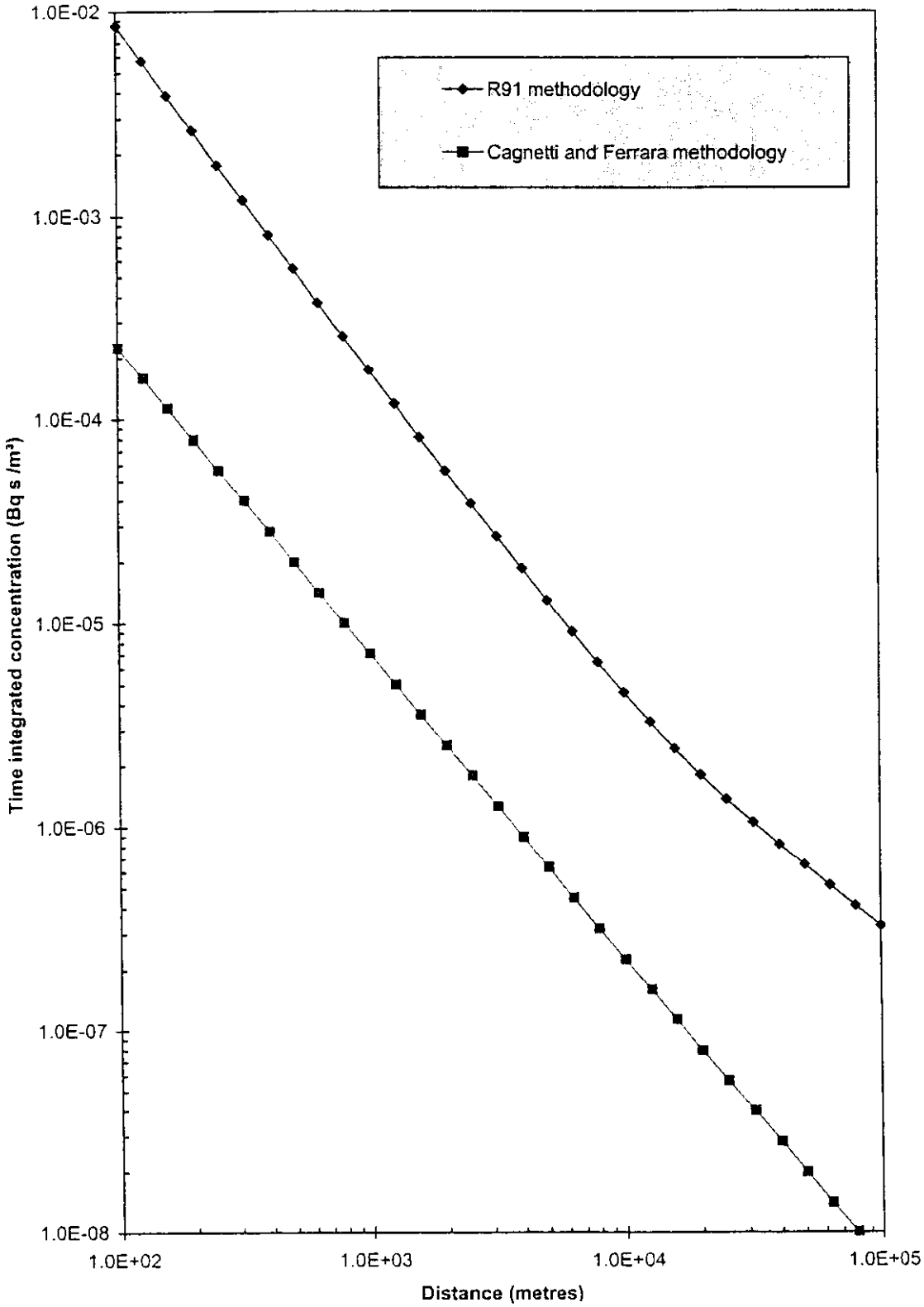

FIGURE 3.9 Results using Cagnetti and Ferrara compared with the standard NRPB-R91 approach for a 1 hour ground-level release in F0.5 conditions

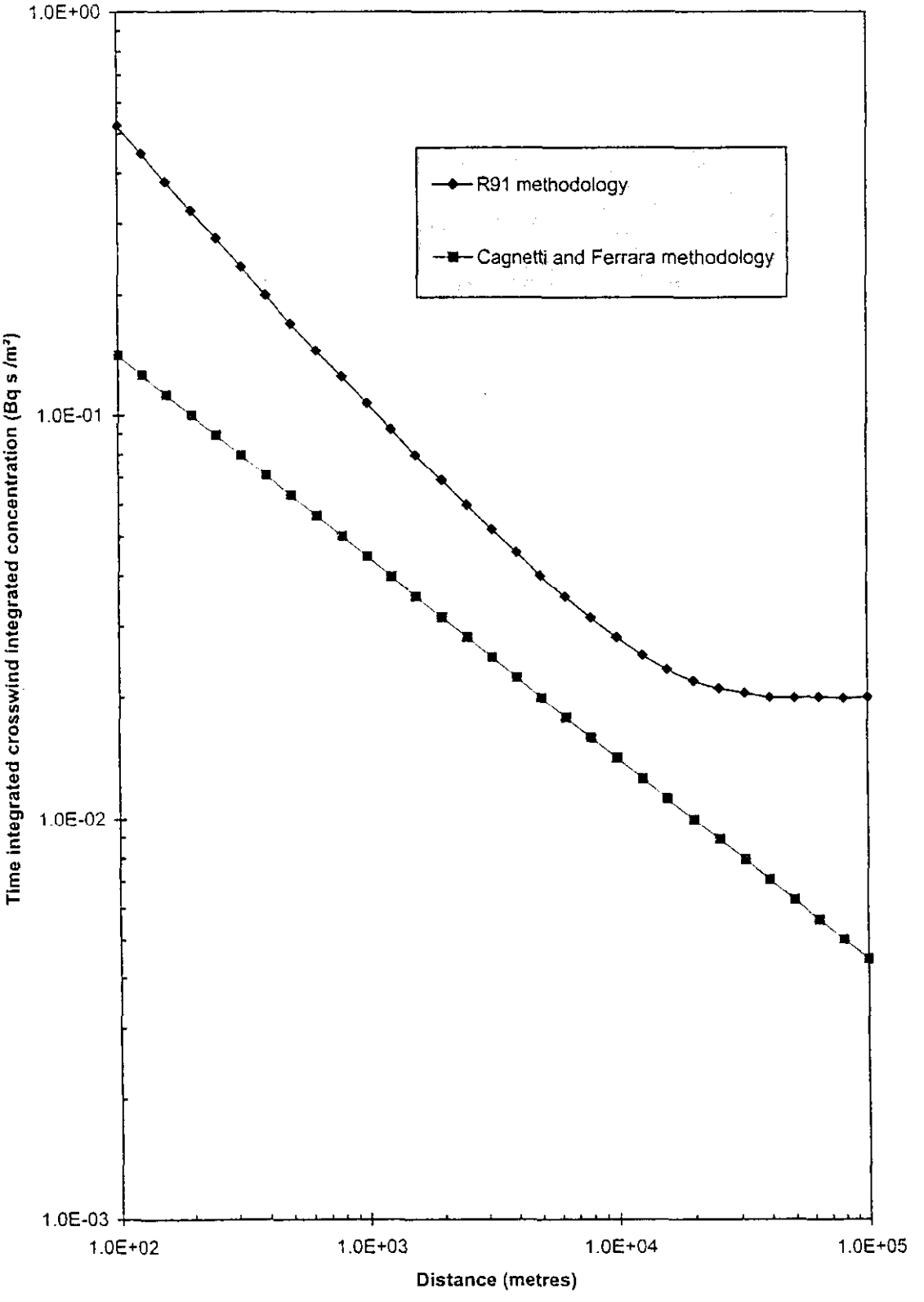

FIGURE 3.10 Cross-wind integrated concentrations for a 1 hour release at ground level in category F0.5 conditions

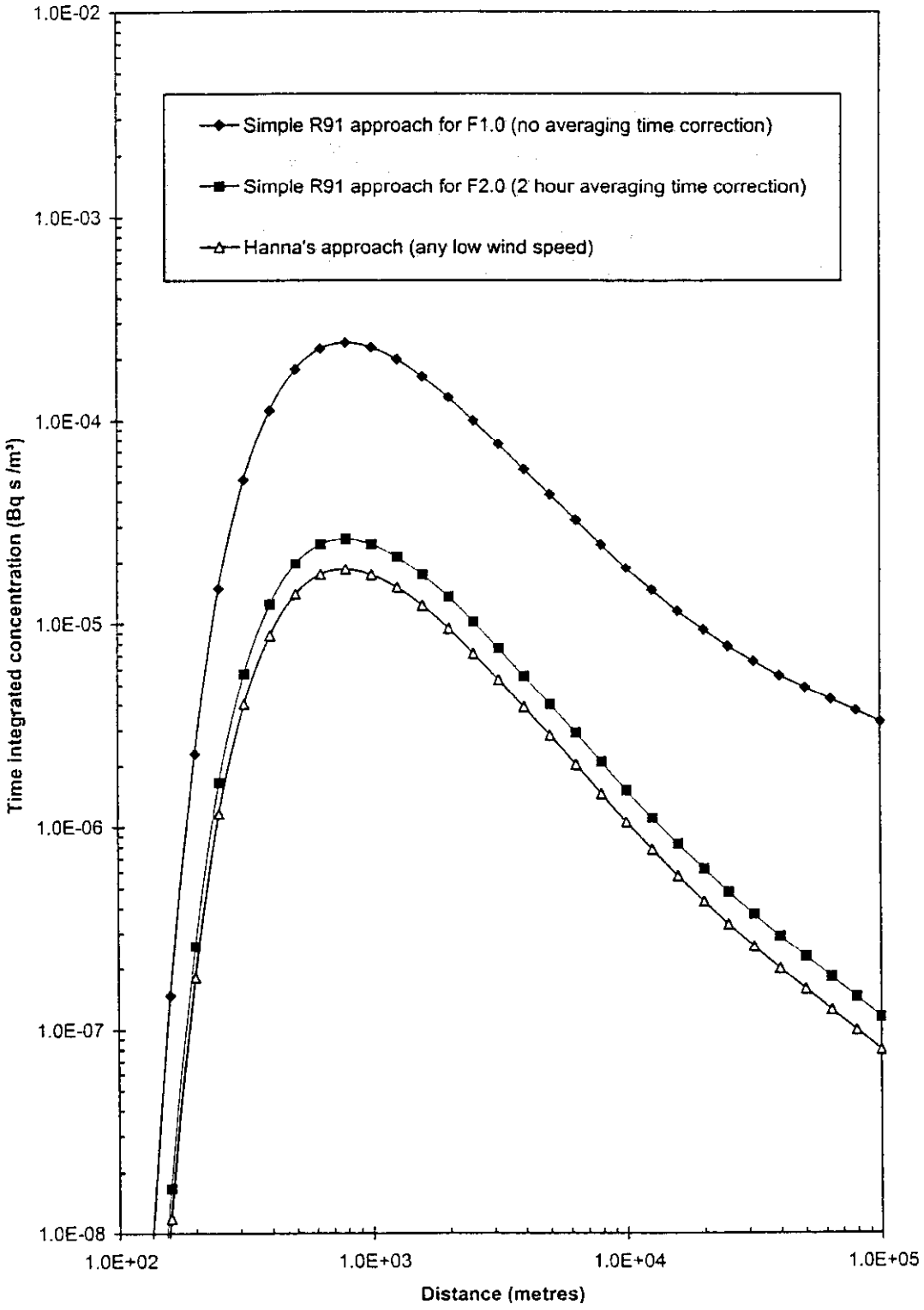

FIGURE 3.11 On-axis ground-level time-integrated concentrations using Hanna's approach for a unit release from a 20 m stack in category F conditions

3.4.6 Arbitrary lower limit on wind speed

This is the approach that was used in Section 3.2 above, and illustrated as the 24 category case in Figure 3.3. It has the following advantages.

(a) It is a well-understood approach, and therefore more likely to be accepted by regulatory authorities when used in safety cases or risk assessments.

(b) It does not involve a step change to a different sort of model. Such step changes are bound to lead to anomalies in the results that could be misleading.

(c) It is easy to apply to annual average or short duration situations.

However, it does suffer from the following disadvantages.

(a) The choice of the arbitrary lower limit is not immediately obvious, although 0.5 $m\,s^{-1}$ appears to be a reasonable estimate for most purposes.

(b) The use of wind speeds as low as 0.5 $m\,s^{-1}$ may not be appropriate when considering medium to long range dispersion in stable conditions, as these conditions are not likely to persist for more than a few hours.

It is emphasised that it is not unreasonable to specify a fairly low arbitrary wind speed limit, such as 0.5 $m\,s^{-1}$, because the averaging time correction will lead to increased values of σ_y at these low wind speeds, which is consistent with the predictions of many low wind speed models.

3.4.7 Summary

The common feature within most of the simple low wind speed dispersion models is that they modify the plume spread σ_y depending on the wind speed. Any such model which only changes σ_y will not change the predicted cross-wind integrated concentration, and therefore such modifications are generally not significant in terms of annual average or risk assessment type applications, as the dose is generally linearly dependent on the time-integrated concentration, and threshold effects are generally not important. In such applications, the most important factor is to ensure that a fully representative set of weather categories is used, as this may have a significant effect on the results.

However, if it is necessary to predict the dispersion of a release in a particular wind direction (eg to determine the maximum distance at which a particular concentration could be reached), then a consideration of low wind speed dispersion will be important. The ideal approach is to use long-term detailed meteorological data collected at the site of interest, but this is rarely practicable, and the required calculations would not be classed as 'simple'. Therefore, for practical purposes, the best current advice for a simple model is to modify the cross-wind spread parameter σ_y according to the wind speed. There are a number of ways in which this can be achieved, many of which are essentially similar, even though they may appear to be quite different. A number of these approaches have been considered above, and Figure 3.12 summarises some of the different approaches in terms of the dependence of σ_y on the wind speed. Having reviewed all of these approaches, it is considered that the most widely applicable simple approach, which is still consistent with the methodology for higher wind speeds, is as follows.

(a) Use refined weather categories, and not the typical wind speed values used in NRPB-R91.

(b) Model calms as 0.5 $m\,s^{-1}$.

(c) Use simple NRPB-R91 Gaussian plume dispersion methodology.

(d) At large distances, determine whether each particular weather category is likely to persist for the required length of time, and if not, then allocate the frequency to the next higher wind speed category.

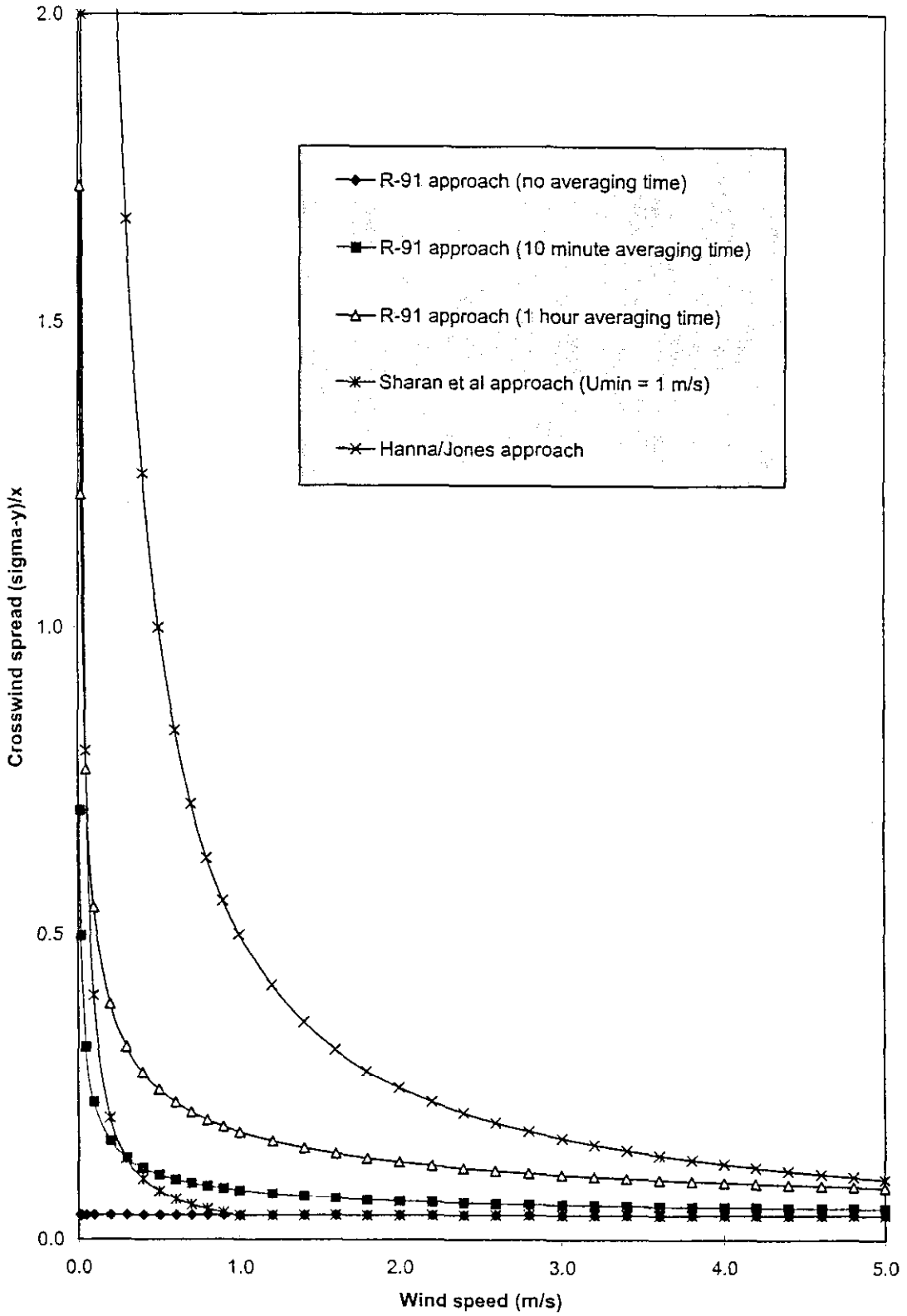

FIGURE 3.12 Comparison of various low wind speed approaches for σ_y (based on F stability conditions)

(e) If explicit consideration of upwind spreading is required (very rarely the case), then use some form of three-dimensional model for distances out to a few hundred metres.

(f) Ensure that averaging time effects are included.

It is emphasised that this approach is far from perfect, but it represents a significant improvement on the simple NRPB-R91 approach.

This approach can be applied to short duration releases and annual average calculations.

3.5 Effects of improved low wind speed modelling on dispersion results

This section summarises the effects of applying the methodology recommended in the summary at the end of Section 3.4 to some of the typical release situations identified in Section 3.1. The results are compared with those that would be obtained using the standard NRPB-R91 type approach, and the key differences are highlighted.

3.5.1 Annual average or risk assessment type applications

The most important improvements are:

(a) use a wider range of representative weather categories (ie 24 instead of 7),

(b) model calms as 0.5 m s^{-1} (the lowest non-zero wind speed category quoted in standard Meteorological Office data),

(c) include the effect of limited persistence of low wind speed conditions, eg

- 0 to 1800 m – use all 24 weather categories including 0.5 m s^{-1},
- 1800–7200 m – model the ≤ 0.5 m s^{-1} categories as 1.0 m s^{-1},
- > 7200 m – model the ≤ 1.0 m s^{-1} categories as 2.6 m s^{-1}.

(It should be noted that, in practice, it would be necessary to examine considerably more persistence data before setting the limiting distances noted above.)

The results of using this approach for an isolated 20 m stack, using Herstmonceux weather data, are shown in Figure 3.13. The results indicate approximately a factor of two increase in the annual average concentrations (or risks) at short to medium ranges due to the inclusion of low wind speeds.

Similar conclusions would be reached for shorter or taller stacks, or for releases in building wakes. However, the importance of the low wind speeds would be reduced if the release had significant positive buoyancy.

3.5.2 *Safety case or specific incident type applications*

When assessing a specific incident that has occurred, or when trying to predict the dispersion of a release in a particular wind direction, the results are more sensitive to the choice of methodology, as we are no longer just interested in the cross-wind integrated concentration. In particular, it may be necessary to identify the 'worst case' weather conditions, and to predict the length and width of a plume in such conditions. 'Worst case' conditions have, in the past, generally been taken as F2, but it appears that it may be more appropriate to consider some lower wind speeds, but with the following three provisos:

(a) low wind speeds should not be used to predict dispersion beyond the 'persistence distance',

(b) a suitable averaging time should be used, which may also be related to the travel time,

(c) a three-dimensional diffusion model may be more suitable for distances of up to a few hundred metres in very low wind speeds.

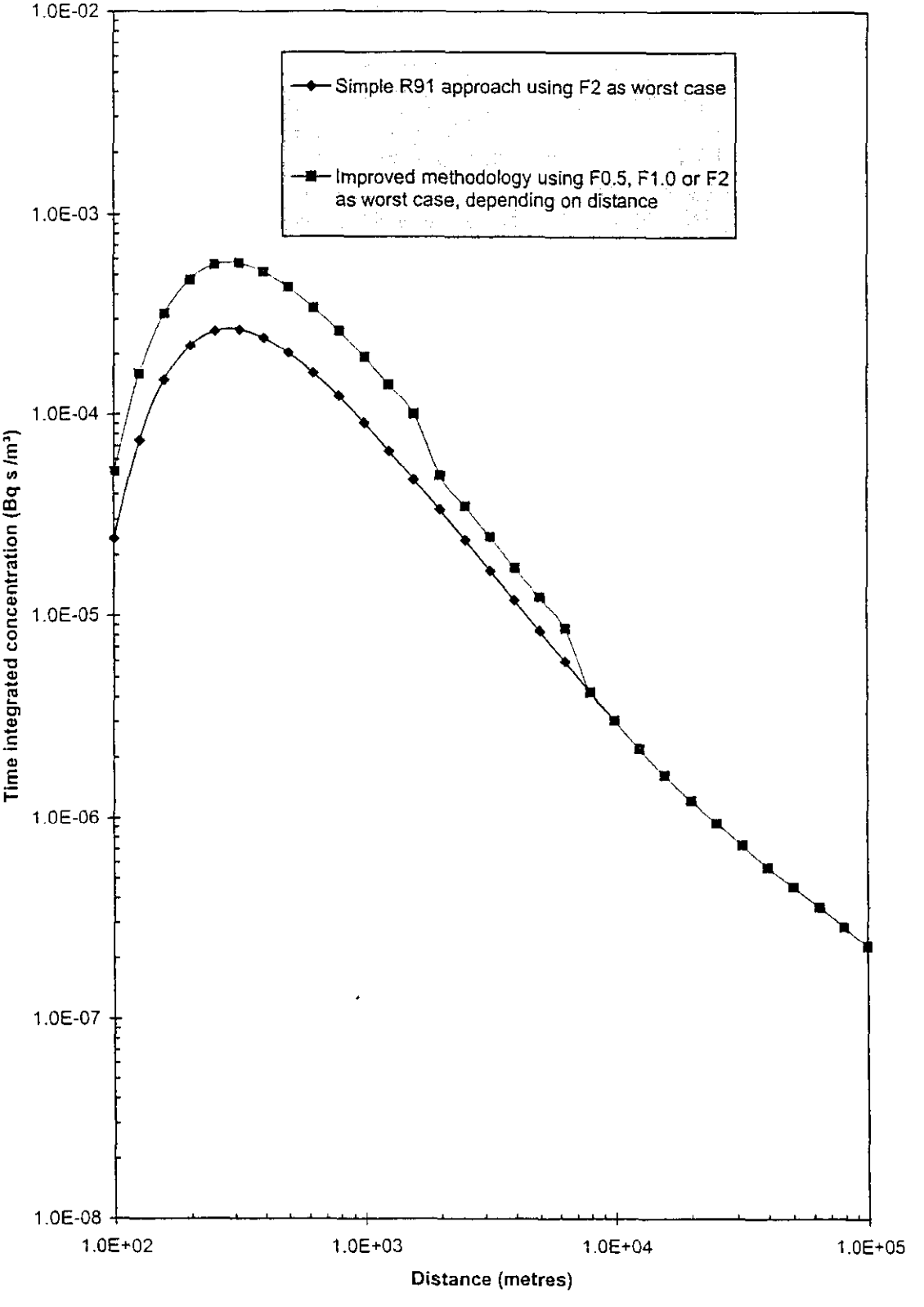

FIGURE 3.13 Effect of improved low wind speed modelling on annual average time-integrated concentrations for a unit release from a 20 m stack

Figure 3.14 shows an example of a 'worst case' weather conditions assessment for a unit release from a 10 m high isolated stack in F stability. It should be noted that a 10 m stack has been adopted in this example in order that the peak ground-level concentration occurs within the first 1800 m. Up to 1800 m, the concentrations are predicted using a wind speed of 0.5 m s^{-1}, and from 1800 to 7200 m a wind speed of 1.0 m s^{-1} is applied. For comparison purposes, Figure 3.14 also shows the predictions of the standard NRPB-R91 method for a wind speed of 2 m s^{-1} (ie the kind of conditions typically regarded as representing the worst case). The conclusion that may be drawn is that, at low to medium distances, the worst case concentrations may be increased if low wind speeds are considered within the analysis. Figure 3.15 shows the extent of the 10^{-4} Bq s m^{-3} contour using these two approaches, illustrating that there is a significant difference in the areas within the contour. It is noted that at larger distances (ie > 1800 m) it may not be appropriate to use 0.5 m s^{-1} as the worst case wind speed, and so the difference between the two approaches would be reduced.

4 Conclusions

The nuclear industry is generally interested in time integrated concentrations, whether from an accidental release or from routine discharges, because dose–response relationships are generally taken to be linear with no lower threshold. This is in marked contrast to other major hazard industries, such as the chemical industry, where the major hazard risks associated with releases of dangerous substances are generally highly dependent on the peak concentration, threshold concentration and on the time-dependent concentration variation. This is the fundamental reason why sophisticated dispersion modelling in low wind speeds is less of a requirement in the nuclear industry than in other areas such as the chemical industry. However, even in the nuclear industry, low wind speeds cannot be ignored altogether, as the likelihood of such conditions is comparatively high, and care should therefore be taken to ensure that any safety case, risk assessment or calculation of annual average or worst case concentrations therefore includes a consideration of low wind speeds.

This project has shown that there are several ways in which simple methodologies can be applied to ensure that the effect of low wind speeds is incorporated. These include:

(a) simply using a greater number of representative weather conditions,
(b) defining additional low wind speed weather categories (eg on the basis of Weibull distributions),
(c) applying simple low wind speed dispersion models for low wind speed or calm conditions,
(d) applying additional conditions/provisos to standard dispersion models

However, having reviewed all of these approaches, it is felt that the best advice is to consider the type of application for which the dispersion modelling is required, and then use an appropriate methodology with suitable assumptions.

In summary, for annual average concentrations or risk assessment type applications, the cross-wind spread of a plume is generally unimportant, as the results depend on the cross-wind integrated concentrations. Many simple low wind speed models essentially just modify the horizontal spread parameter, and so their use would not result in any significant changes to the results. However, this report has shown that the frequency of low wind speed categories may be significant, and it is therefore preferable to use a larger number of representative weather categories in order to ensure that low wind speeds can be included. It should be noted, however, that low wind speed categories should not be used to predict concentrations at distances beyond those which could be reached by the plume (ie considering the persistence of these low wind speed conditions).

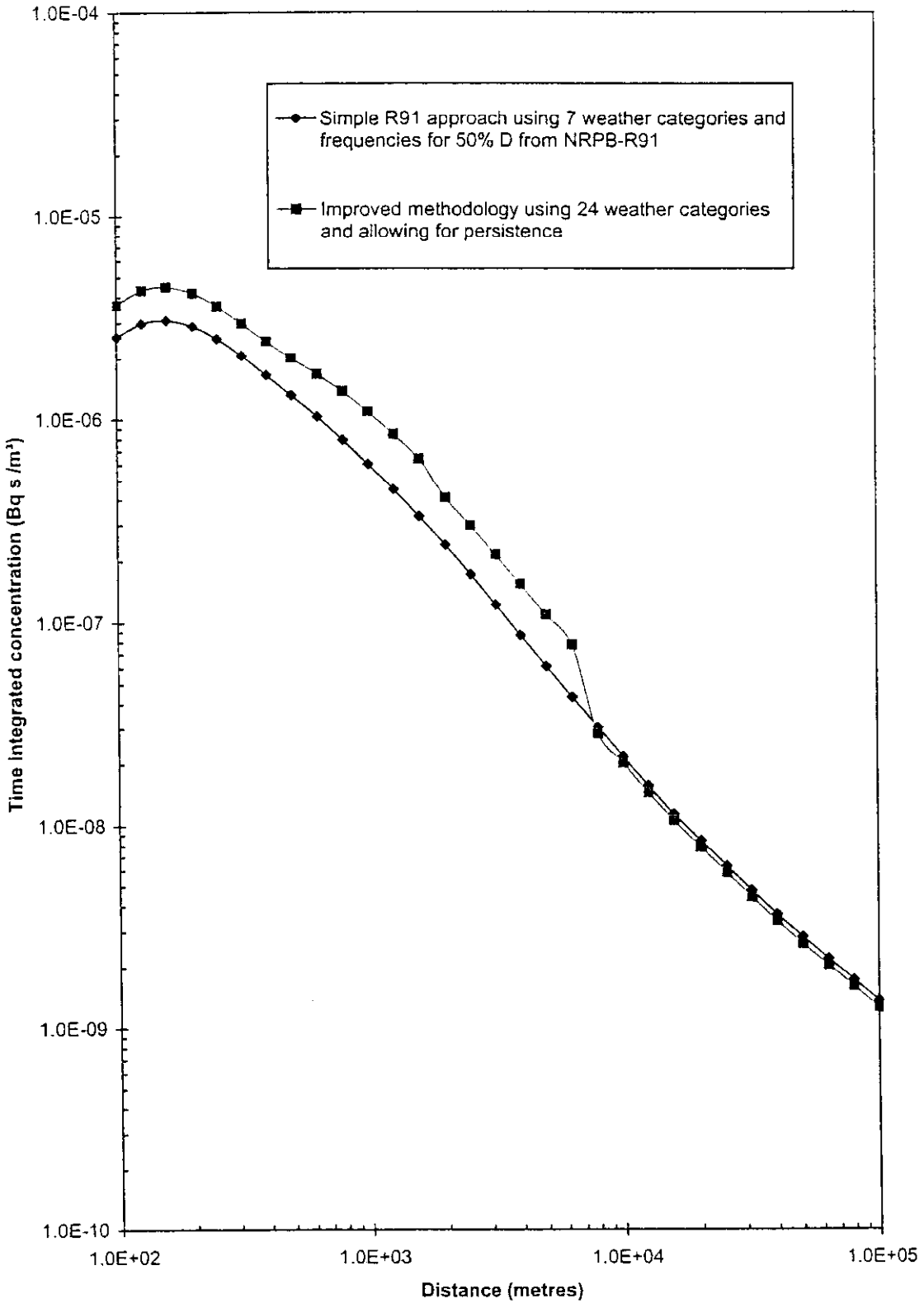

FIGURE 3.14 Worst case predictions using new methodology and the standard approach for a 30 minute release from a 10 m stack in category F conditions

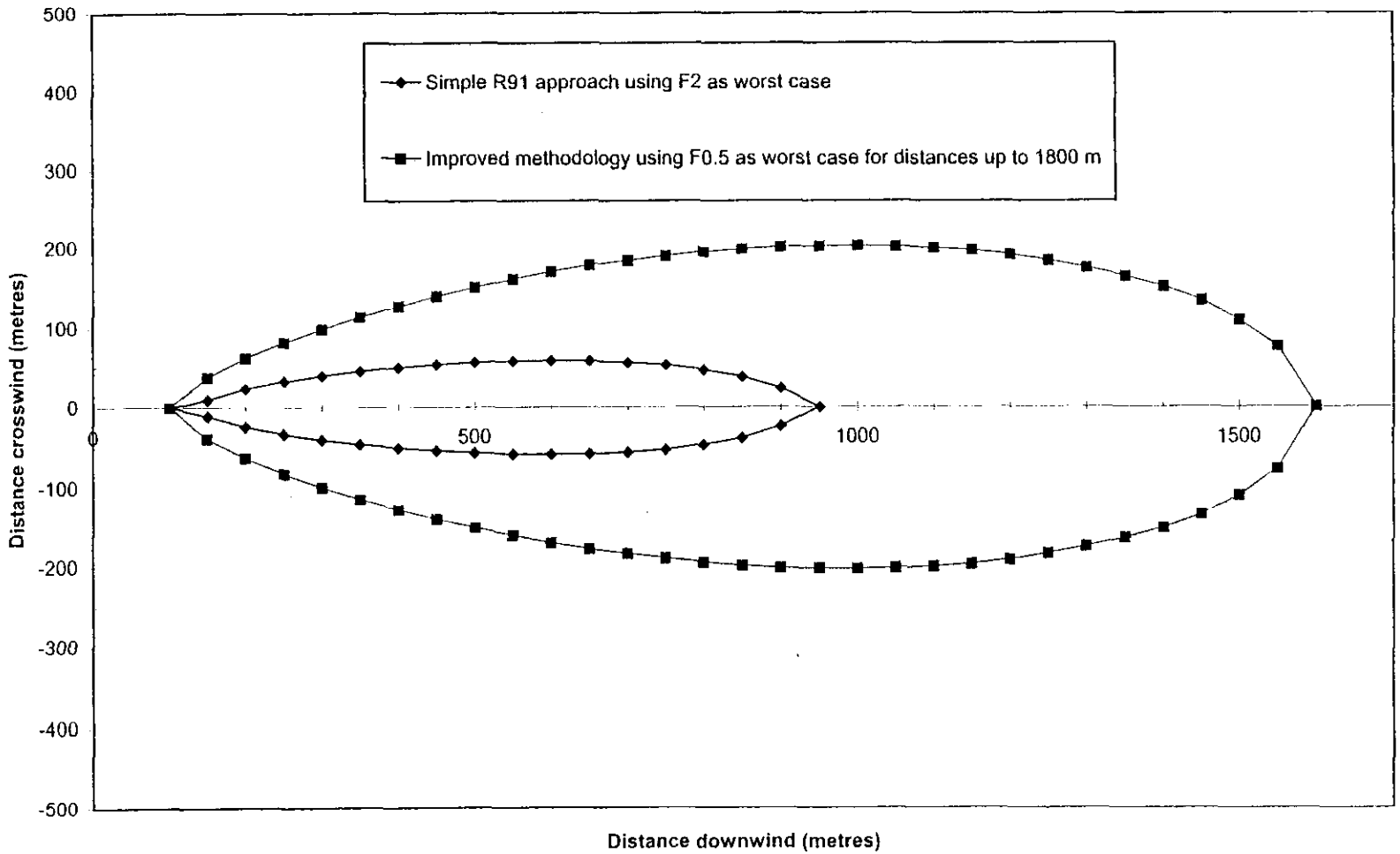

FIGURE 3.15 Worst case predictions of 0.0001 Bq s m^{-3} using new methodology and the standard approach for a 30 minute release from a 10 m stack in category F conditions

For safety case applications, where the requirement is often to consider the dispersion of a release in typical and worst case weather conditions, the assessment of dispersion in low wind speeds is more important.

Firstly, it is necessary to define what constitutes the worst case conditions. In the past, F2 has often been chosen, but this report shows that, at short to medium distances, it may be more appropriate to consider F0.5 or F1 conditions, depending on whether such conditions could persist to the distance of interest. A variety of models may be applied, most of which involve modifying the cross-wind spread according to the wind speed, resulting in wider but less concentrated plumes than would be obtained by simply applying a standard Gaussian plume model approach. Having considered a number of such models, it is felt that, for most practical purposes, the inclusion of a 'meander' or time averaging correction to the standard NRPB-R91 model provides a reasonable approach for use at low wind speeds of 0.5 to 2 m s^{-1}. This approach results in a $u^{-1/2}$ dependence of the concentration on wind speed, rather than the u^{-1} dependence usually quoted for Gaussian plume models. This $u^{-1/2}$ dependence implies a 'softer' singularity as $u \to 0$, implying that it may be appropriate to use such models down to fairly low wind speeds (eg 0.5 m s^{-1}).

In certain special cases, such as when a prediction of upwind spread is required, then it may be necessary to use either a puff type model or some form of three-dimensional diffusion equation, rather than any form of standard Gaussian plume model.

Finally, it should be remembered that numerous studies have shown that the best way to model low wind speed dispersion is to use detailed meteorological data (wind speed, direction, turbulence, etc) measured at various heights over the entire area of interest. However, this is rarely practicable, except in limited dispersion trials, and so it is necessary to accept that accurate predictions at low wind speeds will never be possible using simple models and data. Nevertheless, the simple methods recommended in this report are considered to be reasonably conservative best estimate approaches, which are appropriate for the sort of applications generally of interest.

5 References

Agarwal, P, Yadav, A K, Gulati, A, Raman, S, Rao, S, Singh, M P, Nigam, S, and Reddy, N (1995). Surface layer turbulence processes in low wind speeds over land. *Atmos. Environ.*, **29**, No. 16, 2089–98.

Arya, S P (1995). Modeling and parameterization of near-source diffusion in weak winds. *J. Appl. Meteorol., 34,* 1112–22.

Brown, M J, Arya, S P, and Snyder, W H (1993). Vertical dispersion from surface and elevated releases: an investigation of a non Gaussian plume model. *J. Appl. Meteorol.*, **32**, 490–505.

Cagnetti, P, and Ferrara, V (1982). Two possible simplified diffusion models for very low wind speed. *Rivista di Meteorologia Aeronautica*, **42**, 399–403.

Cirillo, M C, and Poli, A A (1992). An intercomparison of semiempirical diffusion models under low wind speed, stable conditions. *Atmos. Environ.*, **26A**, No. 5, 765–74.

Deardoff, J W (1984). Upstream diffusion in the convective boundary layer with weak or zero mean wind. IN Proceedings 4th Joint Conference on Applications of Air Pollution Meteorology, Portland, OR. American Meteorological Society.

Deaves, D M , and Lines, I G (1997). On the fitting of low mean wind speed data to the Weibull distribution. *J. Wind Eng. Ind. Aero.*, **66**, No. 3, 169–78.

Etling, D (1990). On plume meandering under stable stratification. *Atmos. Environ.*, **24A**, No. 8, 1979–85.

Hanna, S R, and Paine, R J (1989). Hybrid plume dispersion model (HPDM) development and evaluation. *J. Appl. Meteorol.*, **28,** 206–24.

Jones, J A (1997). Atmospheric dispersion at low wind speed. IN ADMLC Annual Report 1995/96. Chilton, NRPB-R292.

Lines, I G, and Deaves, D M (1996). The implications of dispersion in low wind speed conditions for quantified risk assessment. London, HSE Contract Research Report R8000/035 October 1996.

Sagendorf, J F, and Dickson, C R (1974). Diffusion under low wind speed, inversion conditions. Washington DC, US National Oceanic and Atmospheric Administration, Technical Memorandum ERL ARL-52.

Sharan, M, Yadav, A K, and Singh, M P (1995). Comparison of sigma schemes for estimation of air pollutant dispersion in low winds. *Atmos. Environ.*, **29,** No. 16, 2051–9.

Sharan, M, Yadav, A K, Singh, M P, Agarwal, P, and Nigam, S (1996). A mathematical model for the dispersion of air pollutants in low wind conditions. *Atmos. Environ.*, **30,** No. 8, 1209–20.

Smith, FB (1992). Low wind speed meteorology. *Meteorol. Mag.*, **121,** 141–51.

Venkatram, A (1982). A semi-empirical method to compute concentrations associated with surface releases in the stable boundary layer. *Atmos. Environ.*, **16,** No. 2, 245–8.

ANNEX B

Review of Models for Calculating Air Concentrations when Plumes Impinge on Buildings or the Ground

R N Colvile, A S Scaperdas, J H Hill and F B Smith

IMPERIAL COLLEGE CENTRE FOR ENVIRONMENTAL TECHNOLOGY

Summary

This review examines the transport and dispersion of pollution in the vicinity of buildings and hills. While the physical processes occurring for buildings have much in common with those for hills, the different scales involved mean that most methods for calculating concentrations on building and hill surfaces are quite different.

On hills, the change in temperature of the atmosphere with height is important. When the ground is colder than the air above, temperature effects impede the flow of air over hills. Some flow is deflected around the sides of an isolated hill, or stagnates upwind of a ridge. Hills also alter the rates at which pollution is transported and dispersed. On steep slopes, areas of complex recirculating flow may form. All these processes can lead to pollution being transported to the hill surface.

Gaussian plume models developed for use in flat terrain may be adapted for application to hills. Simply ignoring most of the effects of the hill can be useful, providing we have some understanding of the size and sign of errors that will result. Some simple, empirical assumptions about the effects of the hill can be used to reduce those errors, or to ensure that their sign is such as to overestimate concentrations. With a modest increase in computational effort, the Gaussian plume model may be modified by various transformations of source variables and/or receptor locations. Some very simple transformations can be effective under certain conditions, for example normalisation of distances and concentrations using source parameters. Alternatively, various solutions of the flow and dispersion equations for idealised hill shapes can be used to calculate receptor location transformations. This is the approach taken by the American Environmental Protection Agency (EPA) in its CTDMPLUS model. CTDMPLUS is already available as personal computer code, and has been validated in the field. However, this model, and also the simpler more empirical EPA models for dispersion over hills, have been developed primarily for regulatory modelling of industrial sources. During the development of a regulatory model, it may be appropriate to tune the algorithms to achieve consistent performance within a given tolerance or degree of conservatism when predicting certain statistical parameters such as long-term average or percentile concentrations. For other kinds of pollutant and source (for example, accidental release of radioactive material), it is conceivable that a model may have demands made of it that are quite different to those for which it has been developed and validated. It is important to remember that this may affect the performance of the model, and quantifying this effect can be difficult.

An alternative way of adapting the Gaussian plume model to hills, is to use a model of airflow to compute new plume centreline and dispersion parameters that take into account the effects of the hill. This is the approach used in the ADMS modelling system, with the airflow model Flowstar. Computation time using Flowstar is longer than using CTDMPLUS and statistically averaged meteorological data cannot be used to compute long-term average concentrations. ADMS with Flowstar currently does not consider flow recirculation or stagnation or flow around the sides of hills at all. A major advantage of Flowstar over CTDMPLUS, however, is that it takes into account the actual shape of real hills, instead of using parameterisations.

For future development, it is possible to replace Flowstar with a more sophisticated flow model such as a k–ε turbulence model in a computational fluid dynamics (CFD) code. This would allow some treatment of the processes that Flowstar cannot handle. However, the computational expense and user skill required are considerable.

Buildings are even more diverse than hills. Real sites in which there are usually more than one building pose a substantial problem for the development of generally applicable models. A first approach is to define an area of influence for each building. That building can then be modelled as

an individual block if there are no other buildings in its area of influence. If buildings are closer together, and placed inside each other's areas of influence, then existing calculation methods leave little alternative than to model the cluster of buildings as a single block. Exceptions to this are especially common configurations such as urban street canyons, for which some empirical models exist.

Owing to the small size of buildings compared with hills, atmospheric temperature profiles are unimportant in modelling how buildings affect flow. Dispersion near buildings is influenced by flow separation, horseshoe vortices and roof-edge trailing vortices, all of which can cause a plume to impinge on buildings. These form because of the steep sides and sharp edges of building surfaces. Often, for a single building, there are several distinct flow patterns that can arise. Under such circumstances, it may be appropriate to model each pattern individually, and then to carry out a concentration mapping or weighted averaging exercise depending on what information is required. When a source is close to a building, the concentration field can be most variable. Models in such a regime tend to be highly empirical and applicable only to simple building shapes. Uncertainties up to a factor of ten are commonplace.

As the plume becomes larger compared with the building dimensions, the Gaussian plume model and modifications thereof become more applicable. For sources upwind of a building, spreading of the plume at the building causes concentrations to be less than those at the same point in space in the absence of the building, but maximum concentrations tend to be spread over a larger area. Therefore, the Gaussian plume model can be used to calculate the maximum concentration intercepted by the building, and this can be used as a conservative estimate of the concentration everywhere on the face of the building. For sources on the building itself, conservative estimates of concentration elsewhere on the surface can be made as functions of distance from the source relative to the size of the source. Similar expressions may be derived for sources above a building, including the '$2.5H$' rule defining a stack height above which the plume will not impinge on the building at all. In the building wake, the plume may be split into two parts: that which enters the wake and that which remains outside. These two parts may then be modelled as if they come from two separate sources. Such an approach is used in the ADMS modelling system.

In view of the complexity and variety of buildings, CFD and wind tunnel simulations are even more attractive than for hills. Even though the lack of significant atmospheric stability effects makes this less difficult for buildings than for hills, the computing time and user skill required are still considerable.

1 Introduction

Releases of material to the atmosphere can occur in situations where a plume can impinge on other buildings or elevated ground close to the release point. In some instances, the plume can pass over air intakes or windows in the building from which the material is released. This report reviews methods for calculating the concentration on the surface of, or inside, buildings or at ground level on elevated terrain. It identifies situations when plumes might impinge, and describes existing methods for calculating the concentration on the ground or the building surface. Most of these methods are suitable for incorporation in personal computer programs. The extent to which the Gaussian plume model could be modified for application in such situations is addressed.

The review concentrates on existing models. Some possibilities for the development of improved models are identified, but the development of such models is outside the scope of this work.

This review has been carried out at Imperial College Centre for Environmental Technology through ICON Consultants Ltd for the UK Atmospheric Dispersion Modelling Liaison Committee.

There are several physical and mathematical similarities between dispersion around buildings and dispersion around or over hills. However, at the onset of the review, it became clear that many modelling methods and approaches for buildings are quite different to those for hills. Therefore, this review has been prepared in two separate parts. Section 2 provides a survey of methods for calculating concentrations on the ground when plumes impinge on hills. Section 3 provides a similar survey for buildings. In order to facilitate comparison between the two, many of the subheadings are the same in each section. In some cases, this entails some duplication of material between corresponding subsections in the two sections, but there are some differences in the approach depending on whether hills or buildings are being considered – examples of this are the use of wind tunnels and computational fluid dynamics. Section 4 provides some general conclusions concerning choice of model, including a discussion of how modelling might develop given the increasing availability of powerful computers capable of solving the flow equations explicitly for specific configurations of buildings and/or hills.

2 Plumes impinging on hills

2.1 Introduction

2.1.1 Background

The Gaussian plume model is commonly used to calculate concentrations at ground level (Clarke, 1979). In its most basic form, this model assumes flat terrain of constant surface roughness and stationary, homogeneous turbulence. Various versions of the same basic model have been devised, assessed and validated using controlled experiments where the conditions were as close as possible to these ideal conditions (Barad, 1958; Hanna and Paine, 1989; Venkatram, 1996). In reality, these conditions are rarely experienced: turbulence is not homogeneous (especially in the vertical), nor is it Gaussian, nor completely stationary. In particular, terrain is rarely flat. It is therefore necessary for users of Gaussian plume models to be aware of possible effects of departures from idealised conditions, including elevated terrain, as taken into account to some extent by more recent models such as ADMS (Carruthers *et al*, 1994). Of special interest are situations where plumes impinge on elevated terrain. In such cases, ground-level concentrations can differ by orders of magnitude from what would be observed in flat terrain at the same distance from the source. This part of the review therefore addresses physical processes that control dispersion over elevated terrain, and describes currently available methods for calculating concentrations at ground level on

elevated terrain. Modifications to the Gaussian plume model will be considered together with alternative approaches.

The Royal Meteorological Society has produced a policy statement on the justification of choice and use of atmospheric dispersion models, and the communication and reporting of results (Britter *et al*, 1995). Amongst other recommendations, this stresses the importance of scientific assessment as part of the quality assurance of models, especially where it is necessary to investigate conditions that are outside the range within which the models have been validated. In the particular case of dispersion over elevated terrain, models can be validated only for idealised, simple situations such as an isolated round hill or a two-dimensional ridge, or for individual situations of greater complexity. With a few exceptions, every piece of real terrain is unique. The vast majority of real-life applications of dispersion models over elevated terrain are therefore, to some extent, outside the conditions for which the models have been validated. This review therefore aims to provide information that will be valuable in performing such a scientific assessment. In this way, it will be possible to demonstrate the fitness for purpose of a given model for a specific situation, as recommended in the policy statement.

2.1.2 Existing information and modelling techniques

2.1.2.1 Historical overview

Egan (1975) noted that a number of issues requiring knowledge of dispersion processes in complex terrain were not matched by the required research effort to resolve the many technical issues that were then outstanding. Over 20 years later, we find that modelling dispersion in complex terrain still presents considerable difficulties. Nevertheless, we now have the two-fold benefit of a series of experiments observing the effects of hills on dispersion together with increasingly readily available computers of great power capable of solving the complex basic equations.

2.1.2.2 Laboratory and field experiments

Experiments can be divided into two main categories: laboratory and field. These can be subdivided into three categories: isolated round hills, two-dimensional isolated ridges, and more complicated situations. In some cases, field experiments have been repeated in the laboratory.

Laboratory experiments are usually in wind tunnels or towing tanks. In a wind tunnel, the fluid is a gas moving at a speed scaled according to the size of the model hill. In a towing tank, the fluid is a liquid, and a model of the hill is pulled through it (often upside down) at a speed related to the scale of the model and the difference in density and viscosity between the liquid and air.

It can be argued that laboratory experiments benefit from controllability of conditions that is lacking in the field. In principle, however, it is possible to characterise field conditions at least as precisely as in the laboratory. The main advantage of laboratory experiments is therefore one of cost, which allows a much larger amount of data to be collected. It would be prohibitively expensive to wait in the field for natural conditions to vary through all the conditions of interest (coincident with a sufficiently large fraction of the instrumentation functioning correctly) at a single location, yet alone in a variety of situations. The disadvantage of laboratory simulation is that it may differ from field conditions, because it may be impossible to scale down the lengths and velocities to conserve all the governing parameters, especially when thermal effects are involved.

The calculation methods considered in this review have been compared with a mixture of field and laboratory measurements. In undertaking such comparisons, it is important to consider measurement error and, in the case of laboratory measurements, the imperfect representation of the real atmosphere. It is therefore unfortunate that few papers describing model validation exercises

consider such uncertainties. These uncertainties cannot therefore be considered in this review either. In many cases (for example when comparing an extremely naïve modelling approach with one that is much more realistic), the differences between different calculation methods will be much larger than expected experimental errors in field measurements. Nevertheless, when a specific model is applied to a specific problem, consideration of the accuracy of the measurements against which it has been validated is an important part of the scientific assessment of the model, especially when validation has been restricted to the laboratory.

2.1.2.3 Types of calculation method

Existing calculation methods vary immensely in the quality and quantity of information they are designed to provide and also in the computational resources and user effort required to produce results. The NRPB-R91 model (Clarke, 1979) requires only a pocket calculator to obtain concentrations from graphs of dispersion parameters. Computational fluid dynamics models, at the opposite extreme of complexity, can require hours or even days on a Unix workstation or supercomputer. In between are several methods that can be, or have already been, incorporated into programs that will run on a readily available personal computer in a matter of minutes or hours. Some of these models attempt to reproduce short-term average concentrations or ensemble mean concentrations for given broad-brush meteorological conditions, by making as few simplifying assumptions as possible within the constraints of the chosen method of numerical solution. Others intentionally err on the side of overestimating concentrations, as they are intended to be screening models. The theory is, if a screening model predicts that concentrations will not give cause for concern, it is safe to take no further action. If screening identifies a possible problem, then more accurate models should be used to investigate further if time and need so dictate.

In view of the difficulties inherent in modelling dispersion over complex terrain, the use of screening models is an even more valuable step in impact assessment than it is in simpler situations. However, it is still necessary to beware of screening models producing large underestimates of concentration or area-at-risk, where they qualitatively predict the wrong patterns of dispersion. Also, the computational resources or run time of a model are not necessarily related to the amount or quality of information it produces.

Using some simple modelling techniques, for example, annual average concentrations can be much more reliably predicted than short-term average concentrations. This is because, over a year, extreme conditions that are not treated well by the model are averaged out to some extent. However, to model an annual average ideally requires a separate calculation for each hour of a year. In most cases, this is prohibitively time consuming, so statistical meteorological data are used to reduce the computational effort. Research is currently in progress to determine with what resolution meteorological parameters need to be classified in such statistics, in order to avoid erroneous averages. The danger is that extreme conditions may be missed which, owing to the non-linearities that exist, may have a much greater impact on the long-term average than their frequency would suggest. These unusual cases could, of course, have a prolonged effect when toxic pollutants are involved. Furthermore, most studies of the effects of using statistical meteorological data are applicable to flat terrain. In elevated terrain, additional sensitivities can cause finer resolution meteorological data to be required. This will be discussed further in Section 2.1.4.

2.1.3 Classification of types of release

Releases that are liable to impinge on hills may be classified according to their location horizontally relative to terrain features and also according to the height of the release relative to the terrain altitude.

The study of Khurshudyan *et al* (1981) and the results summarised by Snyder (1983) consider releases at three positions horizontally relative to a two-dimensional ridge: on flat ground upwind of the ridge, on the highest point of the ridge, and on flat ground downwind of the ridge. A similar categorisation can apply to a round hill. Most of the calculation methods that will be considered will concentrate on sources upwind of the elevated terrain. However, we will see that it is necessary also to consider the possibility that plumes from sources downwind of the hill can also impinge on the hill surface.

The American Environmental Protection Agency (EPA) defines three different types of terrain according to the height of the source release compared with the maximum altitude of the terrain (Figure 2.1):

(a) simple terrain: maximum terrain height below stack height,

(b) complex terrain: terrain rising above plume centreline height,

(c) intermediate terrain: terrain rising above stack height but not above plume centreline height.

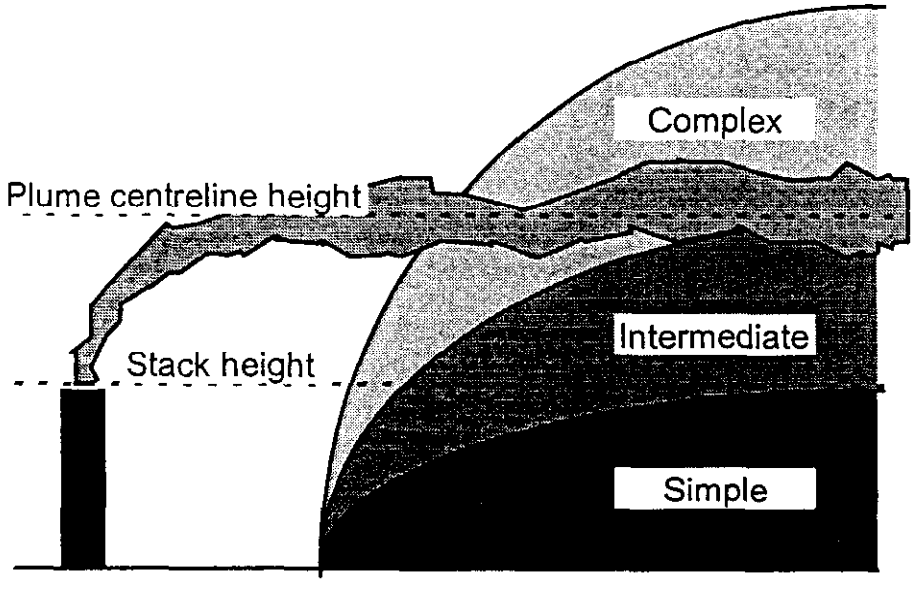

FIGURE 2.1 Terrain types as defined by EPA

2.1.4 Role of atmospheric conditions and stratification

Atmospheric temperature gradients may be classified according to the following three categories.

(a) When there is little or no vertical transport of heat in the atmosphere, temperature decreases with height. This is because rising parcels of air cool by adiabatic expansion and descending parcels of air are heated by adiabatic compression. These conditions are called neutral, because the vertical temperature profile neither encourages nor inhibits vertical motions. Neutral conditions occur typically when it is cloudy and windy.

(b) When the sun heats the surface of the Earth, this causes the drop of temperature with height in the atmosphere to be accentuated. Under such conditions, a rising parcel of air finds itself less dense than its surroundings, so it tends to continue rising. These conditions are therefore called unstable. The most unstable conditions occur when the ground has been heated by the sun and winds are light. Instability is also caused by the advection of cold air over a warmer surface, as behind a cold front.

(c) Conversely, when the surface of the Earth is losing heat to space, the decrease in temperature with height in the atmosphere is reduced, or even air at the surface may be colder than that aloft. A rising parcel of air under such conditions finds itself denser than its surroundings, so tends to sink back down. These conditions are therefore called stable. The most stable conditions occur at night when the sky is clear and the wind is light. Stability is also caused by the advection of warm air over a cold surface, as behind a warm front.

Unstable convection can be enhanced by hills in two ways. Firstly, air approaching a hill is forced to rise. Under circumstances where this process leads to the formation of orographic cloud, the heat released adds to the atmospheric instability. Secondly, south-facing slopes in the northern hemisphere tend to be warmer than flat surfaces, which can cause significant persistent convective cells to lock on to hills. In stable conditions, gravity can cause air to flow down hill slopes locally, regardless of the direction of any light wind elsewhere. The effects of such interactions between hills, stability, flow and clouds are considered in some detailed models (eg Clark, 1977) but not in any of the dispersion calculation methods that will be considered in this review.

When wind blows over the rough surface of the Earth, a turbulent boundary layer is formed, within which thermal and kinetic energy are transported to and from the ground. In stable conditions, the boundary layer may be only tens of metres deep. In unstable conditions, it can extend for kilometres above the Earth's surface. Many hills in the UK are high enough to occupy a large fraction even of a relatively deep, well-mixed, day-time atmospheric boundary layer. Shallow, nocturnal boundary layers are frequently of lesser vertical extent than even the smallest hills. We shall see in Section 2.2.1 that the height of many hills in the UK is sufficient for commonly occurring stable stratification to impede the lifting of streamlines to follow the topography over a hill or ridge. Atmospheric conditions, especially stratification and boundary-layer height or the presence of temperature inversions, thus play a very important role in determining the way in which plumes disperse over hills. This is a major difference between dispersion around buildings and dispersion over and around hills, owing to the difference in size between buildings and hills.

It is known that ground-level concentrations calculated by dispersion models such as ADMS over flat terrain can be extremely sensitive to meteorological inputs. For example, when a plume travels close to the top of the boundary layer, a few tens of metres difference in the boundary-layer height estimated by ADMS using standard meteorological parameters can determine whether or not the plume diffuses down to the ground. This is because there is a positive feedback effect as the dispersion parameters increase from the inversion downwards towards the middle of the boundary layer. The use of meteorological measurements made some distance away from the area of interest can easily cause an error of tens of metres in the boundary-layer height, and thus cause large errors in ground-level concentrations in these conditions. Over elevated terrain, such errors will tend to be larger than they are over flat terrain. Scientific assessment of the assumptions made in a model to be used over elevated terrain is therefore even more important than it is over flat terrain. The importance of this increases as models of increasing complexity are used, as these have a greater potential for marked sensitivity to meteorological input.

In general, the influence of hills on dispersion is much greater in stably stratified atmospheric conditions than when the atmosphere is unstable. This is because, when the atmosphere is not stable, the streamlines can very easily rise to follow the changes in terrain height. Under such conditions, the effect of the hill is slight. We will ignore unstable conditions in which airflow over hills triggers convection, as this is a highly complex turbulence problem not treated by any

short-range models we have found. In the same way, we will not consider plume buoyancy or self-heating releases. We note only that any such process that causes a plume to rise high up in the atmosphere has the potential of causing deposition to the ground hundreds of kilometres or more from the source, as was found in the Chernobyl nuclear plant accident. The effect of hills in unstable conditions therefore perhaps needs to be considered in long-range transport models. This review will concentrate mostly on neutrally buoyant plumes in neutral or stable atmospheric conditions less than 100 km from their source.

Nevertheless, it should be noted that, over flat terrain, the highest ground-level concentrations from elevated sources of pollution are experienced in convective unstable conditions. This is because large turbulent eddies can bring an elevated plume down to the ground close to the source. Complex terrain can have exactly the same effect in less unstable conditions or even in neutral or stable, as the transport of a plume down to the ground is aided by the ground rising up towards an elevated plume. Under unstable conditions where hills cause levels of convective turbulence to be increased, it is possible for emissions from elevated sources to be brought down to the ground even more easily on the hills or in their lee than on flat ground.

2.2 Flow patterns and pollutant dispersion over and around hills

2.2.1 Major characteristics of mean flow over and around hills

Hills influence mean flow in three ways. Firstly, they cause the streamlines to be deflected. This can be either in a vertical or a horizontal direction. Secondly, they cause the air to speed up or slow down. Thirdly, they can cause large disruptions to the flow in the form of separation regions. Each of these will be considered separately below. Hills also generate additional turbulence.

2.2.1.1 Horizontal and vertical deflection of streamlines

The most salient feature of the influence of hills on flow and dispersion is the concept of critical dividing streamline height. This theory has been developed for isolated round hills in stable atmospheric conditions. Air approaching at a height z further from the ground than the critical height is able to rise and pass over the hill. Air approaching below the critical height, however, has insufficient kinetic energy to overcome the downwards force on it due to the stratification of the atmosphere (Figure 2.2).

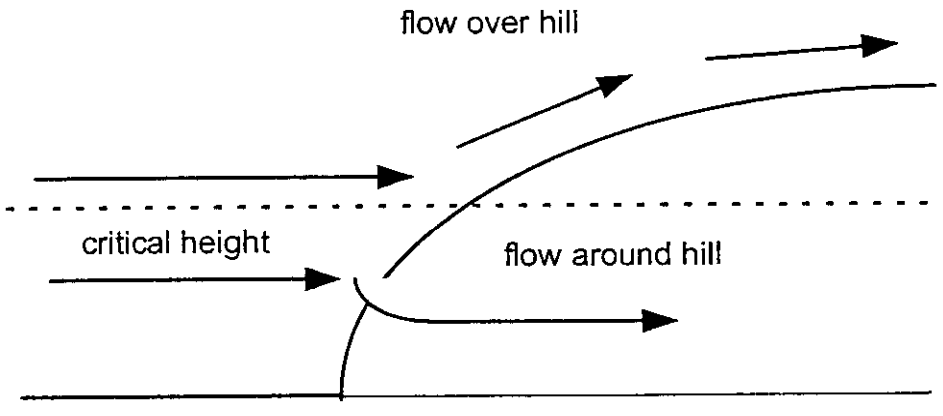

FIGURE 2.2 Critical dividing streamline height

The critical height is a function of the Froude number,

$$Fr = \frac{U}{NH} \tag{2.1}$$

where N is the Brunt-Väisälä frequency

$$N = \sqrt{\frac{-g}{\rho}\frac{\mathrm{d}\rho}{\mathrm{d}z}} \tag{2.2}$$

and U is the wind speed upwind of the hill, H is the height of the hill, g is acceleration due to gravity and ρ is the density of the air. A Froude number much greater than unity describes flow dominated by inertial effects. A Froude number less than unity describes flow dominated by stability.

Hunt *et al* (1978a,b) tested a postulation of Sheppard (1956) and demonstrated the usefulness of a critical height

$$h_c = H(1 - Fr) \tag{2.3}$$

for constant density gradient and uniform upwind velocity profile. This may be generalised (Snyder *et al*, 1982) to arbitrary velocity and density profiles by an iterative solution to the expression

$$\frac{1}{2}\rho(u(h_c))^2 = \int_{h_c}^{h} \rho N^2 (H - z)\,\mathrm{d}z \tag{2.4}$$

For an isolated hill, air approaching below h_c will tend to divide and pass around the sides of the hill. For a ridge, no such route exists, so the air below h_c will tend to stagnate. Either behaviour can potentially influence ground-level concentrations very markedly indeed.

The presence of a temperature inversion in the atmosphere can have a similar effect. If there is a temperature inversion below the height of a ridge, unless the wind is strong enough or the slope gentle enough, the air will tend to stagnate below the inversion in a similar fashion to how it does below the critical height in stably stratified conditions.

Gravity waves are a further mechanism by which flow over hills can cause streamlines to be deflected in the vertical. In stable conditions, these can cause the effect of the hill in bringing a plume close to the ground to occur several hill-lengths away from the hill as well as on the hill itself.

2.2.1.2 Transition from two-dimensional ridge to three-dimensional hill

In cases such as that described above (Section 2.2.1.1), where the major characteristics of the flow are different for a two-dimensional ridge than for a three-dimensional hill, the following method of calculating critical hill size in the horizontal may be tentatively applied. It should be noted that the authors of this review did not find any such calculation in the literature, and so offer this formulation without any field or laboratory validation.

One physical process that will disrupt the flow around a three-dimensional hill, causing it to become more like that upwind of a ridge, is the influence of synoptic-scale horizontal pressure gradients. In Section 2.3.3.1, a model is described which permits calculation of the acceleration of air parallel to the hill surface as it is deflected to flow around a round hill. Using the nomenclature of Section 2.3.3.1, approximating $\sin\theta \approx y/r$ for $r \gg y$ gives

$$\frac{\mathrm{d}y}{\mathrm{d}t} = v_T = \frac{-U(r^2 + R^2)y}{r^3} \tag{2.5}$$

and, differentiating with respect to time to calculate acceleration,

$$\frac{\mathrm{d}^2 y}{\mathrm{d}t^2} = \frac{-U(r^2+R^2)}{r^3}\frac{\mathrm{d}y}{\mathrm{d}t} \tag{2.6}$$

The force exerted by the hill as it deflects the streamlines is therefore balanced by the force due to a horizontal gradient in the pressure, p, when

$$\left(\frac{-U(r^2+R^2)}{r^3}\right)^2 y = \frac{1}{\rho}\frac{\mathrm{d}p}{\mathrm{d}y} \tag{2.7}$$

where ρ is the density of air.

If we consider these forces on a volume of air of approximately the same size as the portion of the hill for which we want to predict the flow characteristics, we can set $y = R$ and $r = 2R$ to yield the condition

$$\left(\frac{5U}{8R}\right)^2 R > \frac{1}{\rho}\frac{\mathrm{d}p}{\mathrm{d}y}\text{, which simplifies approximately to } R < \frac{0.4\rho}{\mathrm{d}p/\mathrm{d}y}U^2 \tag{2.8}$$

for the hill to behave as a three-dimensional obstacle rather than as a two-dimensional ridge. In this context, R is best taken as the half-width or radius of curvature of contour lines for the part of the hill facing the impinging plume, either at the plume height or at the critical dividing streamline height h_c.

For a moderate pressure gradient of a couple of millibars per hundred kilometres ($2\ 10^{-3}$ N m^{-3}) and a wind speed of 10 m s^{-1} away from the hill, this gives a critical hill width or radius of about 20 km, which is towards the upper limit of validity of most of the models considered in this review. It should be noted, however, that this treatment of the problem predicts that the central parts of much smaller hills can behave more like a section of a two-dimensional ridge at lower wind speeds.

The EPA model CTDMPLUS (see Section 2.3.4), which was validated in terrain that included a hill that had a straight side of length about 3 km (Paumier *et al*, 1992), assumes that hills are ellipsoidal and does not seem to include a transition to a two-dimensional ridge for low wind speeds and wide hills (Perry, 1992).

2.2.1.3 Flow deceleration and acceleration

In neutral or stably stratified conditions, the flow of air decelerates on encountering the rising slope at the upwind edge of a two-dimensional ridge perpendicular to the wind direction. It then accelerates at the summit, in order to satisfy conservation of mass as the streamlines are forced closer together. At some distance downwind of the summit of an isolated ridge, the flow must return to the undisturbed upwind flow. In a neutral atmosphere, the flow over a symmetrical ridge is itself symmetrical. Neutral flow therefore slows down again on descending the lee slope. Stably stratified flow, however, or flow that is influenced by an inversion layer above, can be markedly asymmetrical about the axis of a ridge. When the Froude number (see above) is close to unity, strong downslope winds can be generated, which may persist downstream for a distance of several times the height of the hill. Such effects can be accentuated further when the hill summit is close to the top of the boundary layer, especially if an inversion below that height has been deflected upwards to allow air to flow over the hill.

Changes in the mean flow of air over a ridge influence the rate at which a plume is dispersed. Similar considerations apply to flow over a three-dimensional hill, but with the added possibility of streamlines being deflected horizontally as discussed above.

2.2.1.4 Flow separation

If the slope of a hill exceeds a certain gradient, it is possible for the mean flow velocity shear to become zero at some point near the surface (considering linear theory – see Section 2.3.1.2). This shuts off the transfer of momentum to the surface and so causes the mean streamlines no longer to follow the hill surface. Locally, the flow at the surface can be in the opposite direction to the flow aloft. On the upwind side of a hill or ridge, stagnation, blocking and flow around the side of a hill have been considered above (Section 2.2.1.1). In addition, flow separation readily occurs on the downwind slopes of a hill or ridge, associated with the formation of a wake.

Flow separation can be expected for slopes of gradient greater than about 1 : 3 or 1 : 2. The size and position of a zone of separated flow can be influenced by the surface roughness of the hill (Gong *et al*, 1996). For example, the presence of trees can have a strong influence (Kobayashi *et al,* 1994).

2.2.2 Criteria for plume impingement on the ground

Three mechanisms exist that can cause material from a plume to be transported on to elevated ground. These are turbulent diffusion, streamline divergence, and stagnation and separation. Consideration of each of these in turn will allow the meteorological conditions leading to impingement to be identified for a given topographical situation and source location. In addition to plume impingement, it is necessary to remember that gamma radiation can reach the ground from an elevated radioactive plume that does not itself impinge on the ground.

2.2.2.1 Diffusion

For a plume in which material is being advected over the top of elevated terrain, turbulent diffusion will bring material down to the ground if the vertical depth of the plume becomes greater than the height of the plume centreline above the ground. Elevated terrain can influence this in two ways.

Firstly, regions over elevated terrain can exist in which dispersion occurs more rapidly than over flat terrain. A example of this was considered in Section 2.2.1.2, where the mean flow velocity decreases on the upwind slope of a hill, causing dispersion to be enhanced. Alternatively, when the mean flow near the surface accelerates, a special case of enhanced dispersion can occur by the formation of Kelvin-Helmholtz instabilities in regions of high shear. In particular, when a plume travels above the boundary layer, speed-up of the wind inside the boundary layer can cause Kelvin-Helmholtz instabilities (like breaking waves) in the inversion above the hill, bringing tongues of polluted air down through the inversion to the ground. These chaotic Kelvin-Helmholtz instabilities may be contrasted with 'ordinary' turbulent diffusion in that they are more difficult to predict in detail.

Of more significance in many situations is the tendency of the plume centreline over elevated terrain to come closer to the ground than over flat terrain. This was considered briefly in Section 2.1.4, in which it was mentioned that stable stratification of the atmosphere tends to prevent streamlines from rising to pass over elevated terrain.

The same applies in the horizontal when streamlines pass around the side of a hill. Plume spread in the horizontal is nearly always greater than in the vertical, even over flat terrain. Hills have a greater tendency to increase dispersion laterally than vertically. Furthermore, the conditions under which streamlines are deflected past the side of hills are often those in which the flow velocity is reduced and so dispersion is increased. For these three reasons, lateral turbulent diffusion can, under

some conditions, cause a plume to impinge on the ground at an even greater distance from the plume centreline than vertical turbulent diffusion. It should be pointed out, however, that increased dispersion, although able to cause impingement, also reduces concentrations by dilution.

In order to determine whether or not a plume will impinge, the effects of vertical and lateral dispersion need to be considered together with the effects of streamline divergence, which are outlined below.

2.2.2.2 Streamline divergence

In Section 2.2.1.1, the flow of air around the sides of a hill below a critical height was described. This leads to streamline divergence at the hill surface along two lines, as follows.

Below the critical height, there is a line which separates the flow around one side of the hill from flow around the other side. On an ideal, symmetrical hill with constant wind direction, this line will be vertical where a line parallel to the wind direction passing through the centre of the hill intersects the hill surface. Along this line, it is possible for streamlines to approach the hill without deflection to either side. The velocity must decrease to zero to satisfy the boundary condition of an impenetrable hill surface, but the streamline does effectively impinge directly on the ground. (In fact, as the air slows down on approach to the stagnation region, the Coriolis force decreases. The air then tends to follow the pressure gradient to the left parallel to the hill surface. It is, however, difficult to predict to what extent this reduces the impact of streamline divergence, so we shall ignore it here.) The streamline divergence does not of itself increase the concentration above that at the same point in space in the hill's absence. Nevertheless, whatever plume material that is being advected along that streamline can be carried into a stagnant region where it will come into direct contact with the ground. At such a point of direct impingement, ground-level concentrations can *therefore be much higher than they would be in the absence of the hill.*

At the critical height, there is a horizontal line around the hill, above which air flows over the hill and below which air flows around the sides of the hill. In the corresponding situation on a ridge, the air below the critical height will tend to stagnate. If we consider the idealised model in which this transition is sharp, there is a possibility that a streamline travelling along the boundary will impinge on the ground. In reality, this surely cannot occur, as any infinite wind shear would soon be smeared out by a correspondingly large transport of momentum! However, it is prudent to consider the possibility that some more realistic process could occur, at such a transition, that might cause a plume to impinge on the ground. An example of such would be the advection of the plume into a stagnation region below the critical height, with a point of entry close to the hill surface. Also, fluctuations in wind speed will mean that the critical height is constantly changing.

2.2.2.3 Stagnation and separation

As mentioned above, plumes can impinge on the ground at the edge of areas of stagnant or separated flow that were discussed in Section 2.2.1.4. Within such areas, especially in the case of separated flow, the transport of material is complex and difficult to predict. This will be discussed in more detail below.

2.3 Calculating concentrations on hills

2.3.1 Overview of available methods

Where a flow of air encounters a hill, two distinct approaches can be employed to calculate concentrations in a plume carried by that air. The first approach is to attempt a solution to the Eulerian continuity equation for the concentration, using suitable parameterisations to reduce the

number of unknowns to the number of equations, or a Lagrangian expression for the motion of particles in the plume. The second approach is to solve the equations of motion for the flow of air first, without the plume, and then use the resulting field of mean velocity and turbulent fluctuations to calculate how the plume is transported and dispersed. These approaches will be summarised here. Examples of each approach will then be examined in detail in the sections that follow.

2.3.1.1 Derivation of plume equations over flat and elevated terrain

The concentration at a fixed point in a plume may be described by the conservation of pollutant-mass equation. This states that the rate of change of concentration in time is given by a sum of terms, each one of which describes one of the processes of advection, diffusion, reaction, radioactive decay and emission that cause the concentration to build up or to be reduced at that point. The advection term includes fluid velocities, which must satisfy Newton's laws of motion as described by the Navier-Stokes equations. Unfortunately, this leads to a larger number of unknown variables than expressions to solve for them – the well-known closure problem of turbulence. In order to reduce the number of variables, it may be assumed that the mean turbulent flux of material from a more concentrated part of the plume to a nearby, less concentrated part is proportional to the mean concentration gradient between the two. This assumption is valid, providing the turbulent velocities are high but persist only a short time before being replaced, defining length and timescales that are much smaller than those defining the evolving concentration distribution. This Eulerian approach (ie in a fixed coordinate system) leads to the atmospheric diffusion equation. For a source emitting at rate Q, neglecting reaction and decay, this may be written as

$$\frac{\mathrm{d}C}{\mathrm{d}t} + u\frac{\mathrm{d}C}{\mathrm{d}x} = \frac{\mathrm{d}}{\mathrm{d}x}\left(K_{xx}\frac{\mathrm{d}C}{\mathrm{d}x}\right) + \frac{\mathrm{d}}{\mathrm{d}y}\left(K_{yy}\frac{\mathrm{d}C}{\mathrm{d}y}\right) + \frac{\mathrm{d}}{\mathrm{d}z}\left(K_{zz}\frac{\mathrm{d}C}{\mathrm{d}z}\right) + Q(x,y,z,t) \qquad (2.9)$$

where C is the concentration, t is the time, u is the mean wind speed, x is the distance along the mean wind direction, y and z are the distances perpendicular to the mean wind direction, and K_{xx}, K_{yy} and K_{zz} are the diagonal elements of the eddy diffusivity tensor. This eddy diffusivity is the constant of proportionality that was assumed between the flux and the concentration gradient. Usually, the eddy diffusivity is equated to the equivalent momentum diffusivity proportional to the product of the turbulent velocity variance and its length-scale. Diffusivities can be measured in field or laboratory experiments. In simple situations, it is then possible to solve the diffusion equation analytically to obtain the concentration at any point in a plume at time t, given certain boundary conditions such as the concentration field at $t = 0$. In more complex situations, an approximate numerical solution may be found.

An alternative approach is to use a Lagrangian framework instead of the Eulerian one. Instead of considering the amount of plume material arriving at and leaving a fixed point in space, the Lagrangian method follows small volumes of air as they move along streamlines in the mean flow. The probability that one such small volume will be at a certain point is given by the probability that it was at some other point a short time previously multiplied by the probability that it moved from the first point to the second, integrated over all possible first points. This probability that the small volume of fluid moves from one given point to another is called the transition probability. For turbulent flow in general, this is unknown. However, if we assume that the fluctuations in velocity at any point assume a Gaussian distribution and are the same everywhere, the equations derived using the Lagrangian formulation can be solved to yield the well-known Gaussian plume formula for the concentration from an instantaneous point source of strength q at $(x,y,z) = (0,0,0)$, which follows.

$$C(x,y,z,t) = \frac{Q}{(2\pi)^{(3/2)}\sigma_x(t)\sigma_y(t)\sigma_z(t)} \exp\left\{-\frac{(x-ut)^2}{2\sigma_x^2(t)} - \frac{y^2}{2\sigma_y^2(t)} - \frac{z^2}{2\sigma_z^2(t)}\right\} \qquad (2.10)$$

where σ_x, σ_y and σ_z are the variances of the distances that a small volume of air travels in a given time in the x, y and z directions, respectively. A similar expression may be derived by solving the diffusion equation for an instantaneous point source.

In a similar fashion, either the Lagrangian or the Eulerian approach may be used to find analytic expressions for concentrations from releases of finite duration, continuous releases, and extended sources. In this review, we will consider primarily continuous point sources.

The simplest way of adapting these approaches to dispersion over elevated terrain is simply to ignore the presence of hills and to use the above plume formulae without modification, with or without using terrain-following coordinates (Figure 2.3). When using terrain-following coordinates, the assumption that the terrain is effectively flat when it is not, is then just one of several approximations that are made in the derivation of the plume formula. The same applies to the assumption that elevated terrain effectively has no influence over flow or dispersion, that is being made if ordinary flat-earth coordinates are used. In some cases, scientific assessment of such a model will allow the sign and order of magnitude of the error in such a gross simplification to be estimated. Even if the magnitude of the error is unknown, such a model can be used as a screening method if it can be shown that the sign of the error is such as to overestimate the concentration of interest.

The first level of refinement is still to use a plume formula that is essentially derived for flat ground, but to alter some of the assumptions concerning, for example, the boundary layer height and plume centreline position over the elevated terrain.

The alternative is to go back to first principles and re-derive a plume equation specifically over the elevated terrain of interest. The methodology is similar to that by which the Gaussian formula is derived over flat terrain, with the exception that the lower boundary condition is a curved surface instead of a flat one.

Although mathematically elegant, these last methods are of limited applicability. For some such methods, it is simply impossible to solve the equations for situations that are not geometrically extremely idealised. It is therefore appropriate to consider the modelling of airflow and turbulence over hills in some detail.

2.3.1.2 Modelling airflow over elevated terrain

Calculation of mean flow and turbulence over hills suffers from the same mathematical problem as that of dispersion over flat terrain, namely that the Navier-Stokes equations provide more unknown quantities than expressions to solve for them. A widely used assumption to achieve closure and allow analytical solution of this problem in a turbulent boundary layer is known as the mixing-length assumption. In such a mixing-length model, the Reynolds stress at a point is taken to be a linear function of the mean velocity shear (rate of change of a component of the flow velocity with respect to distance perpendicular to the direction of that component) at that point. The constant of proportionality is called the eddy viscosity. This can be calculated as the square of the mixing length multiplied by the magnitude of the mean shear, or some similar expression. It is possible to derive differential equations in this way that are linear. This allows efficient Fourier or Laplace transform methods of solution to be employed, resulting in acceptable resolution and run time using modest computing resources.

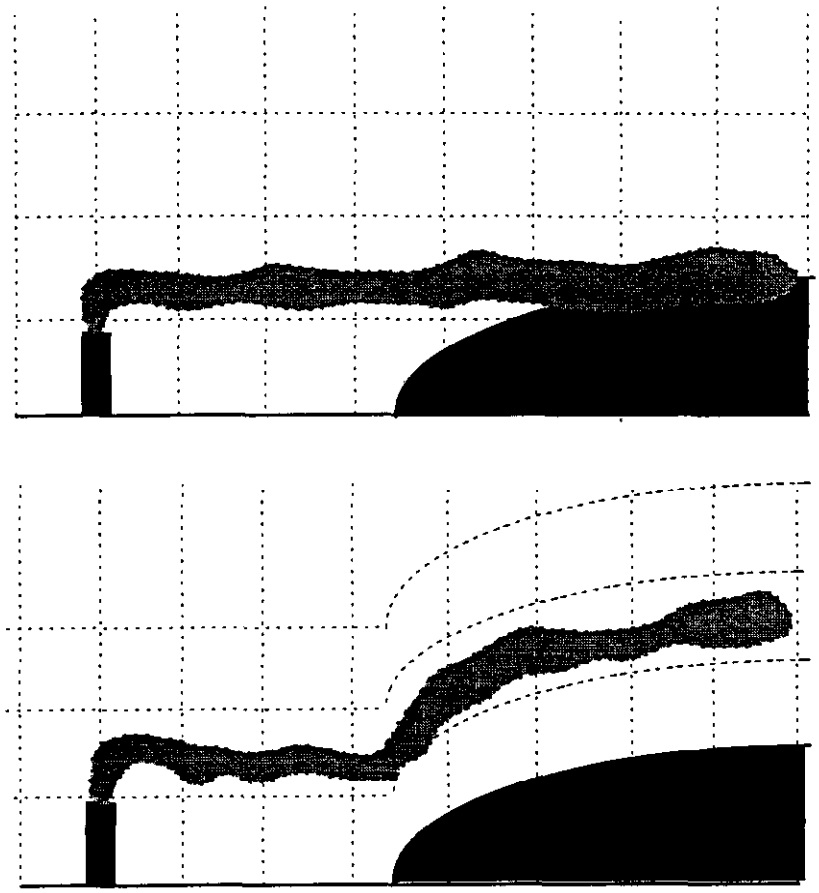

FIGURE 2.3 Terrain following coordinates (lower panel) compared with ignoring the hill altogether (upper panel)

In order to permit analytical solution of the Navier-Stokes equations, however, the mixing-length model assumes that all eddies die out before they can travel far enough to find themselves in a region where the mean flow field is significantly different to that where they started. (This distance, over which eddies lose their identity, is the mixing length. It has to be small, compared with the length-scale of the problem under investigation, for a non-linear term in the equations to become insignificant.) Thus, it is as if the amount of turbulence at a point is determined by the mean velocity shear at that point and nowhere else. This is called local equilibrium of turbulence. The assumptions we are making here for velocity and turbulence are similar to those we made for concentration and flux when we derived the diffusion equation. Observation of the wake behind a bluff body, however, immediately shows that there are situations where local equilibrium of turbulence is a poor assumption. Turbulent eddies are produced in regions of high shear near the surface of the body. These can then be shed and travel downstream. In the wake, turbulence and Reynolds stress are therefore caused not only by the local shear, but also by the transport of turbulent kinetic energy from more highly sheared regions upstream. Local equilibrium also cannot be expected in unstable convective conditions where turbulence is dominated by the sensible heat flux at the ground.

An airflow model that takes into account departures from local equilibrium of turbulence is the k–ε model, where k is the amount of turbulent kinetic energy per unit volume of fluid and ε is the rate of dissipation of k. Because ε is allowed to be smaller or greater than the rate of production of k, turbulence can be transported, as we observe. The term 'k–ε closure' refers to the assumptions

that are made in such a k-ε model, to reduce the number of unknowns such that modified Navier-Stokes equations can be solved for k and ε. The resulting equations, however, are non-linear. The solution method required therefore becomes computationally much more expensive than for linear models. Often, a compromise must be made between resolution and expense. This affects not only the resolution of the model output but also the values of mean-flow and turbulent velocities that are calculated, as the continuous equations are solved on a discrete grid. These errors are analogous to the errors that arise when using a simple rectangle, parallelogram or Simpson's formula to integrate the area under a curve, and are called discretisation errors. In k–ε modelling, it is possible for discretisation errors to become as problematic as errors caused by approximations made in the derivation of the equations themselves.

2.3.1.3 Conclusion

Topographical features in the UK provide a continuum from flat ground through streamlined, gentle hills to bluff bodies such as cliffs. We can therefore expect different approaches to the calculation of concentrations to be appropriate for different situations. What is not immediately apparent is at what height and gradient, and under what meteorological and plume conditions, a hill ceases to be streamlined and becomes a bluff body. This will become clearer as the various solution methods are scientifically assessed in the sections that follow.

2.3.2 Empirical assumptions

2.3.2.1 Unmodified Gaussian plume model

The simplest possible treatment of elevated ground in dispersion modelling is simply to ignore all hills. This is the recommended course of action in the user guide to the ADMS model when hill slopes are less than 1 : 10, owing to the large increase in run time that is incurred on invoking the ADMS hills module. Clearly, this course of action is most suitable when the hill has very little effect on the dispersion.

In stable conditions, it is likely that ground-level concentrations will be higher on elevated ground than on the flat, as the elevated ground rises up towards the plume centreline. In order to err on the side of overestimating concentrations, terrain-following coordinates should therefore not be used in such conditions. Rather, the Gaussian plume equation should be set up for flat terrain, and then calculations performed for receptors at the height of the elevated ground.

In unstable conditions, the plume centreline will tend to follow the terrain, so it will be adequate to use terrain-following coordinates, or rather to assume that all receptors are on flat ground. Furthermore, on low, gentle hills in unstable conditions, the differences between the traditional Gaussian plume model and a second-generation skewed-plume model such as ADMS will almost certainly be greater than the effect of elevated terrain.

Uncertainties in meteorological input can have a significant effect on model results in all conditions, as discussed in Section 2.1.4. This is a strong argument in favour of employing the most simple modelling strategy and diverting effort to ensuring quality of model input. The occasional extreme sensitivity of ADMS to inversion height should give cause for concern, as the presence of elevated ground will introduce even greater uncertainty over inversion height than there is over flat ground.

By simply ignoring elevated terrain, it is possible to underestimate ground-level concentrations when hills cause the plume centreline to be deflected downwards. This method will also tend to overestimate dispersion somewhat near the summit, where speed-up of the mean wind causes dispersion to be reduced over a hill (unless new enhanced turbulence is generated). The

results of this method are clearly inappropriate under conditions when blocking, separation or critical streamline heights are likely to occur.

In stable conditions, if it can be shown that the plume is all above the critical dividing streamline height (see Section 2.2.1.1), a much less conservative estimate may be made by assuming neutral conditions above the critical height and using terrain-following coordinates.

2.3.2.2 Limited terrain adjustment

The EPA industrial source complex model ISC3 (EPA, 1995) is a traditional Gaussian plume model that lacks the hills module of the ADMS modelling system. It does, however, make a few empirical assumptions about the effects of elevated terrain, described as 'limited terrain adjustment'. The EPA modelling guidance recommends the use of this method for rolling terrain that does not exceed the height of the release (also called simple terrain – see Section 2.1.3). In ISC3, any ground rising above this height is simply chopped off. It is important that any model programmed to do this on a computer should issue a clear warning message!

ISC3 assumes that the plume is not deflected in any direction by the elevated ground. The mixing height, however, is assumed to be terrain-following (even though this is not very probable, as the air above the boundary layer is stably stratified). Also, the vertical variation of wind speed is taken from the height of the elevated terrain.

This method is described as a screening method, ie designed to overestimate ground-level concentrations crudely. The assumption of no vertical plume deflection should achieve this in unstable conditions. Unfortunately, these are the conditions in which the ISC3 Gaussian plume formula can fail to bring material down to the ground sufficiently from an elevated release. Furthermore, in any atmospheric conditions, as the mixing height rises to follow the terrain, the strength of any reflections from the inversion will be reduced. Also, dispersion will be increased as the elevated ground causes modelled low wind speeds near the ground to be encountered by an elevated plume. This is why ISC3 is recommended only for simple terrain, below the release height. However, care should be taken to identify any situations where the presence of elevated terrain does not cause ISC3 to predict higher concentrations on elevated terrain than it would on flat terrain, and the physical realism of the assumptions leading to such predictions should be assessed.

2.3.2.3 COMPLEX1 screening model

A first attempt at making some more sophisticated assumptions than the two methods above is represented by the EPA COMPLEX1 screening model. As the name suggests, it is designed for elevated ground at heights above the plume centreline height, but is still a crude model that attempts to err on the side of overestimating concentrations. EPA recommends (*Guideline on Air* Quality Models), that the limited terrain adjustment of ICS3 should be used for lower ground. For intermediate terrain, neither the limited terrain adjustment nor COMPLEX1 is believed to be valid, so the recommendation is to carry out both calculations for every set of meteorological conditions and to accept the higher concentration in each case.

COMPLEX1 makes the same assumptions as the limited terrain adjustment, in that the mixing height and vertical variation in wind speed are terrain-following. In addition, COMPLEX1 does not use the Gaussian lateral spread parameters σ_y. Instead, it assumes uniform concentration throughout a 22.5° sector centred on the mean wind direction. In neutral and unstable conditions, the plume is assumed to be deflected upwards by half the height of the elevated ground – only in stable conditions is no vertical deflection assumed. In addition to these assumptions, the plume centreline is constrained to remain more than 10 m above the ground. In unstable conditions,

concentrations are multiplied by an attenuation correction factor which falls from 1 to 0 as the ground rises from 0 to 400 m above the undisturbed plume centreline height.

There are therefore some situations in which COMPLEX1 could conceivably fail to overpredict, so the same caveats as those for the limited terrain adjustment of ISC3 should be applied.

2.3.2.4 Image source hypothesis

On flat terrain, many routine applications of the Gaussian plume model consider the plume to be reflected from the ground when it impinges on it. Concentrations downwind of the point of impingement are therefore calculated as the sum of a contribution from the source itself and an additional contribution from an image of the source that is apparently below the ground.

An analogous approach can be used in elevated terrain, but in the horizontal plane as well as in the vertical. This is the basis of the EPA Valley model (Burt and Slater, 1977). It is valid where the main effect of a hill is to deflect the plume. Its major weakness is that it makes the same approximation as the Gaussian plume model over flat terrain, namely that the turbulence is the same everywhere. In cases where the hill causes turbulence to be enhanced, models based on this image source hypothesis can therefore greatly overestimate concentrations. The assumptions begin to break down as the plume spreads increasingly over three-dimensional terrain, then loses physical realism altogether where the plume divides to pass on either side of a hill (see Section 2.3.3.1).

2.3.3 Plume equations derived for application over elevated ground

2.3.3.1 Solution of the diffusion equation for flow around a round hill

Hunt *et al* (1979) idealise the flow around the sides of a round hill below the critical streamline (see Section 2.2.1.1). They solve the horizontal diffusion equation in terms of the velocity stream function ψ and velocity potential ϕ for two-dimensional potential flow around a cylinder. The radius of the cylinder is set equal to the radius of the hill at the height of interest.

The functions ϕ and ψ are defined by

$$u = -\frac{\mathrm{d}\phi}{\mathrm{d}x} = \frac{\mathrm{d}\psi}{\mathrm{d}y}$$
$$v = -\frac{\mathrm{d}\phi}{\mathrm{d}y} = -\frac{\mathrm{d}\psi}{\mathrm{d}x} \qquad (2.11)$$

where u is the x-component of the flow velocity and v is the y-component. It is convenient, however, to solve the equations of potential flow around a cylinder in cylindrical polar coordinates, with $\theta = 0$ along $y = 0$ (the x-axis) and increasing anticlockwise. Then v_T is the component of the flow velocity in the θ -direction (positive anticlockwise) and v_R is the component in the r-direction. For a cylinder of radius R, the boundary conditions for potential flow are $v_R = 0$ at $r = R$ and $v \to 0$, $u \to U$ as $r \to \infty$. These are satisfied by

$$v_T = -\frac{U}{r^2}\left(r^2 + R^2\right)\sin\theta$$
$$v_R = \frac{U}{r^2}\left(r^2 - R^2\right)\cos\theta \qquad (2.12)$$

which give

$$\psi = \frac{U}{r}\left(r^2 - R^2\right)\sin\theta$$
$$\phi = -\frac{U}{r}\left(r^2 + R^2\right)\cos\theta \qquad (2.13)$$

Upstream of the stagnation point, the diffusion equation in these coordinates gives the solution, where dashes represent parameters normalised by wind speed and hill radius,

$$C = \frac{Q}{2UR\sigma_z\sqrt{\pi(\phi'-\phi'_s)D}}\exp\left\{-\frac{(\psi'-\psi'_s)^2}{4D(\phi'-\phi'_s)}\right\} \tag{2.14}$$

for the concentration C from a source of strength Q at position (ϕ'_s, ψ'_s), where U is the wind speed, R is the radius of the hill at the height of interest, D is the diffusivity in the horizontal plane (normalised by dividing by the undisturbed wind speed, the hill radius and the source height), and σ_z is the vertical plume spread, which is assumed to be unaltered by the presence of the hill.

Downstream of the stagnation point, the concentration may be calculated using

$$C(\phi',\psi') = \frac{1}{2\sqrt{\pi(\phi'-\phi_s')D}}\int_{L_1}^{L_2} C_1(\psi^*)\left\{\exp\left(-\frac{(\psi'-\psi^*)^2}{4D(\phi'-\phi_1')}\right)+\exp\left(-\frac{(\psi'+\psi^*)^2}{4D(\phi'-\phi_1')}\right)\right\}d\psi^* \tag{2.15}$$

where $L_1 = 0$, $L_2 = \infty$, for $\psi' > 0$ and $L_1 = -\infty$, $L_2 = 0$, for $\psi' < 0$; $C(\psi^*)$ is given by the formula for upstream of the stagnation point with $\phi' = \phi'_1$. The above expression is used round the side of the hill as far as the point where flow separation occurs. The calculation of concentrations in that region will be considered separately in Section 2.3.6.

This model, applied with the normalised diffusivity $D = 0.001$, makes a number of significant predictions for concentrations below the critical streamline on a round hill from a source upwind in stably stratified conditions.

(a) The position of the maximum hill-surface concentration moves rapidly from $\theta = 180°$ for a source directly upwind of the centre of the hill to $\theta = 90°$ for a source more than 10 to 20% of the hill radius away from there in a cross-wind direction.

(b) The plume centreline concentration varies little around the circumference of the hill, and the maximum concentration is not very sensitive to the position of the maximum concentration.

(c) Assuming constant diffusivity, the divergence of streamlines near the stagnation point causes diffusion to be reduced. The concentration where the plume impinges on the hill is therefore greater than the plume centreline concentration in the absence of the hill.

The calculations are compared with predictions of maximum ground-level concentrations from a Gaussian image-source model (see Section 2.3.2.4), and found to agree closely providing the source is offset from the hill centreline by a distance more than double the horizontal plume spread in the absence of the hill. It is concluded that the image-source method overestimates the maximum concentration under conditions when the plume splits to pass both sides of the hill.

2.3.3.2 Solution of the diffusion equation for flow over a round hill

Hunt *et al* (1979) use a similar method to that outlined above (Section 2.3.3.1) for three-dimensional potential flow over a hemisphere. This illustrates how sensitive the ground-level concentration can be to the height of the release relative to the height of the hill. For releases close to the ground and far from the hill (a distance several times the height of the hill), the maximum ground-level concentration is found upwind of the hill. For releases far above the ground (comparable with the height of the hill) close to the hill, the maximum ground-level concentration is found downwind of the hill. In either of these conditions, the effect of the hill is much less

than it is for intermediate release heights. For example, as the release height close to the hill is varied from 0.4 to 0.8 times the hill height, the maximum ground-level concentration is reduced by a factor of ten.

At a release height of 0.4 times the hill height close to the hill, the presence of the hill causes the maximum ground-level concentration to be increased by a factor of five or more from that on flat ground. This is much greater than that on a two-dimensional hill, as the three-dimensional hill causes streamlines to be brought down significantly closer to the hill surface. Whereas, for a two-dimensional hill, the divergence and convergence of streamlines are important, this model for a three-dimensional hill illustrates the primary importance of streamline displacement over a three-dimensional hill.

2.3.3.3 Solution of the diffusion equation in stream-following coordinates for flow over a hill

An alternative to specifying flow in a simplified geometry as above is to use a streamline coordinate system (Ma and Robson, 1995), including the possibility that the flow may not be irrotational. Simplifying assumptions, such as a power-law dependence of vorticity on stream function, lead to analytical solutions. In more general cases, an approximate numerical method of solution can be used. The use of the diffusion equation leads to results of similar applicability to those outlined above. Given a realistic flow field, such as that obtained from an airflow model, this provides an alternative method of obtaining concentrations over irregular terrain to that described in Section 2.3.5.

2.3.3.4 Calculation of maximum concentration value and position using normalised plume parameters

Trombetti and Tampieri (1992) present a hypothesis that, up to a certain distance (of the order of the length of a hill) from the source of a release, dispersion is dominated by parameters at the source rather than by the hill. They test this hypothesis for isolated two-dimensional hills some kilometres in length and some hundreds of metres in height, under neutral stratification in a wind tunnel (Khurshudyan *et al,* 1981).

The distance x_m from the source to the point of maximum ground-level concentration is transformed to a non-dimensional parameter ξ_m using the ratio of advection travel time and vertical diffusion time:

$$\xi_m = \frac{x_m K}{h^2 U} \tag{2.16}$$

where h is the release height, and U and K are the wind speed and vertical eddy diffusivity, respectively, at the release height. The value of the concentration C is transformed to a non-dimensional parameter χ using the source emission rate Q, the wind speed at the source and the release height:

$$\chi = \frac{h^2 U C}{Q} \tag{2.17}$$

Terrain amplification factors (TAFs) are used to test the efficacy of this normalisation for the value of the maximum ground-level concentration. A TAF is the ground-level concentration (C or χ) in the presence of the hill divided by the ground-level concentration that would be found if the hill was not there. TAFs calculated using the maximum normalised ground-level concentration χ_m for the wind tunnel data are found to be closer to unity than TAFs calculated using the maximum

unnormalised ground-level concentration C_m. For example, for a hill of half-length eight times the height, the unnormalised TAF at x_m is reduced from 1.45 to a normalised TAF of 1.08 for a source upwind of the hill at a quarter of the hill height above the ground. In other words, ignoring the hill completely would result in a 45% underestimation of the maximum ground-level concentration but only an 8% underestimation of the normalised maximum ground-level concentration. Similar results are found for different source heights and for releases at the summit of the hill. For releases downwind of the hill, the normalisation reduces the size of the error by about one-third. There are some systematic errors associated with the changes in mean flow and turbulence at various source positions compared with elsewhere on the hill (see Section 2.2.1.2). These become larger as the half-length of the hill is reduced relative to the height from a ratio of eight down to a ratio of three, such that the errors caused by ignoring the hill are reduced by about 50% for a source upwind of the shortest hill studied.

These findings support Trombetti and Tampieri's original hypothesis, as the difference between the unnormalised and normalised TAFs arises from the effect that the hill has on U and K at the source. The way in which one may more readily ignore the hill completely when using normalised parameters than when using unnormalised ones illustrates to what extent the influence of the hill on dispersion is dominated by the effect of the hill on flow and turbulence at the source rather than by its effects at any other points in the flow field.

2.3.4 Modified Gaussian models

Various EPA recommended models incorporate simple screening procedures to capture salient features of dispersion over elevated ground, as discussed above (Section 2.3.1). Until recently, a model similar to the COMPLEX1 algorithm employed in ISC3 was recommended as a model in its own right, called RTDM (rough terrain dispersion model). This has now been superseded by the considerably more sophisticated CTDMPLUS (complex terrain dispersion model plus) (Perry, 1992, and CTDMPLUS source code). CTDMPLUS is arguably the most elegant EPA atmospheric dispersion model to date. It incorporates physical processes that influence dispersion over complex terrain in a way that is computationally highly efficient and that can readily be understood by a non-expert familiar with standard Gaussian plume models. CTDMPLUS is the result of many years of research and validation. However, it is important to remember that EPA develops models primarily for its own regulatory requirements, usually for continuous elevated sources, and the needs for modelling non-stack sources, including many accidental releases, may be different.

CTDMPLUS uses the results of models applicable to complex terrain to modify receptor locations and dispersion parameters so that a Gaussian plume formulation can then be used as if the flow were over flat ground, with just a few alterations to account for impenetrability of the hill where the plume divides around it. The model uses the critical streamline concept outlined in Section 2.2.1.1 to divide the model domain over elevated terrain into two regions above and below a critical height h_c. A different model is used to modify the Gaussian formula in each region.

In the lower region, the hill is approximated to a vertical ellipsoid. It is assumed that the hill causes the streamlines to be deflected and the wind speed to be altered, but that dispersion is not modified by the hill in this region. Analytical solutions to potential flow, similar to those around a cylinder described in Section 2.3.3.1, are used to compute effective distances d from the distorted plume centreline to receptors around the sides of the hill. These values are then used in the following Gaussian plume formula, which is modified to account for the fact that the plume splits into two halves that are separated from each other by the hill.

$$C(s,0,z_R) = \frac{Q}{4\pi U\sigma_y\sigma_z}\exp\left[-0.5\left(\frac{d}{\sigma_y}\right)^2\right]\left[1+\text{sign.erf}\left(\frac{d\sigma_y{}^*}{\sqrt{2}\sigma_{y0}\sigma_y}\right)\right]$$
$$\times\left\{B_1\exp\left[-0.5\left(\frac{z_s-z_R}{\sigma_z}\right)^2\right]+B_2\exp\left[-0.5\left(\frac{z_s+z_R}{\sigma_z}\right)^2\right]\right\} \quad (2.18)$$

The factor (sign) is equal to +1 if the receptor and plume centre are on the same side of the stagnation streamline and equal to −1 otherwise; erf is the mathematical error function

$$\text{erf}\,x = \frac{2}{\sqrt{\pi}}\int_0^x e^{-w^2}\,dw$$

and the factors B_1 and B_2 are given by

$$B_1 = \text{erf}\left(\frac{b_1-b_2-b_3}{b_0}\right)+\text{erf}\left(\frac{b_1+b_2+b_3}{b_0}\right)$$

$$B_2 = \text{erf}\left(\frac{b_1-b_2+b_3}{b_0}\right)+\text{erf}\left(\frac{b_1+b_2-b_3}{b_0}\right)$$

with

$$b_0 = \sqrt{2}\sigma_z\sigma_{z0}\sigma_z{}^*$$
$$b_1 = h_c\sigma_z^2$$
$$b_2 = z_R\sigma_{z0}^2$$
$$b_3 = z_s\sigma_z{}^{*2}$$

Here, z_s and z_R are source and receptor height, respectively, σ_y and σ_z are the plume spread at the receptor assuming no terrain effects, σ_{y0} and σ_{z0} are the plume spread from the source to the point where the plume reaches the hill, $\sigma_y{}^*$ and $\sigma_z{}^*$ are the spread as the plume moves around the hill to the receptor, and s is the distance around the hill.

In the upper region, the hill is approximated to a Gaussian terrain cross-section. Analytical solutions to linearised equations of motion for steady-state Boussinesq flow (Smith, 1980) are used to compute the deflection of the streamlines (the use of such models is discussed also in Sections 2.3.1.2 and 2.3.5). From these results, an effective distance from the plume centreline to the receptor for the Gaussian plume formula is found by comparing the streamline through the source with the streamline through the receptor. The distance s along a streamline to the receptor is found to replace x. Also, the change in distance between streamlines as the air flows over the hill is used to calculate modified dispersion parameters σ_{ze} and σ_{ye}. For example, the modified vertical dispersion is given by

$$\sigma_{ze}^2 = \sigma_{z0}^2+\left(\frac{\sigma_z{}^*}{T_z}\right)^2 \quad (2.19)$$

where σ_{z0} is the plume spread from the source to the point where the plume first meets the hill and $\sigma_z{}^*/T_z$ is calculated from the vertical diffusivity, K_z and the ratio T_h between the vertical streamline separation over the hill to that upwind, using

$$\left(\frac{\sigma_z{}^*}{T_z}\right)^2 = \int_{t_0}^{t} 2K_z(t')e^{-2[T_h(z_m,t')-1]}\,dt' \quad (2.20)$$

where z_m is the streamline height above the surface far upwind (Hunt and Mulhearn, 1973). These are then used in the following adjusted Gaussian plume formula for receptors on the hill surface:

$$C(s, y_R', 0) = \frac{QF_z}{4\pi u \sigma_{ye}\sigma_{ze}} \exp\left\{-0.5\left(\frac{y_R - y_s}{\sigma_{ye}}\right)^2\right\} \tag{2.21}$$

where

$$F_z = 2\exp\left\{-0.5\left(\frac{h_c - z_s}{\sigma_{ze}}\right)^2\right\}\left\langle 1 + \mathrm{erf}\left\{A_z(z_s - h_c)\left(\frac{\sigma_z^*}{T_z}\right)^2\right\}\right\rangle$$
$$+ 2\exp\left\{-0.5\left(\frac{h_c + z_s}{\sigma_{ze}}\right)^2\right\}\left\langle 1 - \mathrm{erf}\left\{A_z(z_s + h_c)\left(\frac{\sigma_z^*}{T_z}\right)^2\right\}\right\rangle$$

and

$$A_z = \frac{T_z}{\sqrt{2}\sigma_{z0}\sigma_{ze}\sigma_z^*}$$

In unstable conditions, the lower layer of flow around the hill does not exist. The streamlines are assumed to follow those calculated by the linear model for neutral stability. The height of the unstable mixed layer is set by fixing streamlines at its top to deflections commensurate with those found in a laboratory study. This adjustment to the mixing layer depth varies from 0.1 to 0.9 times the terrain height. For completeness, it should be noted that CTDMPLUS uses a skewed Gaussian vertical distribution in unstable conditions. In this respect, it is similar to ADMS. The treatment of the effects of the terrain, however, is quite different (see Section 2.3.5).

Both ADMS and CTDMPLUS use linearised flow equations where air travels over the top of the hill, but the assumption of Gaussian hill profiles allows greater computational speed for CTDMPLUS than ADMS at the expense of risking gross approximation to some markedly non-Gaussian hill shapes. Dispersion below the critical dividing streamline height is treated by CTDMPLUS using a formulation that is similar to that above the critical height yet which reflects the quite different flow patterns there. Flow below the critical height is not yet included in ADMS.

The development of CTDMPLUS has included field validation using SO_2 from a power plant stack on the bank of the Hudson River near New York (Paumier *et al,* 1992). This showed that the model overpredicted the top 25-hour concentrations paired by rank by a factor of two, compared with a factor of five by the simpler RTDM model. For 24-hour concentrations paired in time, about half the predictions of both CTDMPLUS and RTDM were within a factor of two of the measured concentrations. On the basis of these statistics, it is possible to recommend CTDMPLUS as a better model for regulatory purposes than RTDM, because its overprediction is desirable without being excessive. However, while RTDM, on average, overpredicted 24-hour averages paired by time by a factor of two, CTDMPLUS on average underpredicted by 30%. Although this is not a problem for a regulatory model in situations where annual averages or percentiles from continuous releases are required, there may be circumstances in which RTDM or some other more pessimistic model might be safer for modelling short-term accidental releases.

2.3.5 Use of an airflow model to calculate Gaussian plume parameters over elevated ground

The approach employed by ADMS (Carruthers *et al,* 1994) to model dispersion over hills is to use the linearised airflow model Flowstar (Carruthers and Hunt, 1990; Carruthers *et al,* 1991; Hunt *et al,*1988) to calculate dispersion parameters over elevated ground. Flowstar finds analytical

solutions to linearised momentum and continuity equations over terrain defined on a grid of up to 64×64 points, including the effects of stratification of the atmosphere. Flowstar divides the atmosphere into three layers. In the upper layer, the pressure field, caused by the interaction of stratification with the terrain elevation, is found by solving the equations for stratified flow that is inviscid, ie neglecting any vertical variation in wind speed and any momentum transfer that would result. In the layer close to the ground, the way in which the hill surface causes the wind to be deflected from straight lines of constant velocity is calculated using Bessel equations. The transport of momentum to the ground via shear and shear stresses is treated by assumption of local equilibrium of turbulence (see Section 2.3.1.2). The discontinuity between these two layers is removed by the insertion of a middle layer in which shear stresses are neglected but the wind speed is allowed to vary with height. The use of linearised equations permits the use of Fourier transform methods of solution, which greatly reduces computing time.

Analogous to the validation of dispersion models by field and laboratory experiment is the series of experiments carried out to validate airflow models, a detailed description of which is beyond the scope of this review. From the results of such experiments, linearised models such as Flowstar are known to perform best in prediction of the mean flow up to the summit of a hill of moderate slope (eg Mason and King, 1985). Performance deteriorates down the lee side of a hill and for hill slopes greater than about 1 : 3. Turbulence parameters are not modelled so well as the mean flow (Bradley, 1980). In some cases, systematic errors cancel out, such as underestimation of speed-up with overestimation of turbulence, such that the calculation of the effect of the hill in causing ground-level concentrations to increase is more accurate than the linear model's calculation of the individual parameters that control the dispersion. Linear models are completely incapable, however, of treating any reverse flow or separation, or instances when air is deflected around the sides of the hill instead of over it. This is a serious limitation, as it is plume division to pass around a hill that can lead to the highest concentrations on the ground. Linear models are only valid when the changes in flow velocity and the lateral displacement of the streamlines are small compared with the mean wind and the size of the hill.

The major advantage of using Flowstar, or a similar model to calculate dispersion parameters over elevated terrain, is that some effects of irregularity and asymmetry in real hills can be taken into account. The amount of computing time for a single set of meteorological and release conditions is relatively short – a few minutes on a typical Pentium personal computer. However, such run times are prohibitively long for long series of meteorological data. The complexity of the problem is simply too great to risk using any statistically aggregated meteorological data to calculate long-term average concentrations. The possibility that effects not treated by linearised models could be important means that the use of such a model for many regulatory modelling purposes can hardly justify the computing time required when some of the more idealised models and methods outlined in Sections 2.3.1–2.3.4 are cheaper and may be more applicable. However, for an accidental release of short duration occurring in specified conditions in which a linearised model is valid, the versatility and realism of a model such as Flowstar can easily justify the significant amount of computer programming involved.

2.3.6 Separated flow regions and stagnation

Most simple methods of modelling dispersion cannot predict details of advection and diffusion in regions where the flow separates as in a wake behind a hill, or where large volumes of air are stagnant as in blocked flow upwind of a ridge in stable conditions. A common way around this is to compute the approximate position of the streamline that bounds the separated region and then to

assume that material is homogeneously mixed within that region (Hunt *et al*, 1979). In evaluating the rate of transfer of material between the separated region and the flow outside, there is a significant difference in theory between two- and three-dimensional hills. Behind a two-dimensional ridge, material can be transferred into and out of a separated flow region only by diffusion. Behind a three-dimensional hill, however, material can enter the separated region by advection.

All models that assume homogeneous mixing of material within a separated or stagnant region will predict that any part of the plume entering that region effectively impinges on the ground. This may not necessarily be true. Alternatively, and more seriously, the predicted concentration may be a significant underprediction.

A non-linear model of airflow and turbulence is required to resolve advection and diffusion in such areas. The most usual example of this is the k–ε model. This is able to produce qualitative or even semi-quantitative calculations of ground-level concentrations in a recirculation zone, including plumes that impinge on the hill surface upwind of the source (relative to the flow aloft) in reverse flow downwind of a hill (Castro and Apsley, 1997). This will be discussed again in Section 2.3.8.

2.3.7 Effect of hill shape

Many of the modelling techniques outlined above assume idealised, geometrical hill shapes, in order to capture the salient features of the dispersion. It should be borne in mind, however, that irregularities in the hill shape, that are removed by idealised models, can have a significant effect on flow and dispersion (Colvile *et al*, 1994). For example, the assumption of an abrupt, level critical height separating regions of flow around the hill and over it may be unrealistic for certain terrain shapes, slopes and orientations (Smith, 1990). Even general conclusions concerning to what extent dispersion is increased over a ridge or a three-dimensional hill may depend on details of the hill slope and cross-sectional shape, as comparison of different wind tunnel studies shows (Gong, 1991). There is therefore a great advantage to be gained from using an airflow model that considers real terrain features. Quite often, the compromise between computer run time and realism will be a hard one. For example, linearised models (Section 2.3.5) fail to consider flow round the hill at all, while a k–ε model to consider this requires significantly greater computational effort (Sections 2.3.1.2 and 2.3.8). However, even if the results are only qualitatively correct or realistic only in certain respects, a model that considers real terrain features can be valuable as a check on the significance of the assumptions made in geometrically more simplified techniques for a given location and meteorological conditions.

2.3.8 CFD modelling applications

In the preceding sections, the importance of irregular hill shapes (Section 2.3.7), flow around the hill as well as over it (Section 2.2.1.1), and separation and stagnation (Section 2.3.6) have been considered. The ability of linear airflow models to consider irregular hill shapes but not flow around a hill, nor separation or stagnation, has been identified (Section 2.3.5). For this reason, as powerful computers become more and more readily available, interest in a more sophisticated solution of the equations of motion of air over hills has been growing steadily.

General-purpose computational fluid dynamics (CFD) codes are available that have user-friendly input and graphical output. However, the main disadvantage of industrial user-friendly and custom designed 'home-made' codes alike is that they are still not suitable for use by non-experts. The user interface of StarCD, for example, includes a large number of options and switches. To assume a simple logarithmic wind profile, it is necessary for the user to write a routine in Fortran and to recompile the model. CFD models specially adapted for environmental applications in general, and hills in particular, may include a number of refinements (Castro and Apsley, 1997).

For example, in the atmosphere, the upper limit on eddy size is imposed by the boundary layer. The standard k–ε representation of turbulence cannot model these large eddies correctly. This can be improved by the use of a correction to the parameter that sets the general level of turbulence production, to take account of the response of turbulence structure to the curvature of the mean flow. Standard k–ε models can also produce unphysical upstream turbulence and trailing eddies caused by strong axial pressure gradients in environmental applications, and this can be corrected for by a modification to the equation describing the production of turbulence. The latter correction has been developed for bluff bodies such as buildings, but has been shown to be applicable for hills as well.

One more easily appreciated pitfall in CFD modelling is the choice of grid resolution. Over-refinement of the grid is impractical because of prohibitively long computer run times. However, for airflow and turbulence, the grid needs to be finest close to steep gradients in the flow and turbulence parameters. For dispersion modelling, the grid needs to be finest close to large concentration gradients. These may not be in the same place. One possible solution to this problem is to compute the flow and turbulence fields first, and then interpolate these on to a different grid on which to carry out the dispersion calculations.

Finally, simpler modelling warns us (eg Section 2.3.3.1) that the flow and dispersion in the vicinity of a hill can be highly sensitive to changes in parameters such as wind direction. Care must therefore be taken in the use of any CFD model on a hill that considers only a single wind direction. One way of considering the variability of wind direction is to consider a point source to be spread out with a Gaussian distribution of source strength as a function of distance perpendicular to the mean wind direction. This is computationally efficient, but is beginning to make some assumptions about the symmetry of the hill, and one of the aims of CFD is to make few such assumptions. Many CFD modelling techniques are capable of explicit treatment of variation in wind direction, by means of a transient solution of the equations of motion. This can also take account of processes such as the deposition and subsequent re-emission of a gas that is deposited on the ground, as the plume doses part of the hill and then moves away. Computing time for such an approach, however, is so many orders of magnitude greater than that for the simple models that an extremely good justification of the effort involved is required.

It is beyond the scope of this review to consider all these details in depth, but the intention is to stress that there are a number of issues that need to be handled with care in the environmental application of CFD.

An example of successful application of a CFD model is the application of SWIFT to the RUSHIL two-dimensional wind tunnel data (Castro and Apsley, 1997; Khurshudyan *et al,* 1981) and the Cinder Cone Butte three-dimensional field measurements (Apsley and Castro, 1997). This illustrates the sensitivity of ground-level concentration to wind direction on a round hill, including the effects of slight asymmetry of Cinder Cone Butte. It succeeds in capturing the recirculation region behind hills and ridges and illustrates how the plume in the recirculation region can impinge on the hill some distance away that is upwind of the source relative to the mean flow over the hill.

2.4 Hills in models of long-range transport of material

This review focuses on calculating concentrations in plumes close to the release point. A brief discussion of additional factors which may be taken into account when considering larger-scale transport (above about 100 km) is therefore included here only for the sake of completeness.

When the scale of a model becomes large compared with the length of hills, it may be appropriate to consider regions of hilly terrain as a change in surface roughness, which can be

estimated from theory and smaller-scale modelling or calculated from aircraft measurements. The main criterion that determines whether to use such a flat surface roughness model, or to go to the considerably greater computational effort of using one that considers individual hills explicitly, is the level of detail that is required of model output. In any case where the effect of elevated terrain on spatial variability in local concentration or deposition at specific points on that terrain is of interest, the elevated terrain should be treated explicitly. In any model that treats hills simply as surface roughness, predicted concentration and deposition values will be completely independent of local hill slope or elevation. Use of such a simple surface roughness model will give concentration and deposition estimates averaged over the whole of the terrain with a similar or slightly greater amount of realism to the simplest empirical hill effect models described in Sections 2.3.2.1–2.3.2.3. In fact, all practical model applications at any scale need to treat as surface roughness individual features that are smaller than a certain size, which often includes objects such as buildings and trees as well as small hills or hummocks. In many cases, the point at which this obstacle size cut-off is made will be determined by the choice of model and the spatial resolution with which that model is applied within constraints imposed by computer programming, memory and execution time restrictions. In any presentation of model results, it is important to demonstrate fitness for purpose of the selected modelling approach and implementation (Britter *et al*, 1995), and this should include, when appropriate, discussion of choice of grid resolution and estimated magnitude of subgrid effects that have been ignored, including terrain features.

Neglecting the detail of individual roughness elements, the increase in roughness due to hills acts to enhance lateral spread of a plume, rather like buildings in a city or trees in a forest. Additional factors such as the aerodynamic drag that hills exert on the atmospheric boundary layer may be considered in models such as weather forecasting models that are also used to compute transport and dispersion of material released into the atmosphere. Sometimes, orographic effects such as terrain-induced convection need to be parameterised as subgrid effects. When the released material can be taken up into cloud droplets or washout out of the air by rain, it may be especially important to consider the seeder–feeder effect. This is where rain from frontal clouds falls through hill cap cloud below and efficiently washes material out of the hill cap cloud by collection of cloud droplets by the falling rain. Where a plume enters a hill cap cloud, this can be an especially efficient way of depositing material to the ground. The seeder–feeder process can result in deposition on to elevated ground being several times higher than on to flat ground. At the very largest scale, large convective motions and weather systems can transport material out of the troposphere into the stratosphere, and so achieve global transport. This includes thunderstorms that can be triggered on elevated terrain.

3 Plumes impinging on buildings

3.1 Introduction

3.1.1 Background

The existing literature on dispersion around buildings is vast, and well over 450 papers can be found on the subject (Hall, 1996a,b). This section is not intended to be a comprehensive review of all relevant previous work, but a brief survey of available information that is directly applicable to situations involving plumes impinging on buildings.

3.1.2 Existing information and modelling techniques

Dispersion modelling techniques fall into mainly two broad categories: scaled flow simulations and mathematical or numerical models.

3.1.2.1 Scaled flow simulations

Scaled flow studies involve the simulation of the flow and dispersion behaviour using a scaled model of a single building, or group of buildings in either a wind tunnel or a water tank. Most of the primary information on dispersion phenomena around buildings has been provided by small-scale wind tunnel experimental data, simulating neutrally buoyant flows. Some studies have been carried out in water tanks, mainly to investigate stratification effects. A few full-scale field experiments have also been carried out, although these have served mainly as a validation of wind tunnel experiments. The most comprehensive reviews of wind tunnel study results on dispersion around buildings are those of Hosker (1981) and Hosker and Pendegrass (1987). Conference proceedings on wind tunnel modelling provide the latest developments in wind tunnel studies such as the recent workshops in Karlsruhe (Robins, 1994), Stevenage (Hall and Robins, 1994), and Japan (EURASAP, 1996). Wind engineering research on wind loading and environmental applications (such as ventilation around buildings and pedestrian comfort) is a source of valuable information on flow patterns around buildings that can also be applicable to dispersion modelling (eg Cook, 1985 and 1990).

3.1.2.2 Mathematical or numerical models

Many mathematical and numerical models exist for dispersion calculations, although given the complexity and diversity of dispersion phenomena occurring around buildings, these models are approximate and strongly case-specific. Apart from a very limited number of theoretical models of some aspects of dispersion around buildings, the vast majority of numerical models are based on semi-empirical, approximate approaches to dispersion calculations. Such models for modelling concentrations on and inside buildings when plumes impinge are discussed in detail in Section 3.3. The main sources of information on available modelling methods are the research papers by Wilson and co-authors who have contributed many useful guidelines for calculating concentrations around and on buildings, other numerical correlations from wind tunnel studies, and descriptions of available Gaussian models, such as NRPB-R91 (Clarke, 1979), ADMS (Carruthers *et al*, 1994), ISC2/3 (EPA, 1995), and OML (Olesen *et al*, 1991). The ASHRAE Handbook (ASHRAE, 1993) is also a useful compendium of information on stack and air vent design to avoid contamination of buildings from roof and wall discharges.

Computational fluid dynamics (CFD) is a type of numerical modelling based on the numerical solution of the fundamental fluid mechanics conservation equations of mass and momentum, with the use of approximate turbulence and dispersion models. At present it is regarded as 'a relatively unproved technique which has contributed little to the research literature' (Hall *et al*, 1996). Nonetheless, there is growing interest in CFD, as computing resources, more robust codes and user-friendly graphical interfaces become more widely available. It is expected to become increasingly popular as a viable alternative tool, to complement or even replace wind tunnel studies in dispersion modelling, as is already happening in fluids research for the aerospace and automotive industry. Section 3.3.8 presents current CFD applications for dispersion modelling around buildings.

The EC COST Action 615 Inventory (Schatzmann *et al*, 1996) is a relevant compendium of information on existing CFD and other numerical models (as well as validation datasets) for modelling pollution dispersion in the urban environment.

3.1.3 Classification of types of release

3.1.3.1 Scales of dispersion behaviour as influenced by buildings

The scales of different types of building influence on an impinging plume range from a few metres in the vicinity of the building, to a few kilometres downstream. Near the building the plume becomes distorted, displaced or trapped by the complicated flow field around it. These

'building effects' can then persist and affect the shape and rate of dispersion of a plume a long way downstream.

Turbulence length scales determine the rate of dispersion in a plume. For a plume impinging on a building, turbulence in the approach flow is enhanced, and becomes dominated by building-generated turbulence caused by flow separation. The simplest length-scale for building-generated turbulence is $L = A^{1/2}$, where A is the frontal projected area of the building. This will be the scale adopted here, although it is not realistic for long, slender obstacles, in which case most of the flow passes around the smallest dimension making this the dominant scale length (Wilson and Britter, 1982).

On the basis of a comparison of plume width to the length-scale of building-generated turbulence, the influence of a building on plume dispersion may be divided into three broad regimes, as follows.

(a) *Plume width* $<< L$. A plume originating from sources on or near a building has a width which is much smaller than the length-scale of building-generated turbulence. As the thin plume interacts with the much larger building, a wide range of potential dispersion scenarios are possible that are difficult to categorise accurately and reliably. Dispersion behaviour is sensitive to a large number of variables, and the phenomena involved are non-steady even under steady weather conditions. Very localised effects dominate dispersion causing highly case-specific behaviour and strong spatial and temporal variation.

(b) *Plume width* $\sim L$. From a source some distance upstream of a building, the plume can disperse sufficiently to have a width comparable with the building dimensions or to encompass a group of buildings. Turbulence generated by buildings influences the growing plume and contributes to plume meandering, but the dispersion patterns are less variable than those in the first case, because only the overall shape of the buildings governs the rate of dispersion, and the plume behaviour is relatively stable.

(c) *Plume width* $>> L$. A longer distance away from the building with a source near the building, or from a source far upstream of a building, the plume is very broad. Turbulence generated by buildings is a small part of the energy causing plume growth; turbulence is dominated by the drag of the surface as it affects the atmospheric boundary layer turbulence. This is the regime modelled by conventional Gaussian dispersion models.

The discussion of models in this section will focus on near-field dispersion, corresponding to the first two regimes. Regime (a) is the most difficult to model, because dispersion patterns are not only complex and temporally variable, but also particularly sensitive to the exact building shape, small changes in incident wind speed and direction, and turbulence characteristics. Scaled flow studies and CFD simulations can represent details of the building shape and incident wind, and provide detailed output. Nonetheless, this regime can be approximated satisfactorily by a variety of simple, yet limited empirical rules, applicable to specific aspects of dispersion behaviour. However, buildings of complex or unusual shape, or complex multiple-building sites fall outside the scope of such approximate, semi-empirical modelling. In those cases, only a scaled flow or CFD study should be used, the former being the more reliable method. The intermediate range (b) is amenable to simpler modelling, and it is possible to use modified Gaussian plume models.

3.1.3.2 Averaging times

When calculating and expressing concentrations, an important consideration is the averaging time. Wind tunnel and short-term full-scale measurements exclude the slow variations in

cross-wind turbulence that are perceived as wind direction shifts in the full scale (Wilson and Britter, 1982). Thus, concentrations predicted on the basis of wind tunnel data will represent average times in the full scale from about 1 to 10 minutes and can possibly be considered as typical of 3-minute averages.

Jones (1983) suggests that if the average concentration over longer periods is required then the effect of a fluctuating wind direction should be taken into account. Once the short-term average concentration C_s at a particular receptor can be determined as a function of any wind direction θ, the concentration for a longer averaging time C_T at a particular point for a particular wind direction θ_p is given by

$$C_T(\theta_p) = \int_0^{2\pi} P(T,\theta)\ C_s(\theta - \theta_p)\ \mathrm{d}\theta \tag{3.1}$$

where T is the averaging time in hours and $P(T,\theta)$ is the probability of the wind direction lying within θ and $\theta + \mathrm{d}\theta$ during that time.

For an averaging duration of up to a few hours, P may be taken to be a Gaussian distribution about the mean wind direction, with a standard deviation σ_θ given by

$$\sigma_\theta = 0.065\left(\frac{7T}{u_{10}}\right)^{0.5} \tag{3.2}$$

or, more simply, by the approximation

$$P = \frac{1}{2\sqrt{3}\sigma_\theta} \text{ for } |\theta - \theta_p| \le \sqrt{3}\sigma_\theta \tag{3.3}$$

$$= 0 \qquad \text{otherwise}$$

This process can be extended to the calculation of longer term averages, eg annual concentration, with the use of wind rose data for the distribution of wind directions.

3.1.3.3 Normalisation

Wind tunnel studies usually express measured concentrations C in non-dimensional form as either

$$\chi = \frac{CUH^2}{Q} \tag{3.4}$$

or

$$\chi = \frac{CUA}{Q} \tag{3.5}$$

where U is the reference wind speed (either at building roof-top level, or the free stream value at a standard height), Q is the rate of discharge of the contaminant, H is the height of the obstacle, and A is the projected frontal area normal to the wind direction. The choice of either H^2 or A usually depends on the particular geometry of the problem. For example, H^2 is usually applied to long buildings and A to more square buildings, but in many cases it may also be completely arbitrary.

3.1.4 *Role of atmospheric conditions and stratification*

The modelling methods to be discussed in this section have been developed using results from wind tunnel studies in neutral conditions. The effect of stable stratification on dispersion

around buildings has been investigated by only a few studies (eg Robins, 1994; Snyder, 1994). However, it is generally agreed that stable stratification is of limited significance to flows around obstacles in the near field, since the mechanical turbulence generated around them tends to overcome turbulence suppression by stratification, until quite pronounced levels of stratification are reached. Stratification is nonetheless important over longer ranges in the far wake where it can dominate dispersion behaviour.

Dispersion calculations are also generally based on the assumption of a steady wind. In the absence of a mean advection velocity, the plume disperses under the action of local atmospheric turbulence or source momentum or buoyancy. Plumes may then move away from the source but return later, or may break into discrete puffs that disperse randomly. As a result, low wind speed conditions introduce considerable uncertainty into the calculation of dispersion rates and direction of travel of plumes (Hall *et al*, 1996). Low or negligible wind speeds ($U < 2$ m s^{-1}) occur about 10% of the time in the UK. However, few papers discuss the subject (Sharan *et al*, 1995, is an exception), and there are as yet few published statistics on the details of frequency, duration and wind behaviour for 'still' air conditions (Hall *et al*, 1996). A description of the current state of knowledge of dispersion in low wind speeds is given by Jones (1998).

3.2 Flow patterns and pollutant dispersion around buildings

3.2.1 Major characteristics of flow around a single building

Dispersion behaviour is the combined effect of the 'advection' of a pollutant plume along the mean flow, and the 'diffusion' or dilution of the plume due to the effect of turbulence, which mixes the plume with the surrounding cleaner air. An understanding of the characteristics of flow around buildings, both mean flow and turbulence, is therefore fundamental to modelling the variety of dispersion situations arising when plumes impinge on buildings.

Figure 3.1 (from Hosker, 1981) illustrates the complexity of the flow arising around a simple rectangular building. These patterns are caused by the presence of the ground plane and the variation of wind speed with height in the approach flow. This diagram can be more easily understood in terms of the major flow regions as illustrated by Hall *et al* (1996) in Figure 3.2. These regions are caused by three main features of the flow: separated flow, the ground-based horseshoe vortex, and roof-top trailing vortices (absent from Hosker's diagram, because it illustrates normal wind incidence for which trailing vortices do not occur).

3.2.1.1 Separated flow

Separated flow regions occur where the flow ceases to follow the surface of the building, forming a recirculating turbulent wake. Separation happens at the downwind side of the edges of a building. Separated flow regions are thus formed at the roof top, at the sides of the building, and immediately downstream of the building. Flow that has separated at the upstream edges of the roof can re-attach forming either distinct roof-top and lateral separation 'bubbles' (as shown in Figures 3.1 and 3.2), or a continuous recirculation region merged with the downwind near wake. This depends on the geometry of the building and the details of the approach flow.

The recirculating flow in these regions is characterised by low wind speeds, large variations in wind direction with respect to the mean free stream velocity and intense turbulence. Within the separation 'bubble', this intense turbulence leads to high rates of mixing and dispersion. However, pollutants can become trapped inside as there is limited exchange with the air outside. This can give rise to high concentrations that can be retained in the bubble over a relatively long time. Emissions inside or entrained into recirculation regions are therefore influenced significantly by the building, and special considerations apply to modelling dispersion in them.

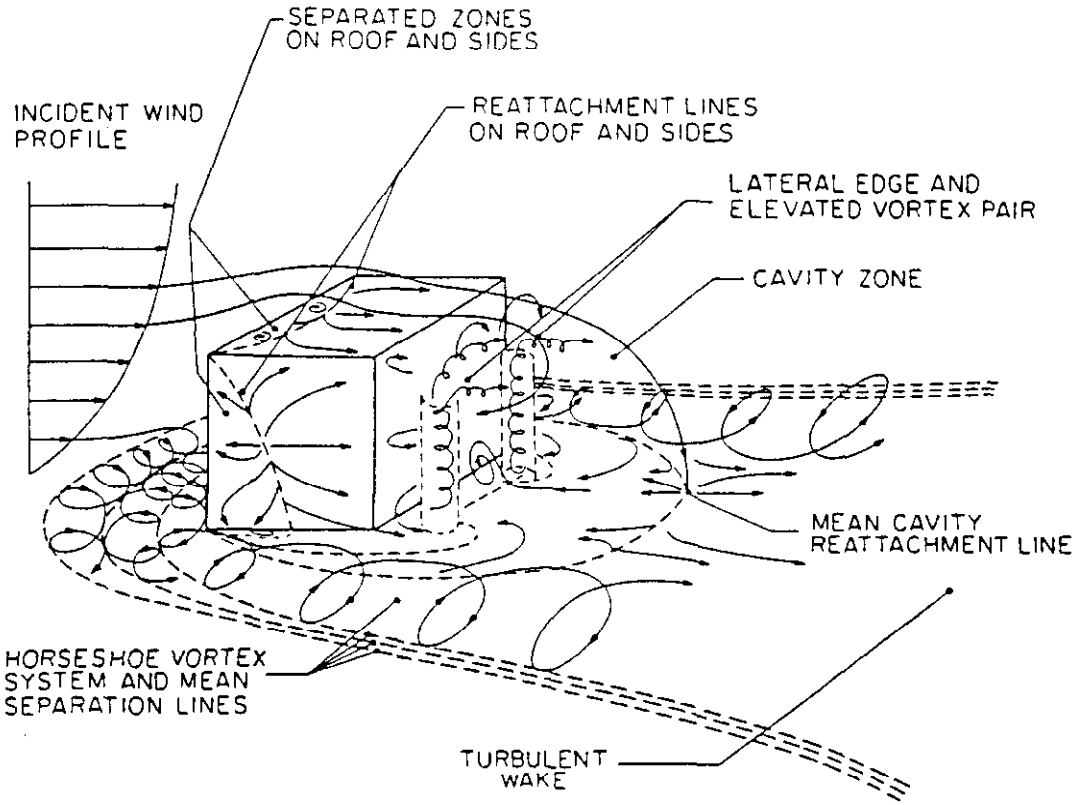

FIGURE 3.1 Major features of flow around a single rectangular building (reproduced with permission from Hosker, 1981)

The near recirculation wake immediately downstream of the building is the largest of the separation regions. It usually extends over $3H$ downwind for near cubic buildings, but for low, wide obstacles it can extend up to $12H$. This region is not a closed bubble, but material is periodically rolled up and ejected laterally (Hunt *et al*, 1978). Above the recirculating region there is a zone in which flow streamlines are deflected downwards significantly, and this can direct plume trajectories over buildings towards the ground, an effect referred to as building downwash. Beyond the near recirculation region is the far wake, in which the building generated turbulence is mild and decays gradually with distance.

3.2.1.2 Ground-based horseshoe vortex

This complex recirculation pattern appears at the ground around the upwind faces of buildings. It arises from the vertical shear that creates vorticity in the approaching boundary layer which rolls around the sides of the building. The vortex becomes stronger as the height of the building increases and intercepts increased amounts of vertical shear. The existence of the horseshoe vortex is critically dependent on the upwind flow stagnating on the upwind face of the building. If a corner of the obstacle is presented to the wind instead of a face (eg for a wind direction at 45°), or if the building is sheltered by another obstacle upwind, the vortex becomes weaker. The importance of the horseshoe vortex in dispersion modelling is that it can bring elevated plumes rapidly to the ground and spread contaminants laterally around the building (instead of over the building). This lateral spread can be significantly larger in width than the separation region behind the building (Hall *et al*, 1996).

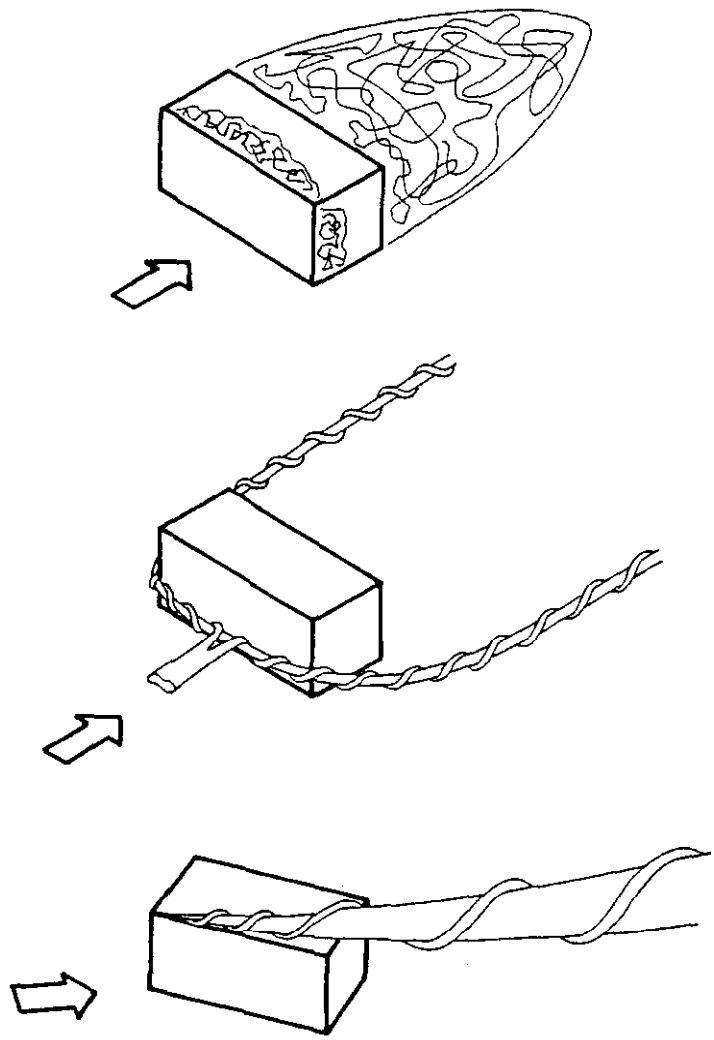

FIGURE 3.2 Major patterns of flow around a single rectangular building (reproduced with permission from Hall *et al*, 1996)

3.2.1.3 Roof-edge trailing vortices

These vortices are shed from sharp edges at the roof at acute angles to the wind direction, due to the separating shear layers from these edges (Castro and Robins, 1977). Rounded corners and low wide buildings ($W/H > 10$) suppress vortex generation. Their strength depends on the length of the edge, the angle of incidence, and the cross-sectional shape of the building. The strongest trailing vortices occur when the wind is at an angle of about 30° to a sharp edge . Little or no vorticity is associated with angles greater than 60°. When trailing vortices are strong they also tend to be particularly persistent. For simple rectangular buildings there are two edges that can shed trailing vortices, and about half of all the wind directions can be expected to generate significant trailing vorticity (Hall *et al,* 1996). Vortices usually occur in pairs, although one vortex can be stronger than its twin and persist longer. Trailing vorticity can have a strong influence on plume paths, by bringing a plume to the roof or the ground very rapidly and with minimum dilution; pollution trapped within a vortex escapes only slowly and so the spread of pollutant may on occasions be surprisingly less than in the absence of the building. The rate at which these vortices decay with downstream distance is enhanced by the action of turbulence, which tends to tear the vortices apart, although very stable atmospheric conditions can allow them to persist further.

The shape and the intensity of each of the flow features discussed above vary considerably with the shape of the building and wind direction, leading to the wide variety of flow patterns observed. Hall *et al* (1996) point out the lack of interest in the effects of the last two features of the flow and illustrate their role on plume dispersion with flow visualisation examples. The downwind near separation region is the most persistent and often the dominant feature of the flow, and it is possible to incorporate the complex effects due to the horseshoe and trailing vortices by combining them in an equivalent wake region. However, this approach may be inappropriate further downstream in the far wake, where strong trailing vorticity may still persist well away from the near wake.

3.2.2 Influence of nearby buildings and other types of obstructions

The majority of studies have focused on dispersion behaviour around a single building, but real dispersion problems more often than not involve groups of obstacles. Interactions between neighbouring buildings can add considerably to the complexities of the possible flow and dispersion patterns. Depending on wind direction, such interactions can either shelter or enhance wind effects, and so increase or decrease concentrations.

Hosker (1981) and Hosker and Pendergrass (1987) have reviewed dispersion near clusters of buildings. Hall *et al* (1996) mention papers on dispersion around specific sites, although, with the exception of the work of Bachlin *et al* (1992), it is difficult to separate general trends from particular site-dependent flow interactions.

The most simple multiple building interaction is that of experiments of two identical cubes placed along the mean direction of flow, as described in Hosker (1981). Effluent emitted from the upwind cube was carried to the lee face of the downwind cube, where concentrations were higher than those at its windward face. Other experiments involving two building interactions with different relative heights, aspect ratios and spacing, led to a wide variety of flow and dispersion behaviour strongly dependent on the above parameters. Gandemer (1976) presents some typical flow patterns and approximate wind speed ratios near building clusters for the mean and turbulent wind speeds.

The complexity of real site modelling is illustrated in Hatcher *et al* (1978), who modelled surface flow patterns and effluent concentrations around an experimental reactor complex. Their visualisations of surface flow patterns around a reactor building differ markedly depending on angles of incidence of flow and also on whether or not auxiliary buildings are included.

A common multiple building configuration is that of a closely packed array of buildings in urban areas. The most prominent feature is the street canyon (a street flanked with buildings on both sides). Figure 3.3 illustrates the typical recirculation pattern due to wind at right angles to the street.

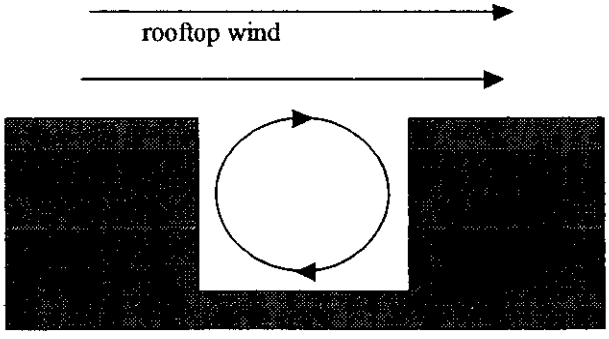

FIGURE 3.3 Recirculation pattern in urban street canyons for normal wind incidence

Smaller obstacles, such as walls, embankments and cuttings can also interact with the dispersion behaviour around a building. Behaving as low, wide obstacles, they can generate separated flow on their downwind side, as well as strong trailing vortices when skewed to the wind. Embankments and cuttings may behave differently depending on their slope; as discussed in Section 2.2.1.4, the flow can remain attached to the ground without separation for slopes of up to one in four.

Porous structures, such as trees and bushes, and industrial lattice structures, are also often encountered in practice, although less is known about the dispersion patterns around these. Trees, for example, can have a significant effect on small-scale dispersion patterns; when in full foliage they can cause plume downwash in a similar way to a solid obstacle. Some relevant information can be found in the experimental work of Raupach *et al* (1986), and of van den Hout *et al* (1989).

3.2.3 Criteria for plume impingement and building downwash

As a plume approaches a building its path is influenced by the shape of the streamlines over and around the building. The plume path may either:

(a) impinge on the building,

(b) be displaced by the building without causing surface contamination,

(c) pass close to the building without impinging, but subsequently be entrained in the wake recirculation region on the downwind side and return to cause surface contamination.

According to a simple criterion proposed by Jones (1983), plume impingement should be assumed to occur if the vertical distance between the plume centreline and the top of the building is less than σ_z and if the cross-wind distance between the plume centreline and the edge of the building is less than σ_y. However, criteria for impinging or non-impinging plumes becoming partially or totally entrained into the near wake or other recirculation zones are more difficult to define and will be discussed separately in Section 3.3.

Considering a thin plume impinging on a building (regime (a) dispersion scale, Section 3.1.3.1), exposure may result via one of the following four source–receptor paths. Firstly, there may be direct exposure to the plume, with both source and receptor in the same unseparated flow region. In this case the plume concentration is high but the probability of exposure is relatively low, due to its small cross-section and its tendency to meander even without the disturbances generated by the building. Secondly, there may be exposure to the entrained part of the plume in the wake of the obstacle, from a source outside the wake. In this case the concentration in the plume may be reduced by one or two orders of magnitude but the probability of exposure is higher, since the wake occupies a larger area and pollutants persist in the wake region for longer. Thirdly, when both the source and the receptor are inside the wake region there may be exposure to a combination of the uniform concentration in the obstacle wake and a near source plume exposure within the wake region (Wilson and Britter, 1982). Finally, with both the source and the receptor in unseparated flow, the plume may still pass through a recirculation region, in which case the plume reaching the receptor is considerably broader and the exposure lower and less variable both spatially and temporally.

There is always uncertainty about which dispersion pattern will occur, which depends not only on the shape of the building, but on small changes in incident wind speed and direction, and turbulence characteristics. Hall *et al* (1996) give examples of 'real' dispersion behaviour which reveal the inherent complexities. Estimates of dispersion behaviour around buildings may therefore be regarded as 'unreliable', although as Hall *et al* (1996) remark, they are in fact 'uncertain', since

any given dispersion pattern will occur reliably for given conditions, even though such conditions may vary unpredictably over time periods of a few minutes.

To quantify and manage this uncertainty Hall *et al* (1996) propose adopting a probabilistic approach for estimating the total exposure of a recipient for relatively short exposure times, when the variability of dispersion behaviour does not average out over time. By considering the probability of different types of exposure occurring (as described above) the total exposure can be estimated either by weighting these estimates and summing them, or by producing some other probabilistic exposure estimate. This could be associated with some form of mapping of the area around a building indicating the regions where the probabilities of plume entrainment into the different recirculation zones are high moderate or low, as well as the probability of exposure to the undiluted plume. This mapping could then be associated with the effects of changing wind direction.

Building downwash can significantly enhance exposure from non-impinging plumes. Building downwash occurs when a plume, following the lines of flow over a building, is directed towards the ground. It also refers to situations when material becomes entrained in the horseshoe vortex or in strong trailing vortices and is brought rapidly down to the ground. The effects of building downwash can be modelled as a reduction of the height and width of the plume, leading to increased ground-level concentrations. Methods for calculating the effects of building downwash are discussed in Section 3.4.

3.3 Calculating concentrations on and inside a single building

3.3.1 Empirical and theoretical models

The aim of this section is to present existing methods for calculating concentrations on and inside buildings from impinging plumes, which have been developed on the basis of theoretical considerations and available experimental data. Owing to the complex flow patterns around even a simple rectangular single building, it is difficult to derive a clear cut general method for the calculation of surface concentrations for buildings corresponding to dispersion regimes (a) and (b) in Section 3.1.3.1. There is no single model that can describe all features of a variety of possible pollution dispersion situations. Instead, we do have a series of semi-empirical rules based on experimental correlations that are applicable in particular situations.

Wilson and Britter (1982) highlight the difficulties inherent in seeking to develop models from experimental correlations. Such correlations have an inherent uncertainty factor of two to five for the concentration, mainly due to the sensitivity of receptor concentration to small shifts in a thin plume trajectory from a point source. The error in predicting local concentrations may be a factor of ten or more when the influence of nearby structures and local terrain are taken into account. With this level of uncertainty, it is argued, it is not necessary to develop complicated models for the interaction of the building with the surrounding flow, and simple diffusion models can usually be sufficient for design purposes. Estimates from some even rudimentary models can in some cases be remarkably accurate. However, some dispersion situations are still not amenable to simple modelling. Examples are localised effects around buildings of unusual shape, or groups of buildings. In such cases, wind tunnel tests are the most appropriate tool for modelling dispersion.

CFD modelling, another type of numerical modelling, is fundamentally distinct to the approximate, case-specific and empirical nature of the other numerical methods discussed in this section. CFD modelling is similar to wind tunnel modelling in the sense that it recreates the flow and dispersion field. Based on solving the fundamental fluid mechanics equations for any given geometry, it gives detailed spatial and temporal information on a wide range of parameters at any point of the flow, and can deal with any complicated building shape. However, CFD modelling is

not as reliable as wind tunnel testing and requires skilful use and careful validation. CFD dispersion modelling applications are discussed in Section 3.3.8.

Dispersion calculations around a simple single (isolated) building with the use of semi-empirical models will be the focus in this review, and only point sources of neutrally buoyant material will be considered. The different near-field dispersion situations involving plumes impinging on a single building can be divided into the following broad categories, according to the position of a source with respect to the building:

(a) sources upwind of the building,
(b) sources on the building,
(c) dispersion in the near-wake recirculation area,
(d) sources above the building.

Methods applicable to calculating concentrations on the building surface are described for each category separately in Sections 3.3.2–3.3.5. Contamination of air inside the building from outside sources is covered in Section 3.3.7. Methods for incorporating the effect of nearby buildings and other types of obstacles on dispersion behaviour around a single building are discussed in Section 3.3.6.

Modular empirical computational modelling programs that incorporate some of these methods for different situations exist for dispersion calculations around buildings. Such computer software can also help decide when and where each model is applicable. A notable example is the PC based, commercially available atmospheric pollution dispersion model ADMS (Figure 3.4), which incorporates the Apsley and Robins (1994) building effects module.

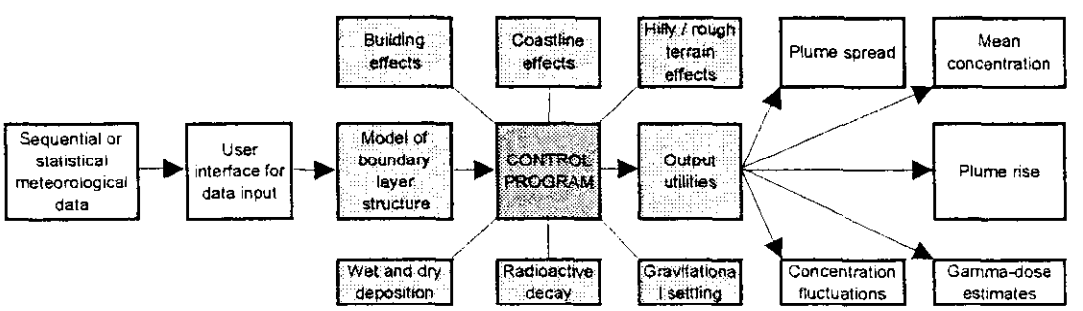

FIGURE 3.4 Components of ADMS

3.3.2 Sources upwind of the building

According to Wilson and Britter (1982), when an impinging plume approaches a building, the streamlines diverge as the flow decelerates towards the upwind face of the building, leading to an increased rate of spreading of the plume. As a result of this spreading, the concentration anywhere on the building surface will always be less than or equal to the maximum concentration on the centreline of the central part of the plume at the distance of the building. This important consideration is supported by the experimental and theoretical study of Britter and Hunt (1982), as referenced in Wilson and Britter (1982). The decrease in concentration is more pronounced the closer the source is to the building, and only becomes significant for $x_s/L < 2$. This holds only for a point source; the effect due to a line source is nearly negligible.

Similarly, Wilson and Netterville (1978) measured the building surface concentration around a rectangular model building in a simulated atmospheric boundary layer. The source was

located at roof level, at about $x_s/L = 5$. Their measurements for two wind directions are summarised in Figure 3.5 which illustrates clearly that, within an experimental uncertainty of about 5%, the maximum building surface concentration was identical to the concentration on the undisturbed plume axis. The increased plume spreading due to the presence of the building is also clearly revealed. Although the maximum concentration on the building surface is the same as that in the undisturbed plume, the area covered by near maximum concentrations is much larger, indicating a proportionately larger risk of exposure when a building is present. This is due to the deceleration of the plume and the divergence of the streamlines in the flow approaching the building, which causes the relatively higher concentrations of the undisturbed plume to become spread over a larger area. Therefore, it is reasonable to adopt Wilson and Britter's (1982) upper bound to the maximum concentration on a building, equal to the maximum undisturbed plume concentration intercepted by its projected frontal area A, as a conservative estimate of the concentration on the building surface from an impinging plume. For groups of buildings, an upper limit for the surface concentration should then be the undisturbed plume maximum intercepted by the building closest to the plume axis. However, a more detailed understanding of the effect of upwind and downwind buildings and terrain irregularities can only be determined by a site-specific wind tunnel model.

Hall *et al* (1996) also found that that large variations in surface concentrations around buildings only occur for sources close to the building, and illustrate the sensitivity of surface concentration patterns to source distance and wind direction with figures similar to Figure 3.5.

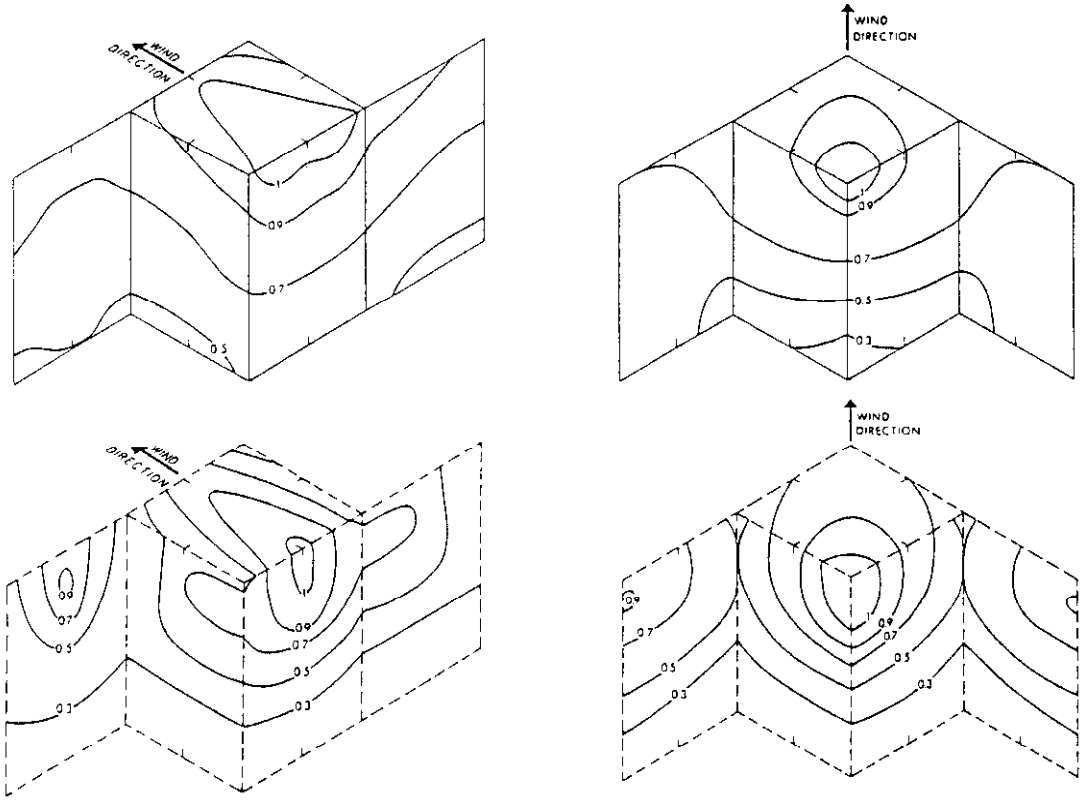

FIGURE 3.5 Concentrations on a building surface due to an impinging plume. Solid lines show edges of a building, with 'flaps' to include data from the far side; diagrams with dashed lines are concentrations in the same space in the absence of the buildings. (Reproduced with permission from Wilson and Netterville, 1978)

The data for side, front, roof and rear vents produce the same constant $B_o = 9.0$ for the maximum surface concentration. This limit was also confirmed by the recent wind tunnel data of Thompson (1991). However, some of the data for sources on the upwind face of the building fall outside of this predicted upper bound. Wilson (1977b) found that these higher concentrations occur for sources on the lower one-third of the building upwind face, and receptors on the lower one-third of the building sides. As discussed in Section 3.2.1, this is apparently the result of the horseshoe vortex that traps and carries the upwind face emissions to the sides of the building with less dilution. These higher concentrations can be accounted for by using $B_o = 30$.

On the basis of these results, Wilson and Britter (1982) recommend the following 'conservative, but realistic' procedure for estimating the maximum building surface concentration C_{max} at a distance r from a surface source:

(a) when the receptor is closer than three source diameters away from the source, assume $C_{max} \approx C_e$, the source exhaust concentration,

(b) when the receptor is greater than three source diameters from the source, assume that plume meandering produces at least a factor of ten dilution so that $C_{max} \leq C_e$,

(c) keeping constraints (a) and (b) in mind, use equation 3.7 with $B_o = 9.0$ to compute the maximum concentration C_{max}, unless both the source and the receptor are on the lower third of the same or adjacent walls, in which case use $B_o = 30$.

3.3.4 Sources above the building

This section will focus on the effect of stack sources on the roof of flat top buildings. The two most important modelling considerations are:

(a) to predict the effect of varying stack height on building surface concentrations,

(b) to determine criteria for the stack height and position so that the plume avoids all contact with building surfaces, and does not become entrained into the near recirculation wake.

Wilson and Britter (1982) estimate the effect of stack height on concentrations at roof level receptors using a Gaussian plume model. For a flat roof building with a stack height h_s above roof level and plume rise Δh, the roof level concentration is given by

$$C_r = \frac{Q}{\pi\, U_c \sigma_y \sigma_z} \exp\left[\frac{-(h_s + \Delta h)^2}{2\sigma_z^2} - \frac{y^2}{2\sigma_y^2}\right] \tag{3.8}$$

with $\sigma_z = 0.21\, R^{0.25}\, x^{0.75}$, where R is a scaling length appropriate for the roof wake, $R = D_S^{0.67}\, D_L^{0.33}$ (subscripts S and L denote the smallest, and the largest building dimension). This relationship was determined by Wilson (1979) and Wilson and Winkel (1982) in a series of experiments on discharge stack heights involving 24 different flat roofed building shapes.

However, this simple Gaussian diffusion model cannot be applied to any situation in which the plume becomes entrained into either the roof wake recirculation region or into the trailing vortices at the edges of the roof. In either of these cases, varying the stack height causes no consistent or predictable concentration reduction, unless the stack is made high enough and located in the centre of the roof away from the edges to avoid these recirculation regions altogether. For shorter stacks or those closer to the recirculation regions, a detailed wind tunnel or CFD study is required.

For low vents and short stacks on the roof of a building, Wilson and Chui (1985) proposed a model for minimum dilution based on two main independent dilution processes: an initial dilution

From a different point of view, Thompson (1993), describes the effect of a building on the impinging plume in terms of building amplification factors (BAFs), defined as the ratio of the maximum ground-level (or building surface) concentration observed in the presence of the building, to the maximum observed for the same source in the absence of the building at ground level. The notion of a building 'amplification' effect may seem to contradict the basic premise of Wilson and Britter discussed above, that the maximum surface concentration on the building is always equal to or less than the maximum concentration in the undisturbed plume at the same downwind location; the 'amplification' is measured with reference to the maximum ground-level value in the absence of the building, which is less than the maximum concentration in the undisturbed plume at the distance of the building. Using BAFs can therefore provide a lower bound to the value of the maximum surface concentration, provided that the source is near enough to the building for the maximum ground-level value to lie downwind of the building.

It is also worth noting, that from sources near the upwind face, material may become entrained into the upwind recirculation region and spread a significant distance upwind of the building of the order of H to $2H$, before being swept around it and becoming entrained into the near wake (Jones, 1983).

3.3.3 Sources on the building

Given the complexity of the flow patterns described in Section 3.2.1, it is nearly impossible to formulate an empirical model for predicting the detailed trajectory of a plume from a building surface release.

Wilson and Britter (1982) have followed an alternative approach by offering simple, yet realistic design guides for stack and vent placement based on the determination of an upper bound to concentration levels on the surface of a building from pollutants discharged from sources on the same building.

Assuming that the maximum possible concentration is due to minimum plume travel time, along the shortest distance along the building surface from source to receptor, a simple theoretical consideration suggests that

$$\frac{C_{max}\, U_H\, s^2}{Q} \approx \frac{U_H}{U_c}\frac{1}{\pi\, i_c^2} \tag{3.6}$$

where s is the shortest, 'stretched string' distance from source to receptor over the surface of the building, i_C is the turbulence intensity normal to the plume axis formed using the local mean velocity U_C, and U_H is the approach free stream wind speed at the height of the building. Wilson (1976, 1977b) found that the combination of variables on the right hand side of the equation above was a constant for most source and receptor locations. Wilson and Britter (1982) then carried out wind tunnel determinations of the value of the right hand side of equation 3.6, for various building shapes and (low momentum) vent locations. Dilution factors, defined as $1/C$, were calculated from concentrations measured at a large number of receptor points on the surface of a building and were plotted as a function of the distance from a source. These show a wide scatter of possible concentration values over several orders of magnitude. However, it is possible to draw a limit line for the upper bound of concentration, within which the vast majority of the measured points fall:

$$\frac{C_{max} U_H\, r^2}{Q} = B_o = 9 \tag{3.7}$$

When designing stacks to avoid building surface contamination from a roof stack source, the stack should be made high enough to ensure that the plume will not impinge on the roof. Wilson (1979) proposed a graphical design procedure based on Figure 3.7. The maximum dimensions of the roof recirculation cavity on the upwind edge correspond to wind directions normal to the upwind face: $H_c = 0.22\ R$, $x_c = 0.5\ R$ and $L_c = 0.9\ R$ (R as defined above). Once these are calculated, a high turbulence zone boundary is constructed with a downward slope of 1 : 10 from the top of the recirculation cavity. Where this boundary crosses the downwind roof edge, the edge of the plume taken at a 1 : 5 slope is projected back upwind over the building is the limit above which all stack heights should be located.

This is a less stringent requirement than that needed to prevent stack plume entrainment into the near recirculation wake, which can cause contamination of the downwind face of the building. A widely used criterion for avoiding entrainment into the near recirculation wake, as well as avoiding building downwash, is the rule that the stack height must be at least two-and-a-half times the height of the building (the $2.5H$ rule), with the exception of tall slender structures for which this criterion can be relaxed to $H + 1.5W$ (Snyder and Lawson, 1976). For wide buildings, Thompson (1993) suggests that an even higher stack (about $3H$) is required to avoid building downwash.

Wilson and Britter (1982) suggest using the following expression to calculate an upper bound on the concentration both on the roof and within the recirculation cavity for roof top stack emissions that become entrained in the near wake recirculation region:

$$\frac{C_{max} U_H (h_s + \Delta h)^2}{Q} = 0.1 \tag{3.10}$$

To account for plume downwash into the building wake, the stack height can be replaced in this equation by an effective stack height, using

$$h_{eff} = h_s - \frac{0.1A}{h_s + 0.1\sqrt{A}} \tag{3.11}$$

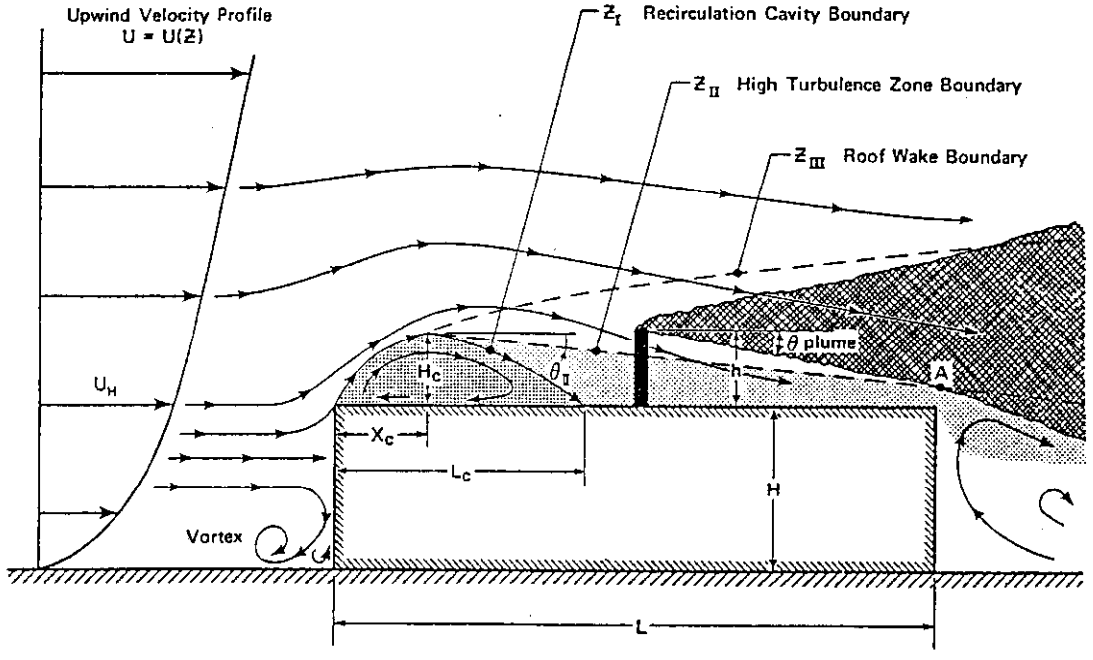

FIGURE 3.7 Illustration of the main roof-level patterns of flow and the graphical method of Wilson (1979) (reproduced with permission)

D_o due to jet and buoyant plume entrainment rate Q_o at the source, followed by 'distance' dilution D_d caused by a constant entrainment velocity into a semicircular uniform concentration plume of radius R bounded by the building surface (Figure 3.6).

The limit equation for minimum dilution is then

$$D_{\min} = \left[D_o^{0.5} + 0.25 \left(\frac{U R^2}{Q} \right)^{0.5} \right]^2 \tag{3.9}$$

Further refinements to this method based on wind tunnel and full-scale studies are proposed in Wilson and Chui (1987) (effects of turbulence from nearby obstacles), Wilson and Chui (1994) (influence of building size), and Wilson and Lamb (1994) (full-scale validation).

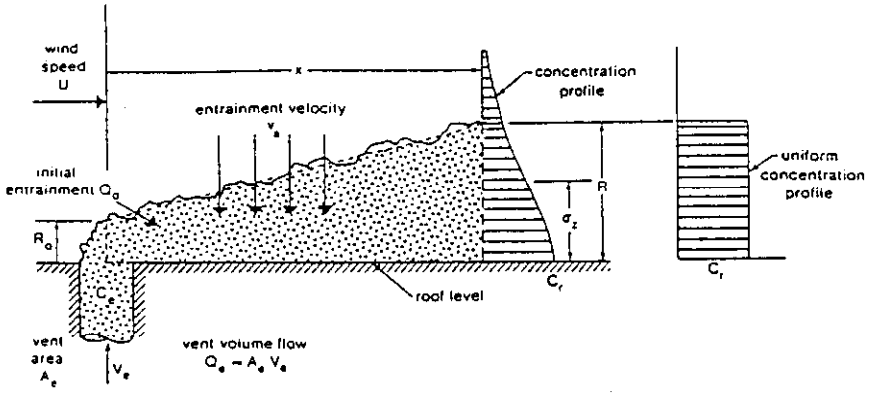

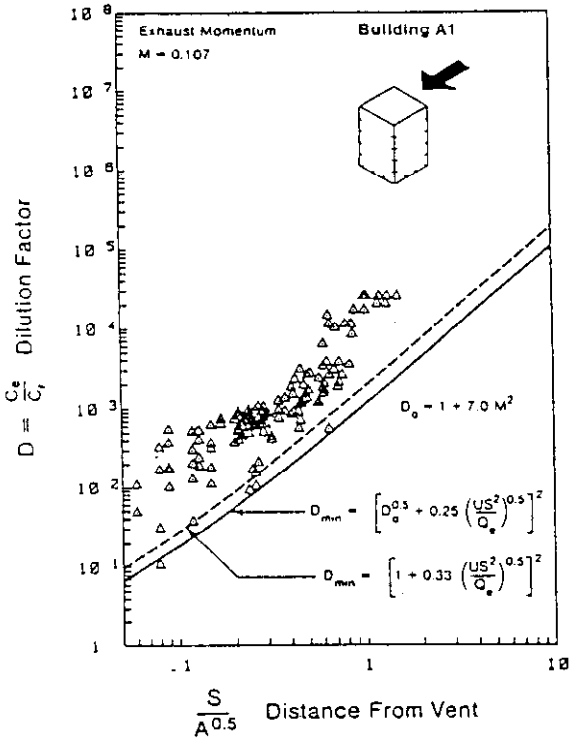

FIGURE 3.6 Calculating the concentrations on a building as a function of distance from a finite area roof-level source using the entrainment model of Wilson and Chui (1985) (reproduced with permission)

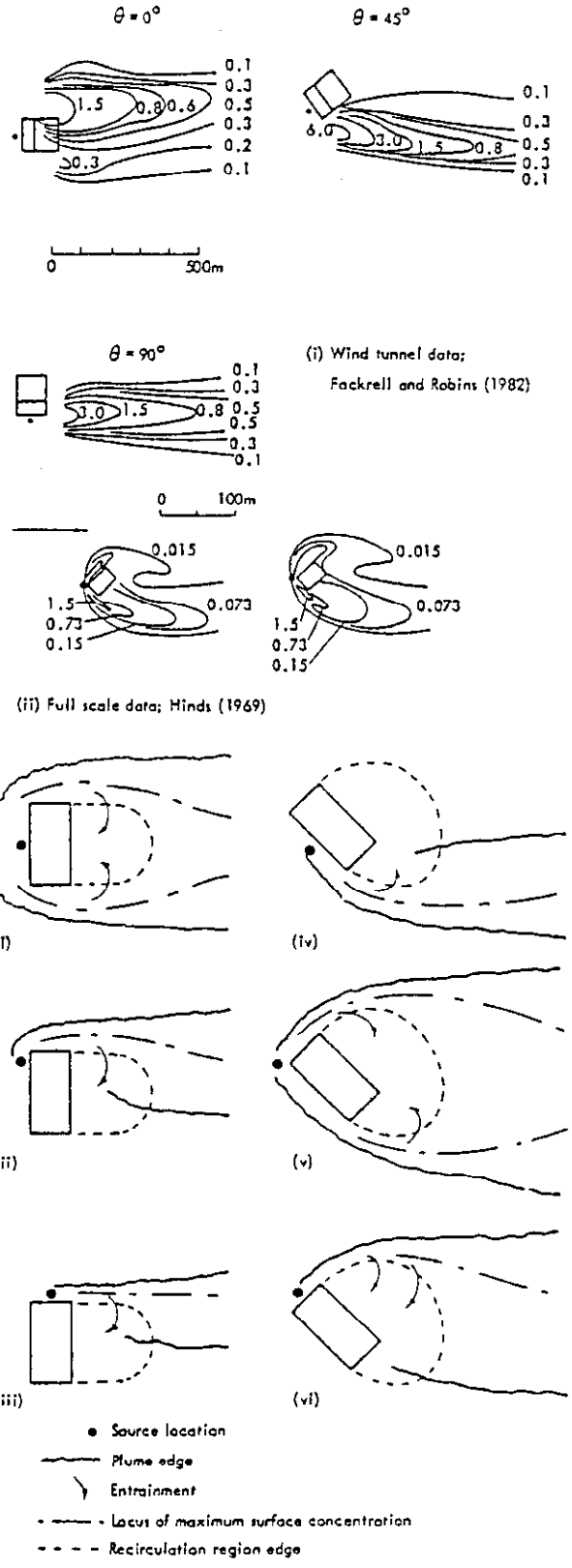

FIGURE 3.8 Contours of concentration in obstacle wakes from ground-level sources (from Robins and Fackrell (1983), copyright Power Technology Centre, Powergen, reproduced with permission)

as derived by Robins and Castro (1977b). Equation 3.10 then becomes

$$\frac{C_{max} U_H (h_s)^2}{Q} = 0.1 \left(1 + \frac{\Delta h}{h_s} - \frac{0.1A}{h^2_s + 0.1\sqrt{h^2_s A}} \right)^{-2} \tag{3.12}$$

3.3.5 Dispersion within the near wake recirculation region

Dispersion in the near wake recirculation region is associated with the following main characteristics: enhanced turbulence leading to increased mixing and dilution, reduced wind speeds, and low air exchange rates that causes contaminant retention inside the recirculation bubble.

Figure 3.8 (Robins and Fackrell, 1983) shows different possible scenarios for plume entrainment into the building wake from sources near the building. Figure 3.9 shows examples of dispersion from ground-level sources located inside the wake. Establishing whether a plume becomes totally or partially entrained into the wake of a building is one of the most important considerations in calculating concentrations on the downwind face of the building, due to either upwind sources, or downwind sources within the recirculation region. It is also crucial for calculating concentrations further downstream.

The Apsley and Robins (1994) building effects model (also part of the commercially available model ADMS) considers the regions of flow around the building to which different plume entrainment criteria apply. In this model, an upwind release may be partially or totally entrained in the recirculation region behind the obstacle, depending both on its lateral spacing from, and height above the obstacle. The plume is then partitioned into a part that is unaffected by the building, and a part that becomes completely entrained. The latter becomes completely mixed throughout the recirculation region and is then re-emitted. The plume issuing from the recirculation region is modelled as a virtual ground level source situated upwind of the building. These two components are treated as independent plumes in the main wake region ('double plume' model) with correspondingly different plume spread coefficients. Modified plume spread parameters are used inside the wake region of the building, to account for the influence that the building has on turbulence downstream. The complete plume from a partial entrainment is obtained by summing concentrations from the two plumes using simple superposition.

This model also assumes (as the model of Gifford, 1960, and Vincent, 1977) that high turbulence intensity and flow recirculation creates a uniform concentration across the entire wake recirculation region. However, as Wilson and Britter (1982) point out, an emission inside the recirculation region is not immediately mixed to a uniform concentration but produces a diffusing plume for a considerable distance from the source. As the plume diffuses further inside the wake, entraining its own recirculated emissions rather than clean ambient air, the concentration in the wake will eventually, far from the source, tend asymptotically to a constant value.

Wilson and Britter (1982) propose a two-part diffusion model for predicting both the constant concentration far from the source, and the near plume diffusion field from sources inside the recirculation wake:

(a) for distances from the source measured along the building and/or along ground level within $r\sqrt{A} \leq 1.73$ use $\frac{C_{max} U_H \; r^2}{Q} = B_0 = 9$ (as in Section 3.3)

(b) for $r\sqrt{A} > 1.73$, use

$$\frac{C_w U_H A}{Q} = B_3 \text{, with } B_3 = 3.0 \pm 2.0 \tag{3.13}$$

These two equations are compared to the measurements from surface releases on the rear of buildings. Thompson (1993) suggests a modification to equation 3.13 above for wide buildings with $W/H > 1$, advising the use of H^2 instead of A as the scaling length.

For sources outside the near wake, a uniform concentration C_w can be assumed to exist within the wake due to contaminant entrainment across the boundary of the recirculation region, and equal to the average concentration over the surface of the recirculation region (Puttock and Hunt, 1979). According to Wilson and Britter (1982), a conservative upper bound to the concentration in the near wake from an upwind source is that given by equation 3.13, which implicitly assumes that all the source material becomes entrained in the wake. A more realistic estimate would, however, be given by equation 3.10 with the term $(h_s + \Delta h)$ replaced, in the case of laterally displaced upwind sources, by the cross-wind distance $(y - W/2)$ that the source is displaced past the edge of the building width W.

All of the models described above are critically dependent on the correct calculation of wake dimensions and ventilation rates. The methods used are briefly described below.

According to the correlation of experimental data from several wind tunnel studies by Hosker (1979), the extent of the recirculation region is given by

$$x_R = \frac{1.75\ W\ H}{H + 0.25\ W} \tag{3.14}$$

for low rise buildings with $W \geq H$, where x_R is the ground-level distance from the downwind face to the point of reattachment.

A simpler form, suggested by Wilson and Britter (1982) is

$$1.5\sqrt{A} \leq x_R \leq 2.5\sqrt{A} \tag{3.15}$$

which approximates equation 3.14 within ±15% over the range $1 \leq W/H \leq 15$.

Fackrell and Pearce (1981) have recommended the following expression (also used by Apsley and Robins):

$$\frac{x_r}{H} = \frac{1.8\ \dfrac{W}{H}}{\left(\dfrac{L}{H}\right)^{0.3}\left(1 + 0.24\dfrac{W}{H}\right)} \tag{3.16}$$

Fackrell (1982) also proposed an expression for the maximum extent of the width of the recirculating region equal to:

$$W_r = 0.6H + 1.1\ W \tag{3.17}$$

The wake ventilation rate α is directly related to the uniform concentration in the wake. It is also inversely proportional to the wake residence time which is an important factor influencing exposure time from instantaneous or transient releases. Material from an instantaneous release that becomes entrained in the wake of the building where the ventilation rate is low, can be retained there for much longer than the duration of the release itself, increasing the time of exposure.

The following analysis by Robins and Fackrell (1980), which calculates the uniform wake concentration C_w due to a source inside the wake of strength Q, illustrates the relationship between the ventilation rate, α, and the wake residence time constant t_d. The recirculation zone is modelled

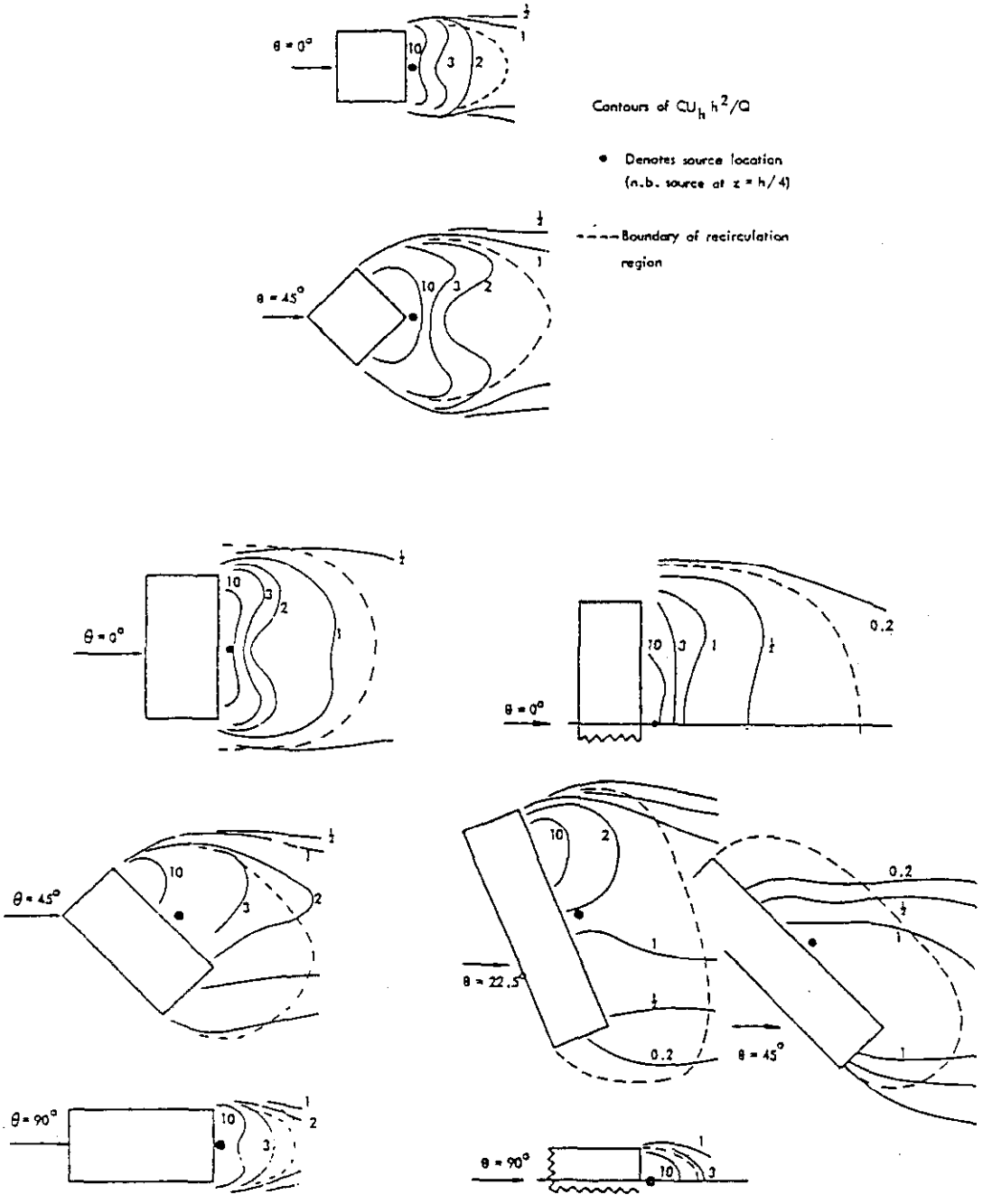

FIGURE 3.9 Contours of concentration in obstacle wakes from ground-level sources (from Robins and Fackrell (1983), copyright Power Technology Centre, Powergen, reproduced with permission)

as a closed cavity with surface area A_w. The mass flux of pollutant across this wake boundary m_w, depends on the amount of air that becomes entrained into the wake, so that

$$m_w = U_H \alpha \ A_w (C_w - C_\infty) \tag{3.18}$$

where C_∞ is the concentration outside the wake. Assuming $C_\infty = 0$, a mass balance for a source emission rate into the wake gives

$$\frac{dC_w}{dt} = \frac{Q - \alpha \ U_H C_w}{V_w} \tag{3.19}$$

where V_w is the wake volume occupied by the uniform concentration C_w. The steady state solution, for $dC_w/dt = 0$, is then

$$C_w = \frac{Q}{\alpha \ A_w U_H} \tag{3.20}$$

and the decay time constant (for the pollutant concentration to fall to 1/e of its initial value for a suddenly stopped source), or wake residence time, is

$$t_d = \frac{V_w}{\alpha \ A_w U_H} \tag{3.21}$$

Vincent (1977, 1978) demonstrated that the building projected frontal area is the appropriate scaling factor for t_d so that

$$\frac{t_d U_H}{\sqrt{A}} = B_1 \tag{3.22}$$

For a surface mounted cube at various angles of incidence and varying approach flow turbulence, $B_1 = 6.8 \pm 1.5$. This result was used by Wilson and Britter (1982).

Fackrell (1984), however, proposed an empirical expression for the wake residence time scaled by H:

$$\frac{t_d U_H}{H} = 11 \frac{\left(\frac{W}{H}\right)^{1.5}}{\left(1 + 0.6 \left(\frac{W}{H}\right)^{1.5}\right)} \tag{3.23}$$

Hunt and Castro (1984) found that this expression was in agreement with their experimental data. It is applicable to rectangular obstacles of $W/H < 8$, and perpendicular to the flow. Wake residence times are typically between 4 and 12. For buildings that are wider than $W/H = 8$, the residence times become greater up to an asymptotic limit, when the wake essentially becomes two dimensional. With oblique wind directions, especially when trailing vorticity is generated, residence times may be significantly lower due to an improved scouring of the wake.

3.3.6 Incorporating the effect of nearby buildings and topography

As discussed in Section 3.2.2 multiple building interactions can be particularly complex and site-specific, especially in the near field. As a result, it is nearly impossible to formulate an accurate empirical numerical method to predict concentrations in complex sites.

A useful empirical concept developed in the wind engineering field for dealing with building interactions is that of an 'area of influence', the area within which the presence of an obstacle will affect the flow around another. Hosker and Pendergrass (1987) report areas of influence of radius R at ground level, centred on a point a distance e downwind of the upwind face of the building, for buildings of varying height H and width W. For buildings with $H > 1.25W$, $R \cong 1.8W$ and $e \cong 0.5W$. For buildings with $1.25W > H > 0.33W$, $R \cong 1.6\sqrt{(WH)}$ and $e \cong 0.9\sqrt{(WH)}$. Finally, for buildings with $H < 0.33W$, $R \cong 2.8H$ and $e \cong 1.6H$. For the tall and intermediate building shapes, the areas of influence are circles; for the wide building shape, the area of influence is bounded by semicircles of radius R with centres at a distance $\cong 1.5H$ from either end of the building, which are joined by straight lines parallel to the long sides of the building.

Cook (1985, 1990) reviews aspects of wind flow effects of multiple building interactions and describes complex procedures for describing the influence of one building on another. Hall *et al* (1996) highlight the potential of this concept for dispersion calculations.

The model of Apsley and Robins (1994) treats groups of buildings in a simplified way, as an equivalent single block of equal frontal projected area A, and orthogonal to the wind direction. The dimensions of this idealised obstacle is used to define a perturbed flow field around the obstacle, with a near wake recirculating region immediately behind the obstacle, and a far turbulent wake further away. This model is used in the ADMS as a building effects module to be used for distances up to $\approx 30H$.

In the far field (see also Section 3.4), the particular arrangement of a cluster of buildings at a site can have a distinct effect on the values of σ_y and σ_z. Singh *et al* (1994) concluded, after assessing dispersion from sources on the BNFL Sellafield site, that 'dispersion in the presence of arrays of buildings can be sufficiently different to that in the presence of fewer discrete buildings, and models developed from tests and observations on the latter cannot be relied upon to predict dispersion from the former'.

3.3.7 Contamination of air inside the building from outside sources

Once the concentration at the surface of the building has been calculated, the indoor pollutant concentration can be modelled based on an understanding of the ways in which indoor air becomes exchanged with outdoor air, together with the deposition or decay dynamics of the pollutants concerned.

Outside air enters into the building due to infiltration through cracks and openings in the building envelope, via natural ventilation when windows are open, as well as via forced ventilation systems that induce air exchange, such as fans, and blowers. The rate of air exchange, λ_v, is usually expressed as the room air volume changes per hour (ACH). Pollutants from the outside air may be removed by the building fabric during infiltration or by air filters in the ventilation system, and this is represented by a filtration factor f. Particulates, as well as chemically reactive pollutants, will deposit on the indoor surfaces at a rate equal to the deposition factor, λ_d. Radioactive contaminants will also decay at a rate of λ, a radioactive decay factor.

Table 3.1 gives a range of typical values for the building specific parameters λ_v, f and λ_d (Roed and Goddard, 1990). It is important to emphasise that these values vary greatly with building type and mode of occupation, and that very few experimental data exist. Air exchange rates also depend on seasonal and shorter term variations of the outdoor wind speed, and the difference between indoor and outdoor temperatures.

TABLE 3.1 Characteristic parameter ranges for λ_r, f and λ_d given by Roed and Goddard (1990)

Parameter		Range	Central
Air exchange	λ_r (h^{-1})	0.33 to 30	3
Filtration	f	0.5 to 1	0.8
Deposition factor	λ_d (h^{-1})	0.002 to 0.43	0.11

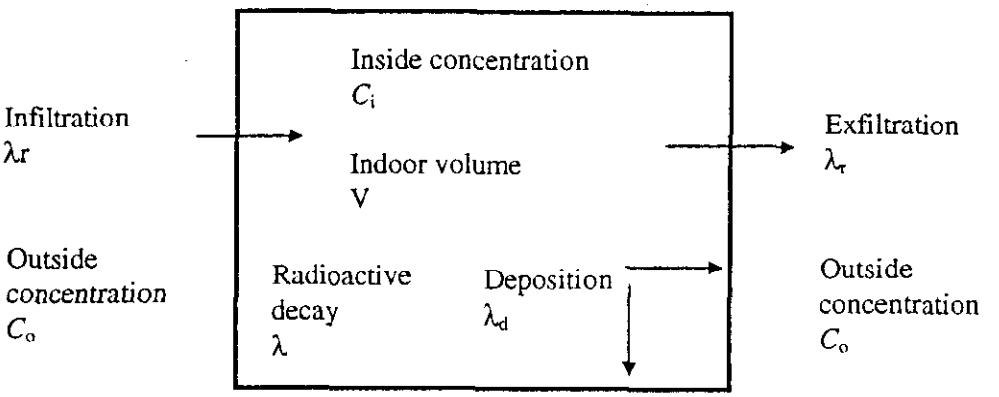

FIGURE 3.10 Simple box model for indoor air concentration

Compartment or 'box' models are the main method employed to calculate the overall concentration inside the building. The indoor space is modelled as one or more, well-mixed boxes of uniform concentration. Figure 3.10 illustrates some of the aspects that can be considered in a simple box model used to model indoor contamination from outside sources.

As a simple example, assume that the outside concentration has a uniform value C_o. (The actual non-uniform concentration on the building is an important consideration however, especially regarding the location of ventilation intakes on the building surface. This could be taken into consideration by using an appropriate apportionment of incoming air and outdoor air concentrations.) A mass balance in the box yields

$$V\frac{dC_i}{dt} = -\lambda_r f\ VC_o - \lambda_r VC_i - \lambda_d VC_i - \lambda\ VC_i \tag{3.24}$$

The steady state solution for the indoor concentration C_i corresponds to $dC_i/dt = 0$, whereby

$$C_i = \frac{\lambda_r f}{\lambda_r + \lambda_d + \lambda} C_o \quad \text{or} \quad \frac{C_i}{C_o} = \frac{\lambda_r f}{\lambda_r + \lambda_d + \lambda} \tag{3.25}$$

The non-dimensional term equal to the ratio of indoor to outdoor concentration, is referred to as the indoor contamination 'transfer factor'. The same term without λ, is also called the 'building protection' factor, since the effect of filtration and deposition (in the case of particulate airborne material, or chemically reactive gases such as SO_2 and NO_2) is to reduce indoor concentrations. However, when the contaminant involved is such that deposition or decay is negligible (eg non-reactive gases such as CO), the steady state concentration inside the building is the same as that outside. Table 3.2 from Goddard and Byrne (1995) summarises reported data on building protection factors (also called 'location factors') from case studies on indoor aerosol contamination.

TABLE 3.2 Ratios of indoor to outdoor concentration (building protection factors) for aerosol concentrations in buildings from available experimental data (as summarised by Goddard and Byrne, 1995)

Reference	Building type	Aerosol type	Indoor/outdoor ratio
Megaw (1961)	UK house	Iodine particulate	0.2+
Biersteker *et al* (1965)	Netherlands, 60 homes	SO_2	0.1 or better
Roed *et al* (1985)	17 Danish homes (14 houses, 3 apartments)	^{7}Be, ^{103}Ru	0.33 (average)
Christensen and Mustonon (1987)	4 Finnish apartments	^{7}Be	0.35 (average)
	1 Norwegian house		0.44 (average)
Roed and Cannel (1987)	1 Danish house	^{7}Be, Chernobyl aerosol	0.4 (iodine) 0.27 (^{137}Cs)
Raunemaa *et al* (1989)	30 Finnish buildings (5 offices, 25 houses and apartments)	Fe, Si, coarse and fine aerosol modes	0.27 (coarse Si) 0.12 (coarse Fe)

A great variety of compartmental models are available, incorporating different parameters and degrees of complexity. Some examples are the code BHOUSE (Qadir, 1990) which incorporates the simple analysis outlined above, and the comprehensive CONTAM model considered as one of the state-of-the-art models (Walton, 1997) and which is freely available on the Internet (gwalton@enh.nist.gov).

CFD modelling is also used increasingly to model the detailed distribution of contaminants inside a building. Examples of CFD modelling of indoor pollution can be found in the work of Chen and Jiang (1992), and the aerosol deposition simulation of Lu and Howarth (1996).

3.3.8 CFD modelling applications

This section is intended to provide a brief overview of CFD applications to near-field dispersion around buildings. For a more comprehensive discussion of CFD applications to near-field atmospheric dispersion modelling, the reader is referred to the recent review by Hall (1996b) which discusses the feasibility and validity of CFD modelling, potential modelling pit-falls, and best practice approaches.

CFD codes are used at an 'exploding' rate as a tool to solve engineering fluid flow problems (Cowan *et al*, 1996; Moin and Kim, 1997). This trend has been mirrored in the study of the flow and dispersion around buildings. CFD was first applied to environmental flows by the wind engineering field to predict wind loading and flow patterns around single, or groups of buildings. This was then followed by studies on the dispersion from and around buildings.

CFD modelling is based on the solution of the governing partial differential equations of the flow, namely those of the conservation of mass, momentum and energy, by numerical means on a computational mesh (a grid that divides the flow domain into individual 'cells'). The differential equations are discretised, ie broken down into an algebraic form amenable to solution by a computer, according to methods such as the finite volume method (Patankar, 1980), and various differencing schemes, eg the upwind or central differencing schemes. Versteeg and Malalakesera (1995) is an excellent introduction to CFD that describes the underlying numerical methods in detail.

Flows around buildings are invariably turbulent, and approximations made in the modelling of turbulence by CFD codes is a fundamental source of error and uncertainty in the prediction. Although turbulence, ie the fluctuating part of a flow, essentially obeys the same fundamental equations as the mean flow, the important constituents of turbulent phenomena take place in eddies of order a millimetre in size when the whole flow domain may extend over hundreds of meters. A grid fine enough to allow an accurate description of a turbulent flow would therefore require an immense and totally impractical number of computations. Full calculations of the turbulent flow for very simple boundary conditions have been carried out only with the use of the most powerful supercomputers available (Moin and Kim, 1997). However, a more useful approach for representing turbulent flows in less detail, is by calculating averaged quantities with the use of approximate, semi-empirical 'turbulence models'. Using these models in conjunction with the conservation equations it is possible to arrive at a satisfactory fluid flow solution on the scale of mean motion with currently available computational power, using workstations or even personal computers.

The k–ε model of Launder and Spalding (1974) is the model of choice for the majority of applications and in the commercial general application CFD codes. Although its deficiencies are well documented (Murakami, 1993; Zhang, 1994), it is a known quantity and many workers prefer a model with known characteristics to a model promising more accuracy but with less history of application. It is likely that improved turbulence models will become more prevalent as experience with them grows. Examples of such models are: further developments of the k–ε model, eg the Chen k–ε (Chen and Kim, 1987) and RNG k-ε models (Yakhot and Orszag, 1986; Yakhot *et al*, 1992), Reynolds stress models (eg Mellor and Herring, 1973), and large eddy simulation models (LES) (eg Nieuwstadt, 1991) which have been shown to return more accurate predictions than the standard k–ε (Murakami *et al*, 1992).

Wilcox (1993) gave a detailed description of turbulence models and their relationship to CFD. Laurence and Mattei (1993) reviewed the current state of turbulence models and concluded that the k–ε model was the safest model to build into a code without presuming the type of application. However, they stated that LES may well be favoured in the future when modelling bluff body aerodynamics, such as the flows around buildings. LES was again reviewed favourably by Murakami (1993) in a comparison of turbulence models applied to flow over a bluff body, whereas the k–ε model was found to overestimate the value of k around the frontal corner due to the production term in the turbulent energy equation.

Apart from the uncertainty inherent in the use of any particular turbulence model, CFD results can also be strongly dependent on the mesh design and the numerical method employed. A critical discussion of the current limitations of CFD can be found in Section 4.3.

Despite the large number of uncertainties and problems associated with CFD, there are many examples of successful application of CFD to modelling flow and dispersion around buildings. Paterson and Apelt (1986) and Hanson *et al* (1986) reported good agreements between predicted flow field and wind loading, and experimental measurements for buildings with sharp profiles. Mathews *et al* (1988) reported good agreement between experimental measurements and numerical predictions, gained from a finite difference code for the case of a building with a smooth profile where the separation point is not as well defined as that of a sharp profile. Murakami and Mochida (1988) carried out a detailed study considering seven cases of flow around a cubic model using the k–ε model. It was concluded that the velocity and pressure fields could be accurately predicted, given a sufficiently fine mesh resolution. However, the turbulent energy (predicted by means of the k–ε model) at the windward edge and in the wake of the building was not in such

good agreement with the experimental measurements. The authors concluded that further efforts should be made to improve the accuracy of the k–ε model.

Benodekar *et al* (1987) developed a methodology to predict flow and dispersion in the vicinity of an isolated reactor building using the finite volume method, which was then applied to a range of cases from an idealised cubic building to a more realistic reactor building. Passive releases in neutral and stable flows were considered, complementing a previous study on buoyant releases (Benodekar *et al*, 1984). In the case of the complex reactor building, plume concentration predictions in the wake region agreed with experimental data at best within 30%, and at worst within a factor of two. The main sources of error were thought to be due to insufficient grid refinement (achievable at an increased computational cost), the k–ε model assumption of isotropy of turbulence and the treatment of the wall boundaries.

Ronold (1993) used CFD to predict detailed air velocity distributions and gas concentration profiles within a petroleum process plant to aid the classification of hazardous areas. Gadilhe *et al* (1993) predicted the wind flow through an urban square, the results comparing well with experimental measurements, although it was concluded that further work was required for a full validation of the model.

The application of CFD models to environmental problems in general, requires the inclusion of a realistic description of the atmospheric boundary layer. Zhang *et al* (1996) presented a comparison of numerical predictions and experimental measurements of flow and dispersion around a building in stable conditions. Fair agreement between predicted and observed centreline ground concentrations was reported for weakly stratified conditions. However, for strongly stratified conditions agreement was poor. Zhang *et al* (1993) also explored the effects of incident wind shear and turbulence levels on the flow around a building and concluded that their CFD model yielded a reasonable simulation of the mean flow, as compared with wind-tunnel data. Richards and Hoxey (1993) suggested appropriate input values for the k–ε model for flows around buildings in the atmospheric boundary layer calculated with reference to full scale measurements. The effect of fluctuating wind directions and wind speeds in the real atmosphere to the flow and dispersion around buildings – as modelled recently by wind tunnel studies (eg Higson *et al, 1994*; Okabayashi *et al,* 1996) can also be modelled with transient CFD simulation techniques, to give a peak and a mean value of parameters (Hill, 1997).

3.4 Dispersion modelling beyond the near wake

Beyond the local influence of a building on plume dispersion, building effects can persist for long distances. Downstream of the near wake recirculation region there is a relatively mildly disturbed wake region associated with enhanced dispersion rates. To model concentrations at longer distances from the building, outside the near wake recirculation region (regimes (b) and (c) according to the classification in Section 3.1.3.1), most of the models found in the literature apply a number of building effect corrections to the standard Gaussian model, expressed as

$$C(x,y,z) = \frac{Q}{2\pi U \sigma_y \sigma_z} \exp\left[-\frac{y^2}{2\sigma_y^2}\right]\left\{\exp\left[-\frac{(z-h_s)^2}{2\sigma_z^2}\right] + \exp\left[-\frac{(z+h_s)^2}{2\sigma_z^2}\right]\right\} \qquad (3.26)$$

where x is the coordinate along the wind direction, y along the cross-wind direction and z along the vertical, the origin being at the source. U is the advection mean speed (usually specified as the wind speed at 10 m height in the boundary layer), σ_y and σ_z are the vertical and lateral plume spreads

expressed as the standard deviation of the horizontal and vertical Gaussian distributions of dispersion, and h_e is the effective height of release.

The main existing Gaussian models are ISC3 (EPA, 1995), NRPB-R91 (Clarke, 1979), ADMS (Carruthers *et al*, 1994) and the Danish OML (Olesen *et al*, 1991). The basic difference between these models is the atmospheric stratification description that they use to calculate σ_y and σ_z. ISC3 and NRPB-R91 calculate σ_y and σ_z based on the discrete Pasquill-Gifford stratification categories, whereas ADMS and the Danish OML use an improved, continuous function of basic physical parameters such as u^*, the Monin-Obukhov length scale, and the roughness length z_o.

The main methods for incorporating building effects in Gaussian plume models are as described by Fackrell (1984) and discussed below.

(a) *Initial dilution of the plume and initial plume width ratio.* Gifford (1960) suggested that the plume downwind of the building can be approximated as a Gaussian with an initial dilution of the plume proportional to wind speed U and the projected building area A. The centreline concentration is then equal to

$$C = \frac{Q}{(\pi\sigma_y\sigma_z + cA)\ U} \tag{3.27}$$

where c has been estimated between 0.5 and 2.0, with $c = 1$ giving the best agreement with experiment in most cases. Although this is a very simple model to use, it is only applicable to centreline concentration.

(b) *Virtual source methods.* To simulate the effect of the building on plume dispersion downwind, these methods assume that the plume comes from a virtual source at positions upstream of the real source. The source position is chosen so that the vertical and lateral plume spreads at the position of the rear face of the building, σ_{yo} and σ_{zo} are some specified fraction of the building height and width. Two models have been suggested and tested:

- Turner (1969):

$$\sigma_{yo} = W/4.3, \quad \sigma_{zo} = H/2.15 \tag{3.28}$$

with the virtual source located at ground level for low level releases, and at roof level, H, to model higher level releases.

- Barker (1982):

$$\sigma_{yo} = W/3, \quad \sigma_{zo} = H/3 \tag{3.29}$$

with the virtual source height equal to $H/3$, for both ground and roof level releases. This is the model adopted by NRPB (Jones, 1983) since it was regarded 'as good as any' of the other available models.

(c) *Increasing σ_y and σ_z by a fixed amount downstream of the building.*
Ferrara and Cagnetti (1980):

$$\sigma_y' = \sigma_y + W/2.5, \ \sigma_z' = \sigma_z + H/2.5 \tag{3.30}$$

This model gives very similar results to that of Halitsky (1977), yet it is easier to apply.

(d) *Virtual source model with interpolation to match near-wake values.* All the above models of the far wake do not match correctly with near-wake calculations as x becomes small. Huber and Snyder (1982) suggested an interpolation for $3H < x < 10H$ as follows:

$$\sigma_y' = 0.7(W/2) + (x - 3H)/15 \tag{3.31}$$

$$\sigma_z' = 0.7H + (x - 3H)/15 \tag{3.32}$$

and for $x > 10H$, a virtual source model is used so that the values at $x = 10H$ match correctly, with the virtual source height used equal to the actual source height. If $\sigma' < \sigma$ for either y or z, then the undisturbed values are used. For source heights greater than the building height no correction is applied for σ_y.

The ISC model (EPA, 1995) uses this method for squat buildings ($H < W$). For tall buildings, the σ_z equation is used with the building height substituted by the building width. For very squat buildings ($W > 5H$), an additional adjustment is included in the σ_y equation when stacks are located near the end of the building.

All the methods described above were tested by Fackrell (1984) who concluded that the behaviour of all the models is similar and that there is usually less than a factor of two difference in their predictions. He stresses that these models cannot be applied very near to the building since the actual plume can be greatly distorted and displaced by the complicated local flow field patterns, but that further downstream ($5H$ to $10\ H$) the local effects become small.

Building downwash effects can also be incorporated into a Gaussian plume model, again by adjusting σ_y and σ_z, or by adjusting the effective height of sources near or on the building (Hanna *et al*, 1982).

The ISC model uses the Schulman and Scire method for stack emissions that become entrained in the near wake, ie when the plume height (stack height plus momentum rise) is greater than $2.5H$ (or $H + 1.5W$ for slender, tall buildings, as in Section 3.3.4). The method incorporates a reduced plume rise due to initial plume dilution, enhanced σ_z as a linear function of the effective plume height, and a specification of building dimensions as a function of wind direction.

The ADMS model uses the building effects model of Apsley and Robins (1994) for distances up to $x \approx 30H$. Use of a shorter distance would reduce computation time, but $x \approx 30H$ is sufficiently far away from the building for discontinuities to be kept small between the buildings effect module and the underlying ADMS dispersion model.

Another practical approach to dealing with Gaussian dispersion calculations is the Gifford and Porch (1993) atmospheric diffusion calculation model GAUS1 incorporated into a pocket size, hand-held calculator. It is a general purpose Gaussian model which incorporates many air-pollution modules/formulas that add refinement to the basic Gaussian calculation. It calculates building effects using the Gifford (1960) method and building downwash according to the method by Briggs *et al* (1982).

4 Conclusions and recommendations for future research and model development

4.1 Field and wind tunnel studies and semi-empirical models

Despite the large number of published papers and reports on wind tunnel studies of buildings effects, the span of the available dispersion database is limited. Studies have tended to concentrate on simple rectangular obstacles only, and little attention has been given to commonly encountered wide and squat, or tall and slender buildings, or groups of buildings in rows or squares

(Hall *et al*, 1996). Obstacles other than buildings such as walls and cuttings, vegetation and lattice structures have also been largely ignored in the literature. The effect on dispersion of the horseshoe and trailing vortices generated by buildings is an issue that also needs further consideration. Additional experimental data are therefore needed to complement this gap of information; experimental data are the foundation on which semi-empirical models are developed, and are also necessary for validating CFD results.

Amongst existing personal-computer-based models, the Apsley and Robins (1994) model is probably the best relatively simple empirical procedure for dealing with dispersion around buildings, since it can accommodate partial plume entrainment in a reasonable way for both elevated and laterally displaced plumes (Hall *et al*, 1996). Although designed as a module for ADMS, it can be used independently.

The practical procedures for estimating maximum building concentrations as described in Sections 3.3.2–3.3.5, are also methods suitable for incorporation in a personal computer program, although such software does not seem to be available.

The value of further general field experiments and wind tunnel studies of dispersion over elevated terrain for idealised symmetrical hill shapes is limited, as a major problem is in the application of their results to more general situations. CFD modelling can be used to produce parameterisations just like those from measurements, although with the non-trivial additional problem of model uncertainty on top of applicability of results. Where new, empirical or theoretical models are developed, for which validation data from existing laboratory and field experiments is lacking, then idealised measurements need to be made for that purpose. Probably of most value, however, are field or laboratory experiments representing specific sites from which releases might occur. An example is the measurements made near the Sellafield reprocessing plant to test the predictions of turbulence parameters that are made by the Flowstar model for use in ADMS (Robinson, 1997). Such an approach is necessary and justifiable, as the number of sites from which releases of radioactive material may occur is quite small, but every site has some local features that may not be handled well by a given model. Scientific assessment of the assumptions made in any model is vital, but should not be used as a substitute for field measurements or at least wind tunnel studies of individual sites.

4.2 *Modifications to the Gaussian plume model*

For buildings, the NRPB-R91 Gaussian plume model is currently designed to model dispersion regime (c) (see Section 3.1.3.1). It is often used incorporating the Barker (1982) correction to the lateral and vertical spreads σ_y and σ_z to account for building effects on impinging plumes (see Section 3.4). In order to consider regimes (a) and (b), it is possible to incorporate more sophisticated σ_y and σ_z corrections, as those employed by the ISC model, and include an improved method for modelling wake entrainment, as for example, the double plume model in the vicinity of the building used by the Apsley and Robins (1994) building effects model. The simple semi-empirical models described in Section 3.3 for estimating an upper bound for the concentration on a building from an upwind source or a source on the building could also be incorporated.

For hills, a model based on modifications of the Gaussian plume model for application when plumes impinge on elevated ground already exists. For details of the EPA CTDMPLUS model, see Section 2.3.4. It seems unnecessary to repeat such a lengthy development and validation procedure in the UK. However, for application in this country, especially to accidental releases which may occur near the ground, it must be recommended that the assumptions made be examined carefully, as CTDMPLUS has been developed primarily for regulation of continuous elevated point

sources in an American environment. It is probably fair to say that the development of all EPA models includes a certain amount of tuning to ensure that model performance suits this specific application. For example, comparability of results between one operator's plant and a competitor's is arguably important as well as the accuracy of the model at a single location. Even though the EPA models are generally rather well documented, the decision process that results in the choice of a given model formulation is inevitably much less well documented (if at all) than the resulting model itself. Furthermore, pressure in American society to limit emissions of chemical pollution such as sulphur dioxide might lead to quite different model requirements to the demands of UK society that radioactive discharges, for example, must be subject to the most stringent control.

The recommendation that model assumptions should be examined carefully, especially when importing American regulatory models for different uses in the UK, is in accordance of the principles of the Royal Meteorological Society guidance (Britter *et al*, 1995), in which demonstration of fitness for purpose of modelling technique requires a scientific assessment of a model whenever it is applied beyond the situations in which it has been validated. There are also some situations, for example releases in reverse flow downwind of a hill, in which the assumptions made in CTDMPLUS are completely invalid, such that its application would produce results that would be most misleading indeed.

In situations in which systematic underprediction of concentrations by CTDMPLUS is likely to give cause for concern, much simpler assumptions – screening methods – become attractive. Alternatively, the ADMS approach of using a linearised airflow model to compute the plume centreline and dispersion parameters is extremely valuable when modelling individual cases under conditions in which the linear model is valid, as the effect of the irregular shape of most hills is considered by the airflow model Flowstar.

The uniqueness of every real-life situation in which a release might impinge on elevated ground makes it extremely difficult to recommend any particular model for application in every situation. This is reflected in the diversity of approaches recommended by EPA in the USA. It is probably necessary to consider the merits and weaknesses of a selection of models for each case individually. The use of more than one model for a given study increases the chances that the user will become aware of likely pitfalls and will be able correctly to estimate the reliability of the model estimates.

4.3 Current limitations and future potential of CFD modelling

Applications of CFD to dispersion calculations around buildings are currently limited by the considerable complexity involved in CFD modelling which results from the many degrees of freedom available through various turbulence models, as well as the choice of appropriate model boundary conditions, meshing approaches, differencing techniques and solution algorithms. CFD fluid simulations are also limited in the sense that they may fail to return a faithful simulation of a flow, and it is always advisable to validate and support CFD results with scaled flow data. See also Hall (1996b).

The success or failure of a simulation depends not only on the code capabilities but also on the way the user defines the problem. Even when input information on boundary conditions is physically realistic and correctly presented to the analysis code, the choice of a given turbulence model, mesh design and differencing scheme can have an effect on the predictions which can be strong, yet difficult to identify or isolate. Leschziner (1993) presents examples of different predictions resulting from changes in the numerical discretisation scheme, along with a wide range of results returned by several specialists groups asked to submit solutions for a simple plenum

chamber problem with given boundary conditions. Leschziner (1993) concludes that considerable expertise, physical insight and experience are essential to obtain meaningful solutions from CFD. A similar conclusion is drawn by Cowan *et al* (1996) who present a comparison between solutions to several flow problems returned by various groups as part of a multi-partner EU project. The solutions are shown to be dependent not only on the turbulence model, but also on the mesh design and numerical method. It is also possible that more accurate numerical procedures can lead to results further from reality, as for example in the case of standard k–ε simulations, coarse grids have returned predictions closer to the experimental measurement than a refined grid, most probably due to numerical diffusion.

Another limitation to the use of available CFD codes to environmental flow modelling is that they are usually industrial-application based and do not incorporate boundary condition options that could be readily used to recreate a realistic description of the atmosphere, in terms of, for example, atmospheric stability, wind profiles, and upwind turbulence (Britter, 1996).

Nevertheless, as discussed in Section 3.3.8, CFD can return accurate predictions of flow, pressure and dispersion in the vicinity of buildings, when used with judgement and experience. There are some guidelines for good operating practice to assist the user of a CFD code and repeated validation plays a key role as the final quality control mechanism (Leschziner, 1993; Versteeg and Malalasekera, 1995; Cowan *et al*, 1996). Although scaled flow studies are still regarded as the most reliable method, there are also unique advantages of CFD over scaled flow simulations, in terms of a substantial reduction of cost and time, the ability to study systems without any interference (eg from walls in a wind tunnel) and under hazardous conditions (eg safety studies and accident scenarios), and the practically unlimited level of detail of the results CFD can offer (Versteeg and Malalasekera, 1995). In the light of the 1991 AIChE workshop on the dispersion of toxic gases over non-flat obstructed terrain, Meroney (1993) concluded that Reynolds stress and large eddy simulation CFD models can reproduce measurements of streamlines, recirculation regions and turbulence magnitude, and that the main obstacle to the use of a CFD operational numerical model to predict diffusion around buildings suitable for regulatory purposes, was available computational power in order to solve on a refined grid.

On hills, it is possible to consider CFD as an alternative to wind tunnel studies. Perhaps, however, any such move away from measurements can be considered to be dangerous. Alternatively, the k–ε model can be considered to be an obvious development from the extremely attractive but of limited applicability linear model, as computing power increases. Increased run-time should, however, restrict the use of k–ε models to those situations where linear models become unreliable.

General application CFD codes that do not require a specialist knowledge of computational techniques or fluid mechanics, are available commercially. The market is at present dominated by four established, industrial-application-based CFD codes, namely STAR-CD, PHOENICS, FLOW3D and FLUENT. They all use the finite volume method (although finite element methods are also available) and employ standard turbulence models, such as the k–ε model, with the added advantage of user-friendly interfaces for the input and display of data and a comprehensive variety of additional modelling features, eg chemical reactions and particle tracking. These models are particularly sophisticated and although detailed documentation is usually provided, it is often far from straightforward to obtain credible predictions, unless the user is equipped with considerable expertise to make the most appropriate use of the code's capabilities for a given specific situation (Cowan *et al*, 1996). Modelling any particular problem requires a wide range of user inputs and decisions (eg meshing details, boundary conditions) and, as a result, different users using the same code, could arrive to quite different solutions (see also Section 3.5.2).

Another commercial CFD code is Fluidyn NS, which is incorporated into Fluidyn-PANACHE. This is an integrated software package for the simulation of atmospheric flow and pollution dispersion. In the version of PANACHE that was demonstrated to the authors of this review, the CFD code is invoked optionally for buildings but not for hills. The EPA Federal Register inclusion of PANACHE as a model that 'may be appropriate' for regulatory use seems to be justified by the fact that the standard Gaussian model that PANACHE uses for most dispersion calculations is similar to that in ISC3. However, it is possible that PANACHE could encourage a non-expert user to employ a 'black box' or 'automatic' approach to CFD. Considering the uncertainties that are inherent in CFD modelling around buildings, this should perhaps give some cause for concern. A more appropriate and potentially extremely valuable way of using such software is that currently favoured by Transoft, the developers of PANACHE, namely to work in a tripartite arrangement between themselves, a university research group and a client. In such an arrangement, the software is used as a tool for investigating different modelling approaches, including software code modification where necessary. Perhaps such an approach, for dispersion around buildings and hills, integrating CFD with Gaussian models and empirical formulae, will prove to be the way ahead for solving problems of specific sites without the constraints of a closed software package such as ADMS. However, the next constraint to the further spread of CFD as a viable modelling method for environmental flows and dispersion is unlikely to be the availability of user-friendly software, but a scarcity of qualified persons able to run the codes making proper judgement based on experience and a good understanding of the internal workings and limitations of the calculations.

5 Acknowledgments

The authors would like to thank everyone who has assisted in the production of this review, especially Dr David Hall and Dr Helen ApSimon for their most valued support and discussion.

6 References

Apsley, D D, and Robins, A G (1994). Modelling of building effects in UK-ADMS. ADMS Technical Specification. Cambridge Environmental Research Consultants Ltd, UK-ADMS 1.0 P16/01K/94.

Apsley, D D, and Castro, I P (1997). Numerical modelling of flow and dispersion around Cinder Cone Butte. *Atmos. Environ.*, **31**, 1059–71.

ASHRAE (1993). *ASHRAE Handbook.* Fundamentals Volume, Chapter 14. Atlanta GA, American Society of Heating, Refrigeration and Air Conditioning Engineers, Inc.

Barad, M L (1958). Project Prairie Grass – a field program in diffusion, Volumes I and II. Geophysical Research Paper No. 59. Bedford MA, Air Force Cambridge Research Center, NTID PB 151424, PB 1514251.

Barker, C D (1982). The application of the virtual source entrainment model in nuclear safety calculations. Ratcliffe on Soar, PowerGen, CEGB Report No. RD/B/5238/N82.

Benodekar, R W, Goddard, A J H, and Gosman, A D (1984). Predicting lift-off of major self heating releases under the influence of a building. Report SR-016-(UK) for the European Commission.

Benodekar, R W, Goddard, A J H, and Gosman, A D (1987). Computer modelling of gaseous effluent dispersal from nuclear reactor installations. Joint Report No. GR/D/07824 and GR/D.51520 for the European Commission.

Bradley, E F (1980). *Quart. J. Roy. Meteorol. Soc.*, **106**, 101.

Britter, R E (1996). Personal communication.

Britter, R, Collier, C, Griffiths, R, Mason, P, Thomson, D, Timmis, R, and Underwood, B (1995). Atmospheric dispersion modelling: guidelines on the justification of choice and use of models, and the communication and reporting of results. Policy Statement. Reading, Royal Meteorological Society.

Burt, E W, and Slater, H H (1977). Evaluation of the valley model. Presented at AMS-APCA Joint Conference on Applications of Air Pollution Meteorology, Utah.

Carruthers, D J, and Hunt, J C R (1990). Fluid mechanics of airflow over hills: turbulence, fluxes and waves in the boundary layer. IN *Atmospheric Processes over Complex Terrain* (W Blumen, Ed). *Meteorol. Monogr.*, **23**, 83–108. Boston, American Meteorological Society.

Carruthers, D J, Hunt, J C R, Britter, R E, Perkins, R J, Linden, P F, and Dalziel, S (1991). Fast models on small computers of turbulent flows in the environment for non-expert users. IN *Computer Modelling in the Environmental Sciences* (Farmer and Rycroft, Eds). Oxford, Clarendon Press.

Carruthers, D J, Holroyd, R J, Hunt, J C R, Weng, W S, Robins, A G, Apsley, D D, Thompson, D J, and Smith, F B (1994). UK-ADMS: a new approach to modelling dispersion in the earth's atmospheric boundary layer. *J. Wind Eng. Ind. Aerodynam.*, **52**, 139–53.

Castro, I C, and Robins, A G (1977). The flow around a surface-mounted cube in uniform and turbulent streams. *J. Fluid Mech.*, **79**, 307.

Castro, I P, and Apsley, D D (1997). Low and dispersion over topography: a comparison between numerical and laboratory data for two-dimensional flows. *Atmos. Environ.*, **31**, 839–50.

Chen, Q, and Jiang, Z (1992). Air supply method and indoor environment, *Indoor Environ.*, **1**, 88–102.

Chen, Y S, and Kim, S W (1987). Computation of turbulent flows using an extended k–ε closure model. NASA CR-179204.

Clark, T L (1977). A small scale numerical model using terrain following coordinate transformation. *J. Comput. Phys.*, **24**, 186–215.

Clarke, R H (1979). A model for short and medium range dispersion of radionuclides released to the atmosphere. Harwell, NRPB-R91.

Colvile, R N, Sander, R, Choularton, T W, Bower, K N, Inglis, D W F, Wobrock, W, Schell, D, Svenningsson, I B, Wiedensohler, A, Hansson, H-C, Hallberg, A, Ogren, J A, Noone, K J, Facchini, M C, Fuzzi, S, Orsi, G, Arends, B G, Winiwarter, W, Schneider, T, and Berner, A (1994). Computer modelling of clouds at Kleiner Feldberg. *J. Atmos. Chem.*, **19**, 189–229.

Cook, N J (1985). *The Designer's Guide to Wind Loading of Building Structures. Part 1.* Garston, Building Research Establishment/London, Butterworths.

Cook, N J (1990). *The Designer's Guide to Wind Loading of Building Structures. Part 2 – Static Structures.* Garston, Building Research Establishment/London, Butterworths.

Cowan, I R, Castro, I P, and Robins, A G (1996). Uncertainty in CFD modelling of wind engineering problems. Presented at 3rd UK Conference on Wind Engineering, Oxford.

Egan, B A (1975). Turbulent diffusion in complex terrain. IN *Lectures on Air Pollution and Environmental Impact Analyses,* Workshop Proceedings. Boston, American Meteorological Society.

EPA. Guideline on air quality models. Available on the Internet: http://134.67.104.12/html/scram/gaqm.htm.

EPA. CTDMPLUS Fortran source code and PC executable code. Available on the Internet: http://134.67.104.12/html/scram/reg.htm.

EPA (1995). User's guide for the industrial source complex (ISC3) dispersion models, EPA-454/B-95-003a. Washington DC, Environmental Protection Agency. Also available on the Internet: http://134.67.104.12/html/scram/dreg.htm.

EURASAP (1996). 6th EURASAP International Workshop on Wind and Water Tunnel Modelling of Atmospheric Flow and Dispersion, Aso, Japan, 25–27th August 1996. *Atmos. Environ.*, **30**, 2811–8.

Fackrell, J E (1982). Flow behaviour near isolated rectangular buildings. Ratcliffe on Soar, PowerGen, CEGB Report 7PRD/M/1254/N82.

Fackrell, J E (1984). An examination of simple models for building influenced dispersion *Atmos. Environ.*, **18**, 89–98.

Fackrell, J E, and Pearce, J E (1981). Parameters affecting dispersion in the near wake of buildings. Ratcliffe on Soar, PowerGen, CEGB Report No. RD/M/1179/N81.

Ferrara, V, and Cagnetti, P (1980). A simple model for estimating airborne concentrations downwind of buildings for discharges near ground level. Presented at the European Commission Seminar on radioactive releases and their dispersion in the atmosphere following a hypothetical reactor accident, Risø, Denmark.

Gadilhe, A, Janvier, L, and Barnaud, G (1993). Numerical and experimental modeling of the three-dimensional turbulent wind flow through an urban square *J. Wind Eng. Ind. Aerodynam.*, **46–47**, 755–63.

Gifford, F A (1960). Atmospheric dispersion calculations using the generalised Gaussian plume model. *Nucl. Saf.*, **2**, 56–9.

Gifford, F A, and Porch, W M (1993). Atmospheric diffusion calculations on the HP-48 series pocket calculators.

Goddard, A J H, and Byrne, M A (1995). A briefing note on the temporal and spatial variation of the location factor for air concentration in buildings. IN Radiation Protection: Deposition of Radionuclides, Their Subsequent Relocation in the Environment and Resulting Implications, Final Report. Luxembourg, European Commission, EUR 166604 EN.

Gong, W (1991). A wind tunnel study of turbulent dispersion over 2-dimensional and 3-dimensional gentle hills from upwind point sources in neutral flow. *Boundary Layer Meteorol.*, **54**, 211–30.

Gong, W M, Taylor, P A, and Dornbrack, A (1996). Turbulent boundary-layer flow over fixed aerodynamically rough 2-dimensional sinusoidal waves. *J. Fluid Mech.*, **312**, 1–37.

Halitsky, J (1977). Wake and dispersion model for the EBR II building complex. *Atmos. Environ.*, **11**, 577–96.

Hall, D (1996a). Personal communication.

Hall, D J, and Robins, A G (1994). Introduction to the 5th EURASAP International Workshop on Wind and Water Tunnel Modelling of Atmospheric Flow and Dispersion. *Atmos. Environ.*, **28**, 1813–18.

Hall, D J, Spanton, A M, Macdonald, R, and Walker, S (1996). A review of requirements for simple urban dispersion models. Garston, Building Research Establishment, BRE Client Report CR 77/96.

Hall, R C (1996b) Application of computational fluid dynamics to near-field atmospheric dispersion. IN Atmospheric Dispersion Modelling Liaison Committee Annual Report 1995/96, Annex B. Chilton, NRPB-R292.

Hanna, S, and Paine (1989). Hybrid plume dispersion model (HPDM) development and evaluation. *J. Appl. Meteorol.*, **28**, 206–24.

Hanna, S R, Briggs, G A, and Hosker, R P (1982). *Handbook on Atmospheric Diffusion.* Oak Ridge TN, Department of Energy, Technical Information Center, DOE/TIC 11223.

Hanson, T, Summer, D M, and Wilson, C B (1986). A three-dimensional simulation of wind flow around buildings. *Int. J. Num. Methods Fluids*, **6**, 113–27.

Hatcher, R V, Meroney, R N, Peterka, J A, and Kothari, K (1978). Dispersion in the wake of a model industrial complex. NRC Report NUREG-0373. Washington DC, Nuclear Regulatory Commission, NTIS.

Higson, H L, Griffith, R F, Jones, C D, and Hall, D J (1994). Concentration measurements around an isolated building: a comparison between wind tunnel and field data. *Atmos. Environ.*, **28**, 1827–36.

Hill, J H (1997). A method to enable the inclusion of wind speed and directional fluctuations within a computational fluid dynamics code. *To be submitted.*

Hosker, R P (1979). Empirical estimation of wake cavity size behind block-type structures. IN Proceedings Fourth Symposium on Turbulence, Diffusion and Air Pollution, 15–18 January, Reno, Nevada, American Meteorological Society, pp 603–9.

Hosker, R P (1981). Flow and diffusion near obstacles. IN *Atmospheric Science and Power Production* (D Randerson, Ed), Chapter 7. Oak Ridge TN, Department of Energy, Technical Information Center.

Hosker, R P, Jr, and Pendergrass, W R (1987). Flow and dispersion near clusters of buildings. NOAA Technical Memorandum ERL ARL-153.

Huber, A H (1991). Wind tunnel and Gaussian plume modelling of building wake dispersion. *Atmos. Environ.*, **25A**, 1237–49.

Huber, A H, and Snyder, W H (1982). Wind tunnel investigation of the effects of a rectangular-shaped building on dispersion of effluents from short adjacent stacks. *Atmos. Environ.*, **16**, 2837–48.

Hunt, A, and Castro, I P (1984). Scalar dispersion in model building wakes. *J. Wind Eng. Ind. Aerodynam.*, **17**, 89–115.

Hunt, J C R, and Mulhearn, R J (1973). Turbulent dispersion from sources near two-dimensional obstacles. *J. Fluid Mech.*, **61**, 245–74.

Hunt, J C R, Abell, C J, Peterka, J A, and Woo, H (1978). Kinematical studies of the flows around free or surface mounted obstacles, applying topology to flow visualisation. *J. Fluid Mech.*, **86**, 179.

Hunt, J C R, Snyder, W H, and Lawson, R E, Jr (1978). Flow structure and turbulent diffusion around a three-dimensional hill: fluid modeling study on effects of stratification. Part I: flow structure. Washington DC, Environmental Protection Agency, Report No. EPA 600/1-78-041.

Hunt, J C R, Puttock, J S, and Snyder, W H (1979). Turbulent diffusion from a point source in stratified and neutral flows around a three-dimensional hill – Part I. Diffusion equation analysis. *Atmos. Environ.*, **13**, 1227–39.

Hunt, J C R, Leibovich, J, and Richards, K J (1988). Stratified shear flow over low hills. I: effect of wind shear. *Quart. J. Roy. Meteorol. Soc.*, **114**, 1435–70.

Jones, J A (1983). Models to allow for the effects of coastal sites, plume rise and buildings on the dispersion of radionuclides, and guidance on the deposition velocity and washout coefficients. Chilton, NRPB-R157.

Jones, J A (1997). Atmospheric dispersion at low wind speeds. IN Atmospheric Dispersion Modelling Liaison Committee Annual Report 1995/96, Annex A. Chilton, NRPB-R292.

Khurshudyan, L H, Snyder, W H, and Nekrasov, I V (1981). Flow and dispersion of pollutants over two-dimensional hills. Washington DC, Environmental Protection Agency, Report No. EPA-600/4-81-067.

Kobayashi, M H, Pereira, J C F, and Siqueira, M B B (1994). Numerical study of the turbulent-flow over and in a model forest on a 2D hill. *J. Wind Eng. Ind. Aerodynam.*, **53**, 357–74.

Launder, B E, and Spalding, D B (1974). The numerical computation of turbulent flows. *Comp. Methods Appl. Mech. Eng.*, **3**, 269–89.

Laurence, D, and Mattei, J-D (1993). Current state of computational bluff body aerodynamics. *J. Wind Eng. Ind. Aerodynam.*, **49**, 23–44.

Leschziner, M A (1993). Computational modelling of complex turbulent flow – expectations, reality and prospects. *J. Wind Eng. Ind. Aerodynam.*, **46–47**, 37–51.

Lu, W, and Howarth, A T (1996). Numerical analysis of indoor aerosol particle deposition and distribution in a two-zone ventilation system. *Building Environ.*, **31**, 41–50.

Ma, J, and Robson, R E (1995). Turbulent dispersion of pollutant over complex terrain. *Boundary Layer Meteorol.*, **72**, 149–75.

Mason, P J, and King (1985). *Quart. J. Roy. Meteorol. Soc.*, **111**, 617.

Mathews, E H, Crosby, C P, Visser, J A, and Meyer, J P (1988). Numerical prediction of wind loads on buildings. *J. Wind Eng. Ind. Aerodynam.*, **31**, 241–50.

Mellor, G L, and Herring, H J (1973). A survey of the mean turbulent field closure models. *AIAA*, **11**, 590–99.

Meroney, R N (1993). Bluff-body aerodynamics influence on transport and diffusion of hazardous gases. *J. Wind Eng. Ind. Aerodynam.*, **49**, 141–56.

Moin, P, and Kim, J (1997). Tackling turbulence with supercomputers. *Scientific American.*

Murakumi, S (1993). Comparison of various turbulence models applied to a bluff body. *J. Wind Eng. Ind. Aerodynam.*, **46–47**, 21–36.

Murakami, S, and Mochida, A (1988). 3-D numerical simulation of airflow around a cubic model by means of the k–ε model. *J. Wind Eng. Ind. Aerodynam.*, **31**, 283–303.

Murakami, S, Mochida, A, Hayashi, Y, and Sakamoto, S (1992). Numerical study on velocity pressure field and wind forces for bluff bodies by k–ε, ASM and LES. *J. Wind Eng. Ind. Aerodynam.*, **41–44**, 2841–52.

Nieuwstadt, F T M (1991). A large-eddy simulation of a line source in a convective atmospheric boundary layer – 1. Dispersion characteristics. *Atmos. Environ.*, **26A**, 485–95.

Okabayashi, K, Ide, Y, Kitabayashi, K, Okamoto, S, and Kobayashi, K (1996). Effects of wind directional fluctuation on gas diffusion over a model terrain. *Atmos. Environ.*, **30**, 2871–80.

Olesen, H R, Lofstrom, P, Bercowicz, R, and Jensen, A B (1991). Paper presented at the 19th International Technical Meeting on Air Pollution and its Applications, Ierapetra, Crete, 29 September – 4 October 1991.

Patankar, S V (1980). *Numerical heat transfer and fluid flow. Hemisphere.*

Paterson, D A, and Apelt, C J (1986). Computation of wind flows over three-dimensional buildings. *J. Wind Eng. Ind. Aerodynam.*, **24**, 193–213.

Paumier, J O, Perry, S G, and Burns, D J (1992). CTDMPLUS: a dispersion model for sources near complex topography. Part II: performance characteristics. *J. Appl. Meteorol.*, **31**, 646–60.

Perry, S G (1992). CTDMPLUS: a dispersion model for sources near complex topography. Part I: technical formulations. *J. Appl. Meteorol.*, **31**, 633–45.

Puttock, J S, and Hunt, J C R (1979). Turbulent diffusion from sources near obstacle with separated wakes. Part I: an eddy diffusivity model. *Atmos. Environ.*, **13**, 1–13.

Qadir, N (1990). A box model for indoor particulate transport. London, Imperial College Report.

Raupach, M R, Coppin, P A, and Legg, B J (1986). Experiments on scalar dispersion within a model plant canopy. *Boundary Layer Meteorol.*, **35**, 21–52.

Richards, P J, and Hoxey, R P (1993). Appropriate boundary conditions for computational wind engineering models using the k–ε turbulence model. *J. Wind Eng. Ind. Aerodynam.*, **46–47**, 145–53.

Robins, A G (1994). Flow and dispersion around buildings in light wind conditions. IN *Stably Stratified Flows – Flow and Dispersion over Topography* (I P Castro and N J Rockliff, Eds). Oxford, Clarendon Press, pp 325–58.

Robins, A G, and Castro, I P (1977a). A wind tunnel investigation of plume dispersion in the vicinity of a surface mounted cube: I. The flow field. *Atmos. Environ.*, **11**, 291–7.

Robins, A G, and Castro, I P (1977b). A wind tunnel investigation of plume dispersion in the vicinity of a surface mounted cube: II. The concentration field. *Atmos. Environ.*, **11**, 299–311.

Robins, A G, and Fackrell, J E (1980). Laboratory studies of dispersion near buildings. Ratcliffe on Soar, PowerGen, CEGB Internal Report MM/MECH/TF 235.

Robins, A G, and Fackrell, J E (1983). Mean concentration levels around buildings due to nearby low level emissions. Ratcliffe on Soar, PowerGen, CEGB Report No. TPRD/M/1261/N82.

Robinson, L M (1997). PhD Thesis. Department of Physics, UMIST.

Roed, J, and Goddard, A J H (1990). Ingress of Radioactive material into dwellings. Presented at a Seminar on Methods and Codes for Assessing the Off-site Consequences of Nuclear Accidents, Athens.

Ronold, A (1993). Modeling of flow and ventilation within petroleum process plants. *J. Wind Eng. Ind. Aerodynam.*, **46–47**, 675–80.

Schatzmann, M, Rafailidias, S, Britter, R, and Arend, M (1996) Database, monitoring and modelling of urban air pollution. Inventory of models and data sets, COST Action 615, Luxembourg, European Commission.

Sharan, M, Kumar, A, and Singh, M P (1995). Comparison of sigma schemes for estimation of air pollutant dispersion in low winds. *Atmos. Environ.*, **29**, 2051–9.

Sheppard, P A (1956). Airflow over mountains. *Quart. J. Roy. Meteorol. Soc.*, **82**, 528–9.

Singh, S, Fulker, M J, and Marshall, G (1994). A wind-tunnel examination of the variation of sigma *y* and sigma *z* with selected parameters. *Atmos. Environ.*, **28**, 1837–48.

Smith, R B (1980). Linear theory of stratifid hydrostatic flow past an isolated mountain. *Tellus*, **32**, 348–64.

Smith, R B (1990). Why can't stably stratified air rise over high ground? IN *Atmospheric Processes over Complex Terrain* (W Blumen, Ed). Boston, American Meteorological Society, pp 105–7.

Snyder, W H (1983). Fluid modeling of terrain aerodynamics and plume dispersion: a perspective view. IN Extended Abstracts, Sixth Symposium on Turbulence and Diffusion. Boston, American Meteorological Society.

Snyder, W H (1994). Some observations of the influence of stratification on diffusion in building wakes. IN *Stably Stratified Flows – Flow and Dispersion over Topography* (I P Castro and N J Rockliff, Eds). Oxford, Clarendon Press, pp 301–23.

Snyder, W H, and Lawson, R E, Jr (1976). Determination of a necessary height for a stack close to a building: a wind tunnel study. *Atmos. Environ.*, **10**, 683–91.

Snyder, W H, Thompson, R S, Eskridge, R E, Lawson, R E, Jr, Castro, I P, Lee, J T, Hunt, J C R, and Ogawa, Y (1982). The structure of strongly stratified flow over hills. Diving streamline concept. Appendix A. Washington DC, Environmental Protection Agency Report No. EPA 60013-83-015.

Thompson, R S (1991). Concentrations from above roof releases of laboratory exhausts: a wind tunnel study. *ASHRAE Trans.*, **97**, Part 2.

Thompson, R S (1993). Building amplification factors for sources near buildings: a wind-tunnel study. *Atmos. Environ.*, **27A**, 2313–25.

Trombetti, F, and Tampieri, F (1992). Analysis of wind tunnel dispersion data over two-dimensional obstacles. *Boundary Layer Meteorol.*, **59**, 209–26.

Turner, D B (1969). Workbook of atmospheric dispersion estimates. Washington DC, Department of Public Health Publication No. 999-AP-26.

van den Hout, K D, Baars, H P, and Duijm, N J (1989). Effects of buildings and trees on air pollution by road traffic. IN *Proceedings 8th World Clean Air Congress*. Oxford, Elsevier.

Venkatram, A (1996). An examination of the Pasquill-Gifford-Turner dispersion scheme. *Atmos. Environ.*, **30**, 1283–90.

Versteeg, H K, and Malalsekera, W (1995). *An Introduction to Computational Fluid Dynamics. The Finite Volume Method.* Harlow, Longman.

Vincent, J H (1977). Model experiments on the nature of air pollution transport near buildings. *Atmos. Environ.*, **11**, 765–74.

Vincent, J H (1978). Scalar transport in the near aerodynamic wakes of surface mounted cubes. *Atmos. Environ.*, **12**, 1319–22.

Walton , G (1997). Personal communication.

Wilcox, D C (1993). Turbulence modeling for CFD. DCW Industries Inc.

Wilson, D J (1976). Contamination of air intakes from roof exhaust vents. *ASHRAE Trans.*, **82**, 1024–38.

Wilson, D J (1977a). Effect of vent stack height and exhaust velocity on exhaust gas dilution. *ASHRAE Trans.*, **83**, 157–66.

Wilson, D J (1977b). Dilution of exhaust gases from building surface vents. *ASHRAE Trans.*, **83**, 168–76.

Wilson, D J (1979). Flow patterns over flat-roofed buildings and application to exhaust stack design. *ASHRAE Trans. Part 2*, **85**, 284–95.

Wilson, D J, and Netterville, D D J (1978). Interaction of a roof level plume with a downwind building. *Atmos. Environ.*, **12**, 1051–9.

Wilson, D J, and Britter, R E (1982). Estimates of building surface concentrations from nearby point sources. *Atmos. Environ.*, **16**, 2631–46.

Wilson, D J, and Chui, E H (1985). Influence of exhaust velocity and wind incidence angle on dilution from roof vents. *ASHRAE Trans.*, **91**, 1693–706.

Wilson, D J, and Chui, E H (1987). Effect of turbulence from upwind buildings on dilution of exhaust gases. *ASHRAE Trans.*, **93**, 2186–97.

Wilson, D J, and Chui, E H (1994). Influence of building size on rooftop dispersion of exhaust gas. *Atmos. Environ.*, **28**, 2325–34.

Wilson, D J, and Lamb, B K (1994). Dispersion of exhaust gases from roof-level stacks and vents on a laboratory building. *Atmos. Environ.*, **28**, 3099–111.

Yakhot, V, and Orszag, S A (1986). Renormalization group analysis of turbulence 1: basic theory. *J. Sci. Comput.*, **1**, 1–51.

Yakhot, V, Orszag, S A, Thangam, S, Gatski, T B, and Speziale, C G (1992). Development of turbulence models for shear flows by a double expansion technique. *Phys. Fluids*, **7**, 1510–20.

Zhang, C X (1994). Numerical predictions of turbulent recirculating flow with a k–ε model. *J. Wind Eng. Ind. Aerodynam.*, **51**, 177–201.

Zhang, Y Q, Arya, S P, and Snyder, W H (1996). A comparison of numerical and physical modeling of stable atmospheric flow and dispersion around a cubical building. *Atmos. Environ.*, **30**, 1327–45.

Zhang, Y Q, Huber, A H, Arya, S P S, and Snyder, W H (1993). Numerical simulation to determine the effects of incident wind shear and turbulence level on the flow around a building. *J. Wind Eng. Ind. Aerodynam.*, **46–47**, 129–34.

Permissions

APPENDIX

List of Symbols

A	projected building frontal cross-sectional area, m^2
A_w	surface area of wake recirculation boundary, m^2
B_0, B_1, B_3	empirical constants
C	concentration, kg m^{-3}
C_-	concentration outside the wake, kg m^{-3}
C_e	contaminant concentration in the gas at the source, kg m^{-3}
C_i	indoor concentration, kg m^{-3}
C_{max}	maximum concentration, kg m^{-3}
C_o	outdoor concentration, kg m^{-3}
C_r	roof-level concentration, kg m^{-3}
C_w	uniform wake concentration, kg m^{-3}
c	empirical constant
D	dilution factor (= $1/C$), kg^{-1} m^3
D_d	'distance' dilution, kg^{-1} m^3
D_L	larger of building height or width, m
D_{min}	minimum dilution, kg^{-1} m^3
D_o	an initial dilution due to jet and buoyant plume entrainment, kg^{-1} m^3
D_S	smaller of building height or width, m
f	building filtration factor
Fr	Froude number
g	acceleration due to gravity, m s^{-1}
H	building height, m
H_c	maximum height of the roof recirculation cavity on the upwind edge, m
H	hill height, m
h	release height above ground, m
h_c	critical streamline divergence height
h_s	stack height above roof level, m
h_{eff}	effective stack height above roof level incorporating effect of building downwash, m
Δh	plume rise above stack exit, m
i_c	rms intensity of isotropic turbulence
K	diffusivity
k	turbulent kinetic energy density
L	building length or length-scale for turbulence, m
L_c	maximum width of the roof recirculation cavity on the upwind edge, m
m_w	mass transfer rate of contaminant across wake boundary, kg s^{-1}
N	Brunt-Väisälä buoyancy frequency, s^{-1}
p	atmospheric pressure, Pa
Q	rate of discharge of contaminant, kg s^{-1}

Q_o	entrainment rate at the source, $m^3 s^{-1}$
r	raidal distance from centre of round hill, m
R	length scale for roof top wake turbulence, m
R	radius of round hill, m
s	stretched string distance from source, m
T	time, h
t	time, s
t_d	wake ventilation time constant, or residence time
U	reference advection windspeed, $m s^{-1}$
u	local wind speed (or component thereof) in x-direction, $m s^{-1}$
u_*	friction velocity, $m s^{-1}$
u_{10}	mean free stream velocity at 10 m, $m s^{-1}$
U_c	local mean velocity, $m s^{-1}$
U_H	windspeed at roof level far upwind of the building, $m s^{-1}$
V_w	volume of the near wake recirculation region, m^3
v_T, v_R	components of flow velocity in polar coordinate system
W	building width, m
x	longitudinal distance, or distance parallel to reference wind direction, m
x_c	maximum length of the roof recirculation cavity on the upwind edge, m
x_m	distance from source to point of maximum ground-level concentration, m
x_R	distance from the downwind building face to the reattachment point of the near-wake recirculation region, m
x_s	distance from an upwind source to the upwind building face, m
y	lateral distance or horizontal distance perpendicular to reference wind direction
z	height above ground, m
z_o	aerodynamic roughness length, m
α	entrainment constant for recirculation region
χ	non-dimensional concentration
ε	rate of dissipation of turbulent kinetic energy
λ	radioactive decay factor, s^{-1}
λ_d	deposition factor, s^{-1}
λ_r	rate of air exchange, h^{-1} (ACH)
ρ	fluid density, $kg m^{-3}$
θ	angle from x-axis in polar coordinate system
σ_x	longitudinal plume spread, m
σ_y	crosswind plume spread, m
σ_y	vertical plume spread, m
σ_θ	angular standard deviation of wind direction, degrees
σ_y', σ_z'	modified plume widths due to obstacles, m
σ_{yo}, σ_{zo}	virtual source plume widths at the source, m
ϕ	velocity potential
ψ	stream function
ζ	normalised distance in x-direction

On sale through the Stationery Office
£22.50

Stationery Office Publications Centre
PO Box 276, London SW8 5DT

Stationery Office Bookshops
49 High Holborn, London WC1V 6HB
71 Lothian Road, Edinburgh EH3 9AZ
16 Arthur Street, Belfast BT1 4GD
The Stationery Office Oriel Bookshop,
The Friary, Cardiff CF1 4AA
9–21 Princess Street, Manchester M60 8AS
68–69 Bull Street, Birmingham B4 6AD
33 Wine Street, Bristol BS1 2BQ

Also available through booksellers

ISBN 0 85951 422 6